Monitoring tropical forest dynamics using Landsat time series and community-based data

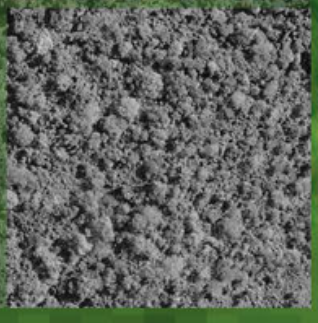

Ben DeVries

Monitoring tropical forest dynamics using Landsat time series and community-based data

Ben DeVries

Thesis committee

Promotor:
Prof. Dr M. Herold
Professor of Geo-information Science and Remote Sensing
Wageningen University

Co-promotors:
Dr L. Kooistra
Assistant Professor, Laboratory of Geo-information Science and Remote Sensing
Wageningen University

Dr J. Verbesselt
Assistant Professor, Laboratory of Geo-information Science and Remote Sensing
Wageningen University

Other members:
Prof. Dr L. Poorter, Wageningen University
Dr M. Wulder, Canadian Forest Service, Victoria, Canada
Dr R. Fensholt, University of Copenhagen, Denmark
Dr I. Jonckheere, Food and Agriculture Organization of the United Nations, Rome, Italy

This research was conducted under the auspices of the C.T. de Wit Graduate School
of Production Ecology & Resource Conservation (PE&RC)

Monitoring tropical forest dynamics using Landsat time series and community-based data

Ben DeVries

Thesis
submitted in fulfilment of the requirements for the degree of doctor at
Wageningen University
by the authority of the Rector Magnificus
Prof. Dr A.P.J. Mol,
in the presence of the
Thesis Committee appointed by the Academic Board
to be defended in public
on Friday 16 October 2015
at 4 p.m. in the Aula.

Ben DeVries
Monitoring tropical forest dynamics using Landsat time series and community-based data
170 pages.

PhD thesis, Wageningen University, Wageningen, NL (2015)
With references, with summary in English

ISBN 978-94-6257-476-2

Acknowledgements

This PhD thesis represents four years of research, learning, discovery and collaboration. While the contents herein are the final product of many hours of hard work, they cannot completely reflect the input I have had from so many people along the way.

First of all, I would like to thank my promoter, Martin Herold, under whose guidance I have developed tremendously in the past four years. Your commitment to your students and department is clearly evident and very much appreciated.

Second, I would like to thank my co-promoters, Jan Verbesselt and Lammert Kooistra. After countless discussions over coffee, hashing through details, debating methods and results, I am honoured to have been able to work together with you both on this thesis. Thank you also to Valerio Avitabile for your valuable assistance and guidance along the way, both while in the field and in the office.

I consider myself very fortunate to have had the chance to carry out much of my research in the field in Ethiopia. This work would not have been possible without the continued support of NABU. From the German office, I would like to thank Svane for her strong leadership, Dani for the very dependable support and company while in Bonga, and Bianca for keeping this wonderful project running. I would like to give a big thanks to Bekele, Sisay and Bety in Addis Ababa and Mesfin, Wondu, Fiseha and Wolde for the leadership and support on the ground in Ethiopia. Finally, my work was also made possible with the kind assistance from partners, especially EWNHS in Addis Ababa: thank you to Ato Mengistu, Alemayeu, Tewabe and especially Tesfaye for your assistance in these past years.

While in Ethiopia, I benefited from a very fruitful partnership between NABU and the Kafa Zone Bureau of Agriculture. Thank you to Terefe for your continued leadership in Kafa. I would like to give a huge thank you to the forest rangers who continue to show an incredible dedication to their work, and have made a concrete contribution to this research: Serkalem, Mitiku, Atnafu, Admasu H., Zintalem, Admasu A., Matiwos, Kasim, Tadalech, Gizachew, Zinabu, Asegadech, Abdu, Bethelihem, Girma, Nasir, Mekonnen, Israel, Bizuayehu, Mamo, Getinet, Siraj, Abera, Tesfaye, Tadesse, Mohammed, Abebe, Wodajo, Teka, and Adinew - Yeerimba! Finally, I would like to thank Muluken for his

constant support and facilitation during my five field campaigns in Kafa.

A big thanks goes out to the very vibrant Laboratory of Geo-Information Science and Remote Sensing group at Wageningen University. Arun, Johannes R., Roberto, Niki, Tsoefiet, Mathieu, Richard, Simon, Michael, Manos, Maria, Arend, Philip, Eskender, Loïc, Peter, Kim, Johannes E., Sytze, Eliakim, Harm, John, Ron, Jan C., Arnold, Angela, Brice, Nandika, Hans, Jose, Sarah, Astrid, Alvaro, Rosa, Erika, Jessica, Kathleen, Juha, Aldo, Willy, Frans, Roland, Lucasz, Corne, Ben, Giulia, Yang, Marston, Konstantin, Qijun, Marcio, Jalal, Laure, Valerie, Titia, Rogier, Daniel, Daniela - thanks for four great years and keep up the excellent work! A special thanks goes to Truus and Antoinette for your endless support and problem solving on the administrative side. Finally, I would like to thank the MSc thesis students whom I have had the pleasure to supervise: Frehiwot, Kalkidan, Stephan, Elias and Dereje.

I did not spend all of my time behind the desk and in the field, of course. My other great passion - music - helped to keep me on track and well-balanced in these past years in Wageningen. For this, I would like to thank the entire music community in Wageningen and surroundings. An especially big thanks goes out to Caperune: Johan, Jimi, Sam, Erikwim, Erik, Jelmer, Daniel, and the countless guest musicians who have helped to make this project the success it was. A big thanks goes to Guus Tangelder and the Big Band Sound of Science, and all of the other musicians and friends with whom I have had the pleasure to meet and get to know in this small but very charismatic town.

Finally, I would like to give a big thanks and much love to my wonderful family, both immediate and extended, near and far. Ik wil de Dykstra familie hier in Nederland bedanken voor alles tijdens de afgelopen zeven jaar in Nederland. Ik ben zo blij dat ik jullie beter heb leren kennen. Bovendien wil ik Max en Tineke bedanken voor hun steun vanaf mijn allereerste dag in Wageningen. To my family in Canada: I've missed you and am grateful for everything you've given me over all these years. First, to my parents - Andy and Siska DeVries - thanks for your unfailing love and support in all of my endeavours, without which I would never had made it this far. A huge thanks goes out to my brothers and their families as well: Chris, Amanda, Joe, Elle, Aaron, Sarah, Maya, Julian, Raine, Helena, Nolan and baby number three (who I can't wait to meet!). I'm honoured to call you all family, and couldn't have asked for a better one!

Contents

Summary

Tropical forests cover a significant portion of the earth's surface and provide a range of ecosystem services, but are under increasing threat due to human activities. Deforestation and forest degradation in the tropics are responsible for a large share of global CO_2 emissions. As a result, there has been increased attention and effort invested in the reduction of emission from deforestation and degradation and the protection of remaining tropical forests in recent years. Methods for tropical forest monitoring are therefore vital to track progress on these goals. Two data streams in particular have the potential to play an important role in forest monitoring systems. First, satellite remote sensing is recognized as a vital technology in supporting the monitoring of tropical forests, of which the Landsat family of satellite sensors has emerged as one of the most important. Owing to its open data policy, a large range of methods using dense Landsat time series have been developed recently which have the potential to greatly enhance forest monitoring in the tropics. Second, community-based monitoring is supported in many developing countries as a way to engage forest communities and lower costs of monitoring activities. The development of operational monitoring systems will need to consider how these data streams can be integrated for the effective monitoring of forest dynamics.

This thesis is concerned with the monitoring of tropical forest dynamics using a combination of dense Landsat time series and community-based monitoring data. The added value conferred by these data streams in monitoring deforestation, degradation and regrowth in tropical forests is assessed. This goal is approached from two directions. First, the application of econometric structural change monitoring methods to Landsat time series is explored and the efficacy and accuracy of these methods over several tropical forest sites is tested. Second, the integration of community-based monitoring data with Landsat time series is explored in an operational setting. Using local expert monitoring data, the reliability and consistency of these data against very high resolution optical imagery are assessed. A bottom-up approach to characterize forest change in high thematic detail using *a priori* community-based observations is then developed based on these findings.

Chapter 2 presents a robust data-driven approach to detect small-scale forest disturbances driven by small-holder agriculture in a montane forest in southwestern Ethiopia. The

Breaks For Additive Season and Trend Monitoring (BFAST Monitor) method is applied to Landsat NDVI time series using sequentially defined one-year monitoring periods. In addition to time series breakpoints, the median magnitude of residuals (expected versus observed observations) is used to characterize change. Overall disturbances are mapped with producer's and user's accuracies of 73%. Using ordinal logistic regression (OLR) models, the extent to which degradation and deforestation can be separately mapped is explored. The OLR models fail to distinguish between deforestation and degradation, however, owing to the subtle and diffuse nature of forest degradation processes.

Chapter 3 expands upon the approach presented in Chapter 2 by tracking post-disturbance forest regrowth in a lowland tropical forest in southeastern Peru using Landsat Normalized Difference Moisture Index (NDMI) time series. Disturbance between 1999 and 2013 are mapped using the same sequential monitoring method as in Chapter 2. Pixels where disturbances are detected are then monitored for follow-up regrowth using the reverse of the method employed in Chapter 2. The time of regrowth onset is recorded based on a comparison to defined stable history period. Disturbances are mapped with 91% accuracy, while post-disturbance regrowth is mapped with a total accuracy of 61% for disturbances before 2006.

Chapter 4 and 5 explore the integration of community-based forest monitoring data and remote sensing data streams. Major advantages conferred by community-based forest disturbance observations include the ability to report on drivers and other thematic details of forest change and the ability to detect low-level forest degradation before these changes are visible above the forest canopy. Chapter 5 builds on these findings and presents a novel bottom-up approach to characterize forest changes using local expert disturbance reports to calibrate and validate forest change models based on Landsat time series. Using random forests and a selection of Landsat spectral and temporal metrics, models describing forest state variables (deforested, degraded or stable) at a given time are produced. As local expert data are continually acquired, the ability of these models to predict forest degradation are shown to improve.

Chapter 6 summarizes the main findings of the thesis and provides a future outlook, given the prospect of increasing availability of satellite and *in situ* data for tropical forest monitoring. This chapter argues that forest change methods should strive to utilize satellite time series and ground data to their maximum potential. As "big data" emerges in the field of earth observation, new data streams need to be accommodated in monitoring methods. Operational forest monitoring systems that are able to integrate such diverse data streams can support broader forest monitoring goals such as quantitative monitoring of forest dynamics. Even with a wealth of time series based forest disturbance methods developed recently, forest monitoring systems require locally calibrated forest change estimates with higher spatial, temporal and thematic resolution to support a variety of forest monitoring objectives.

Chapter 1

Introduction

Parts of this chapter are adapted with permission from:

DeVries, B. & Herold, M. 2013. The Science of Measuring, Reporting and Verification (MRV). In R. Lyster, C. MacKenzie, & C. McDermott (Eds.), *Law, Tropical Forests and Carbon: The Case of REDD+*, pp. 151-183. Cambridge: Cambridge Univ Press.

1.1 Monitoring Tropical Forest Change

The tropical forest has long held a place of wonder and mystery in the collective imagination of the Western world. Thomas Belt, a 19th century English naturalist, said of the cloud forests of Nicaragua:

> "Though I had dived into the recesses of these mountains again and again, and knew that they were covered with beautiful vegetation and full of animal life, yet the sight of that leaden-coloured barrier of cloud resting on the forest tops, whilst the savannahs were bathed in sunshine, ever raised in my mind vague sensations of the unknown and the unfathomable." (Belt, 1874)

To many, the tropical forest was wild, pristine and untouchable. The fragility of these environments was not lost on Belt, however. What he observed was a highly dynamic system left vulnerable by human activities:

> "I have been led to the conclusion that the forest formerly extended much further towards the Pacific, and has been beaten back principally by the agency of man." (Belt, 1874)

Deforestation in the tropics came to the attention of the broader scientific community nearly one century following Belt's observations (Myers, 1979). Several studies revealed tropical forest removal using aerial photography and field observations (Bernstein et al., 1976), linked conversion of tropical forests to other land uses to climate change and air pollution (Bach, 1976) and issued calls for the establishment of protected forest areas for primates and other wildlife (Veblen, 1976; Bernstein et al., 1976).

1.1.1 Tropical forests and carbon emissions

Today, tropical forests cover 15% of the earth's surface (FAO, 2014). In the absence of disturbances, tropical forests have been shown to act as carbon sinks as CO_2 is actively removed from the atmosphere and assimilated into biomass (Lewis et al., 2004; Phillips et al., 1998). This carbon-absorbing function is not limited to pristine primary forests, as secondary forests have been shown recently to be key players in the mitigation against global climate change (Bongers et al., 2015). Due to these changes, tropical forests are estimated to be a net source of CO_2 emissions since 1990, with gross emissions outweighing atmospheric removals by 1.3 billion tonnes per year (Pan et al., 2011).

Curbing deforestation in the tropics has the potential to contribute significantly to carbon emission reductions globally (Gullison et al., 2007). The role of tropical forests in climate change mitigation has been recognized through negotiated mechanisms such as the Reducing Emissions from Deforestation and Forest Degradation (REDD+) programme, which aims to credit developing countries who enact measures to stem emission due to

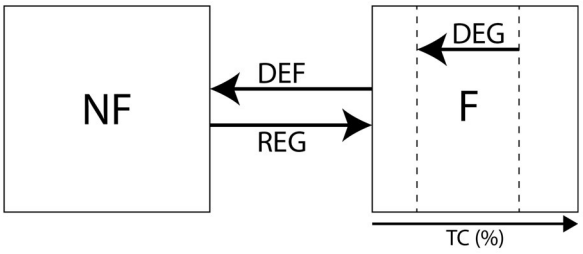

Figure 1.1: Schematic outlining the concept of forest change employed in this thesis. Deforestation (DEF) is a transition from a forested (F) to non-forested (NF) state, while regrowth (REG) is the reverse process. Degradation (DEG) is a decrease in percent tree cover (TC) within a preserved forested state.

forest loss and conserve remaining forests (Schmidt & Scholz, 2008). The successful implementation of REDD+ depends on the Measuring, Reporting and Verification (MRV) of emissions reductions (DeVries & Herold, 2013; UNFCCC, 2009b), where activity data (forest area change) and emission factors (carbon stock per unit forest area) are linked to derive estimated CO_2 emissions (Penman et al., 2003).

MRV is concerned with three broad forest change processes: deforestation, forest degradation and forest regrowth. Making a distinction between these processes requires a robust definition of forests (DeVries & Herold, 2013). Thresholds defined at the UNFCCC 7$^{\text{th}}$ Conference of Parties (COP7), commonly known as the Marrakech Accords, are often used to define forests as follows: "a minimum area of land of 0.05-1.0 hectares with tree crown cover (or equivalent stocking level) of more than 10-30 percent with trees with the potential to reach a minimum height of 2-5 metres" (UNFCCC, 2001). Deforestation thus refers the process by which forested land is converted to non-forest lands (Figure 1.1). Degradation, on the other hand, is defined by the IPCC as "reductions in carbon stocks within forests remaining forests" (Penman et al., 2003). Forest regrowth can thus be defined as the reverse of either of these two processes, where forest carbon stocks recover, removing atmospheric CO_2 in the process. The definitions of forest change employed in this thesis are shown in Figure 1.1. These change classes are defined below and are explained in more detail in each chapter.

- **Deforestation** is defined as a transition from a forested stated to a non-forested state, where "forest" is defined based on a tree cover threshold within one Landsat pixel.
- **Degradation** is defined as a reduction in tree cover where the end result is still defined as a forest. This definition is analogous to that recommended by the IPCC (Penman et al., 2003), except that the definition used here only considers the forest canopy, rather than height and area.
- **Regrowth** is defined as a transition from a non-forest state to a forested state.

In reality, the regrowth forest canopy and structure differ greatly from that of the original intact forest in terms of carbon stocks and other variables. The definition used here is simplified for the purpose of detecting changes at the Landsat pixel scale.

1.1.2 Understanding tropical forest dynamics

Forest monitoring extends beyond the measurement of forest cover loss and carbon emissions and removals. Changes in forest cover and structure have been shown to have an effect on the resilience of forest systems, bringing them closer to critical forest/non-forest transitions as tree cover is reduced (Hirota et al., 2011). Such non-linear transitions between forest and non-forest states are in line with modern thinking around ecosystem dynamics (Holling, 1973; van de Leemput et al., 2015). A detailed understanding of forest dynamics is necessary to unravel the complex interactions between forests, climate and human systems (Bonan, 2008). Such an understanding requires information on forest status with high spatial, temporal and thematic detail. While conventional plot-based forest research has the most potential for addressing the thematic dimension, key barriers are faced in the spatial and temporal domains (Salk et al., 2013).

1.2 Monitoring Forests from Space

Remote sensing technologies, including aerial and space-borne sensors, have become prominent in operational forest research and monitoring in the past few decades (De Sy et al., 2012) and are poised to fill the spatio-temporal gaps present in plot-based forest research. At present there are numerous satellite constellations monitoring the earth's surface using a variety of wavelength ranges, including optical and radar sensors. Optical sensors detect reflected radiation from the earth's surface at wavelengths in the visible, Near-Infrared (NIR), Short-Wave Infrared (SWIR) and Thermal Infrared (TIR) ranges. At these ranges, spectral characteristics of the detected radiation can reveal a great deal about the physical characteristics of the earth's surface, including land cover and vegetation cover. Optical sensors suffer several drawbacks, however. First, most space-borne optical sensors are passive, meaning they can only collect data during the day when the sun is illuminating the earth. Second, optical radiation is not able to penetrate cloud cover, a problem which plagues many areas within the humid tropics (Asner, 2001). Radar sensors can overcome some of the shortcomings of optical sensors. For example, as active sensors (meaning they act as the source and receiver of electromagnetic radiation at the same time), they do not rely on reflected solar energy and can make observations at day or night (Thiel et al., 2006). Additionally, radiation at wavelengths in the radar range is able to penetrate clouds (De Sy et al., 2012), thus providing an alternate data source

for areas with high cloud cover. Future applications of remote-sensing science to forest monitoring will likely include the integration of radar and optical remote-sensing based methods (Reiche et al., 2013, 2015a,b). Although each of these types of sensors provides unique advantages to the field of forest and land cover change monitoring, this thesis focuses on the use of optical sensors, as they currently provide the most widely accessible data and associated methods.

1.2.1 Spectral Response to Forest Changes

As the bulk of the sun's optical radiation does not penetrate the forest canopy, monitoring forest changes using passive optical sensors is mostly concerned with changes to the forest canopy. A simplified illustration of some of the forest change processes studied in this thesis is shown in Figure 1.2. Here, reflectance over a single pixel (bottom row) is shown for forest stands under different disturbance conditions (top row). In this illustration, a hypothetical index is shown, with darker values related to forest canopies and lighter values related to soil reflectance. Reflected radiation from intact forests (Figure 1.2A) describes vegetation characteristics with no background influence of soil or understorey vegetation. Forest degradation, due to selective logging for example, often results in canopy gaps, whereby a fraction of the pixel contains background soil reflectance from the forest floor, with the remaining fraction containing forest canopy reflectance (Figure 1.2B). Spectral un-mixing algorithms are commonly used to disentangle these contributing reflectance profiles towards degradation mapping (Souza et al., 2005). Complete removal of a forest stand within a pixel results in a completely altered reflectance profile, the result being dominated by bare soil or other vegetation reflectance characteristics (Figure 1.2C). Finally, regrowing forests following a stand-replacing disturbance can result in canopy closure by woody successional species within several years (Finegan, 1996; Howorth & Pendry, 2006). Research using optical Landsat data has suggested that reflectance in the SWIR domain may be used to distinguish young successional forest canopies from intact forest canopies, since primary and secondary forest canopies have different moisture contents, a physical parameter to which these wavelength ranges are sensitive (Fiorella & Ripple, 1993; Gao, 1996; Wilson & Sader, 2002; Jin & Sader, 2005).

1.2.2 The Landsat legacy

The launch of the first Landsat sensor in 1972 marked the beginning of the longest ever continuous earth observation record (Roy et al., 2014; Williams et al., 2006). Since that time, a suite of Landsat-bound sensors have facilitated the collection of terrestrial imagery over the globe. The Multi-Spectral Scanner (MSS) sensors capture reflected radiation from the visible and near infra-red (NIR) wavelengths. The Thematic Mapper (TM) on board Landsat-4 and Landsat-5 and the Enhanced Thematic Mapper Plus (ETM+) on board

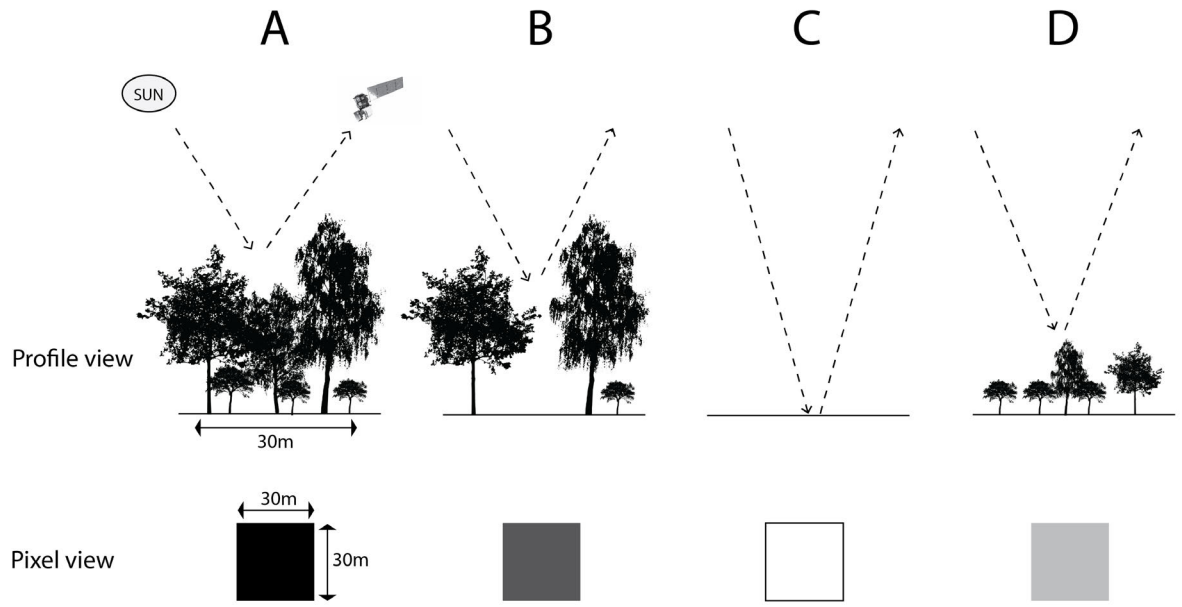

Figure 1.2: Illustration of canopy reflectance as detected by passive optical sensors. Intact forests (A), degraded forests with canopy gaps (B), cleared forests (C) and regrowing forests (D) differ in canopy refectance due to varying degrees of background soil reflectance, understorey vegetation, canopy structure and moisture content. The bottom row illustrates the impact of these reflectance profiles on a hypothetical vegetation index over a 30m Landsat pixel.

Landsat-7 have been responsible for a spectrally richer dataset, with the capabilities of recording radiation at a much wider range of wavelengths. The Landsat programme has not been without its disappointments, however. First, the Enhanced Thematic Mapper (ETM) on board Landsat 6 failed to reach orbit, a loss which was partially compensated by the unanticipated lifespan of the Landsat-5 TM sensor. Second, the scan-line corrector (SLC) on board the ETM+ sensor failed in 2003, resulting in a loss of approximately 22% of data from each scene acquired thereafter (Maxwell et al., 2007). ETM+ data have nevertheless remained an important component of the Landsat archive, especially in light of the end of the TM sensor's life in 2011. The eighth Landsat mission, featuring the Operational Land Imager (OLI), was launched in 2013 (Irons et al., 2012), once again filling the gaps left by the ETM+ SLC-off errors and the decommissioned TM sensor. OLI expands on the spectrum of wavelengths offered by TM and ETM+, including extra bands for enhanced atmospheric correction and cloud masking (Irons et al., 2012).

In recognition of the importance of the Landsat archive, recent efforts have been placed in consolidating (Loveland & Dwyer, 2012), pre-processing (Masek et al., 2006b; Vermote et al., 1997) and publicly releasing (Wulder et al., 2012) Landsat data across the globe. This effort has led to a surge in high temporal resolution change detection methods, not least of which have been designed expressly for forest monitoring purposes (Banskota

et al., 2014). Landsat-based multi-temporal methods have taken their cues from time series approaches developed with coarse resolution datasets with frequent return times and higher-level products available (Cihlar et al., 1997; Roerink et al., 2000; Cihlar et al., 2004; Roerink et al., 2003). More recently, these types of approaches have been developed using Landsat Time Series (LTS), either on annual composites (Kennedy et al., 2010; Huang et al., 2010), or by ingesting all available observations in the archive to derive higher level thematic products (Broich et al., 2011; Potapov et al., 2012; Zhu et al., 2012b; Zhu & Woodcock, 2014). A more detailed background on methods developed for LTS is given in Chapters 2 and 3.

1.2.3 Operational forest monitoring systems

A number of examples of operational forest monitoring systems designed to support REDD+ MRV or other forest monitoring objectives have emerged as a result in advances in time series based change detection methods. The Brazilian Space Agency (INPE), for example, has developed systems for reporting forest cover changes at annual time scales (INPE, 2014b) and on a near real-time basis (INPE, 2014a). The Global Forest Watch initiative (World Resources Institute, 2014) provides an open access platform for the visualization and analysis of LTS-based forest cover change estimated at unprecedented spatial scale and resolution (Hansen et al., 2013). These forest monitoring systems represent significant and important steps towards bringing remote sensing based forest monitoring methods into public use. The interpretations, conclusions and applications that can be drawn from such large area datasets remain controversial, however (Hansen et al., 2014; Tropek et al., 2013). Describing forest change in greater thematic detail using the full spectral and temporal arsenal of Landsat and similar datasets therefore represents a key research gap.

1.3 Structural Change Monitoring

Many of the methods applied to satellite time series data for terrestrial monitoring have their roots in different disciplines. For example, methods such as dynamic time warping, originally developed for voice recognition algorithms, and statistical control charts, developed as a multivariate process monitoring method (Reynolds & Cho, 2011), have found their place in the satellite time series literature to map land cover changes (Petitjean et al., 2012; Brooks et al., 2014). Structural change monitoring encompasses a series of methods used to track breaks in a time series that were originally developed for application to econometric models (Bai, 1997; Bai & Perron, 2003; Zeileis et al., 2005). Structural change monitoring is based upon hypothesis tests regarding stability of a time series compared to a previously established stable period. Under the null hypothesis,

data being monitored do not significantly deviate from expected patters established in a history period. Rejection of this null hypothesis is thus interpreted as a significant break (e.g. based on a 95% probability threshold) in the time series (Zeileis et al., 2005).

Rather than testing the null hypothesis on singular observations within the time series, structural change monitoring employs cumulative or temporal neighbourhood statistics, thus preserving the structural characteristics of the time series (Chu et al., 1992; Zeileis et al., 2005). One such measure is based on moving sums of residuals (MOSUM), where residuals are calculated as the difference between expected values and actual observations in a monitoring period. The MOSUM (MO_t) corresponding to an observation y at time t is computed as follows:

$$MO_t = \sum_{i=t-h+1}^{t} \frac{y_i - \hat{y}_i}{\hat{\sigma}\sqrt{n}} \tag{1.1}$$

In this form, a bandwidth (h) is typically set as a fraction of the number of observations (n) in the time series such that MO_t is the "normalized" sum of all residuals within the window preceding (and including) observation y_t. This sum is normalized by the estimated deviance from the stable history period ($\hat{\sigma}$), implying that with a noisy time series (i.e. with high variance throughout), there is less chance that the null hypothesis will be rejected due to noise alone. In other words, a statistically significant and persistent break is required to trigger a breakpoint (Zeileis et al., 2005; Verbesselt et al., 2010, 2012). Structural change monitoring thus provides a data-driven method for detecting change, whereby the threshold above which change is detected is not determined externally (e.g. by a user), but depends on the local structure of the time series residuals (the numerator of Equation 1.1) and the level of noise expected in the time series (the denominator of Equation 1.1).

1.3.1 Applying the theory: BFAST

Structural change monitoring based on the MOSUM has been previously applied to coarse resolution satellite time series in the form of the Breaks For Additive Season and Trend (BFAST) family of algorithms (Verbesselt et al., 2010, 2012). These algorithms have been designed either to divide a time series into a number of stable segments based on a number of breaks (Verbesselt et al., 2010), to select the single most important break in a time series, if any (de Jong et al., 2013), or to monitor incoming observations in a time series against a defined stable history period (Verbesselt et al., 2012). These approaches rely on the additive fitting of a season-trend curve to the data as follows:

$$y_t = T_t + S_t + \epsilon_t \tag{1.2}$$

where T_t is the trend component, S_t is the seasonal component and ϵ_t is the remainder (related to $\hat{\sigma}$ in Equation 1.1). By combining Equations 1.2 and 1.1, the BFAST-family

of algorithm allow for robust monitoring of time series changes above and beyond what might be expected due to seasonality, monotonic trend or random noise. Few studies have applied structural change monitoring methods to irregular time series such as LTS (Reiche et al., 2015a; Dutrieux et al., 2015), and whether such a data-driven approach can work in an operational forest monitoring setting is unknown.

1.4 Community-Based Forest Monitoring

Ground-based forest monitoring approaches have developed in parallel with, and in many cases in synergy with, satellite-based technologies. One such data source which is especially relevant for tropical countries engaging in REDD+ originates from Community-Based Monitoring (CBM) of forest. CBM data are a product of community forest management systems, which have been promoted and supported throughout the tropics (Pratihast et al., 2013; Bowler et al., 2012). CBM has been promoted in REDD+ MRV systems for a number of reasons. First, involvement of local people in REDD+ monitoring activities is seen as a way to enhance the acceptance, sustainability and equity of REDD+ projects on the ground (Palmer Fry, 2011). Second, where CBM is effectively implemented, monitoring costs have been shown to dramatically decrease, giving added incentives to countries to invest in REDD+ MRV systems (Pratihast et al., 2012).

Aside from the obvious social and practical benefits to including communities in forest monitoring activities, CBM has the potential to complement existing forest monitoring technologies, such as satellite-based monitoring, towards enhanced monitoring systems. In this sense, communities can be viewed as "human sensors" who measure and monitor important forest-related variables *in situ*. This concept is analogous to volunteered geo-information (VGI) or citizen science data, where volunteers or lay people provide geo-localized qualitative or quantitative data which are used as reference data for various land monitoring applications (Goodchild, 2007). CBM has been shown to be useful and cost-effective in measuring forest carbon stocks at the plot level (Pratihast et al., 2012; Brofeldt et al., 2014) and has been put forward as a key component in national-level forest monitoring systems in support of REDD+ MRV (Pratihast et al., 2013).

CBM data have the potential to support satellite-based forest change analysis in two key ways. First, these data could play a vital role in validation of change estimates. Validating change maps is notoriously difficult due to the simple fact that we cannot travel back in time to verify if and when a change occurred. Validation thus often relies on other imagery (such as very high resolution optical imagery), which is difficult to access in many cases. Other studies have used human interpreters and the same LTS source data that were used to derive the change maps to validate changes (Cohen et al., 2010), which has been shown to be effective in the absence of other reference data (Kennedy et al., 2010). CBM data could therefore help to fill this gap by tapping into the knowledge of local people, thereby

supplying a bottom-up data stream for forest change monitoring.

The second potential value added of CBM data to satellite-based change estimates is the addition of thematic details to change estimates. Human sensors have the distinct advantage of being able to document forest changes underneath the canopy independently of satellite-based alerts. This capability is a key advantage in forest areas where low-level degradation is driven by fuelwood collection in the understorey, for example (Herold et al., 2011; Dresen et al., 2014), and could serve as an early warning for degradation before changes to the forest canopy become visible. Additionally, this "bottom-up" monitoring of forest changes could result in additional training data to gage the extent to which subtle forest canopy changes can be detected from space.

While the idea of CBM is gaining considerable traction in the frame of REDD+ and other similar forest-related schemes, the potential of CBM to support forest change monitoring from the ground remains largely unexplored. Several research questions need to be addressed before CBM can be integrated with satellite data in an operational setting. First, the question of quality and reliability of CBM-based forest change observations needs to be addressed. Differences in forest change interpretations between local communities and professionals, or inadequate technical support (e.g. GPS devices for geo-location) may preclude the effective integration of CBM data with satellite-based observations. Second, the question regarding the level at which integration of CBM and satellite data should be integrated remains. As noted above, this integration could occur at the calibration or validation stages of forest change monitoring. Addressing these research gaps represents a significant step towards operational integration of CBM and satellite-data in a forest monitoring system.

1.5 Problem Statement and Research Objectives

With the rich Landsat archive stretching back to the 1970's and the ever-expanding prospects of continuous satellite-borne data streams in the future, time series based methods such as those developed for Landsat data will become increasingly important. While forest disturbance monitoring using LTS has been operationalized in many cases, most of the methods that have been developed still under-utilize the time series or rely on user-defined or otherwise arbitrary thresholds. There is a need for more robust, data-driven methods that can detect forest changes in high temporal, spatial and thematic resolution.

As described above, CBM has seen similarly significant advances in recent years. Evolving technologies are opening the doors to enhanced *in situ* and community-based monitoring of forest resources. CBM has the potential to help address some of the gap in LTS-based forest monitoring identified above. Despite a growing body of research into the topic of

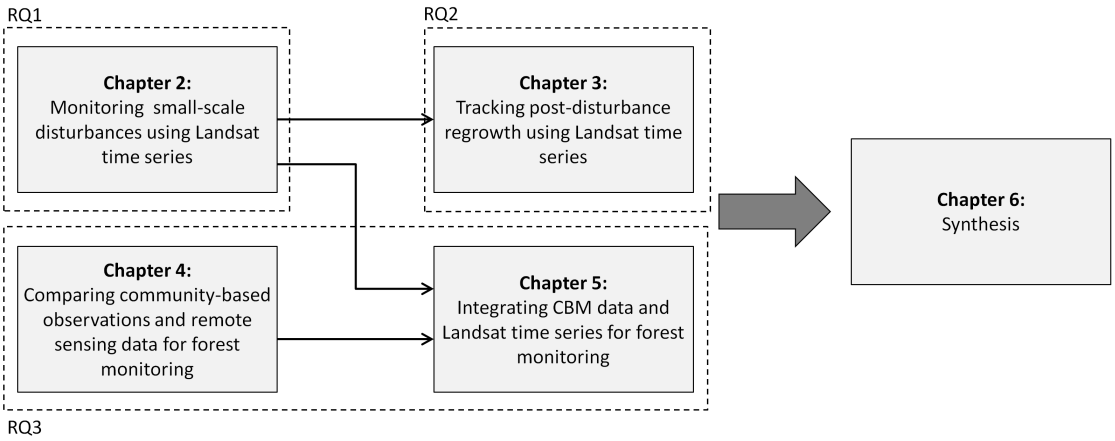

Figure 1.3: Flowchart for the chapters in of this thesis in relation to each of the research questions (RQ).

CBM for forest monitoring, however, very little research has been done to address the question as to how such a data stream can complement satellite-based time series for operational forest monitoring.

The research described in this thesis seeks to address these two research gaps by exploring two potential bridges: (1) that between robust structural change monitoring methods and satellite-based time series; and (2) that between satellite-based time series and CBM data streams. To this end, I pose the following research questions:

1. To what extent can we track small-scale forest disturbances in complex forest landscapes using dense LTS?
2. Can structural change monitoring be used with LTS to monitor post-disturbance regrowth in tropical forests?
3. How can community-based monitoring data and Landsat time series be integrated to enhance forest monitoring?

1.6 Thesis Overview and Study Sites

This thesis includes six chapters, including this Introduction Chapter. The outline of subsequent chapters is presented in Figure 1.3.

Chapter 2 describes a robust approach for monitoring small-scale forest disturbances in a forest-agriculture matrix landscape in southern Ethiopia. Structural change monitoring methods are applied iteratively on Landsat Time Series data and a change magnitude

method is derived statistically to map small-scale agriculture-driven deforestation and degradation.

Chapter 3 extends on the methodology developed in Chapter 2 and presents data-driven method for detecting post-disturbance forest regrowth using Landsat Time Series. By applying the method over a lowland tropical forest system in southern Peru, advantages and limitations to using Landsat Time Series for post-disturbance regrowth monitoring are shown, and a framework for continuous monitoring of forest dynamics is proposed.

Chapter 4 presents an assessment of consistency between community-based monitoring data, professional forest monitoring data and very high resolution remote sensing data for forest change monitoring. A dataset of local expert observations is compared with professional forest observations and very high resolution satellite imagery over a site in southern Ethiopia.

Chapter 5 presents an integrated forest monitoring approach using Landsat time series and community-based forest monitoring data in southern Ethiopia. Using a suite of spectral-temporal metrics derived from dense Landsat time series combined with a continuous stream of local expert monitoring data in random forest models, local expert data are shown to improve estimates of deforestation and forest degradation over time.

Chapter 6 discusses the results of the thesis and addresses the research questions presented above. The implications of the results on integrated forest monitoring are discussed and an outlook regarding the future of satellite-based and *in situ* monitoring of forest dynamics is presented.

I conducted my research through two case studies in the tropics. First, the UNESCO Kafa Biosphere Reserve in southwest Ethiopia is featured in Chapters 2, 4 and 5. The moist forests in this area represent some of the last remaining Afro-montane forests (Schmitt et al., 2010a), and harbour valuable *Coffea arabica* genetic resources (Aerts et al., 2015; Hein & Gatzweiler, 2006). The second study area, on which Chapter 3 is based, is found in Madre de Dios, southeastern Peru. This lowland forest has recently been opened up to rapid developments, including for pasture, croplands and gold mining (Nepstad & Carvalho, 2001; Shepard et al., 2010; Asner et al., 2013; Alvarez-Berríos & Mitchell Aide, 2015). Specific characteristics of the study areas are explained further in their respective chapters.

Chapter 2

Monitoring small-scale disturbances using Landsat time series

This chapter is based on:

DeVries, B., Verbesselt, J., Kooistra L. & Herold, M. 2015. Robust monitoring of small-scale forest disturbances in a tropical montane forest using Landsat time series. *Remote Sensing of Environment*, 161:107-121.

Abstract

Remote sensing data play an important role in the monitoring of forest changes. Methods are needed to provide objective estimates of forest loss to support monitoring efforts at various scales, and with increasing public availability of remote sensing data, accurate deforestation measurements at high temporal resolution are becoming more realistic. While several time series based methods have recently been described in the literature, there are few studies focusing on tropical forest areas, where low data availability and complex change processes present challenges to forest disturbance monitoring. Here, we present a robust data-driven method to track tropical deforestation and degradation based on Landsat time series data. Based on the previously reported Breaks For Additive Season and Trend Monitor (BFAST Monitor) method (Verbesselt et al., 2012), we show that BFAST Monitor, when applied to Landsat NDVI time series data using sequentially defined monitoring periods, can be used to track small-scale forest disturbances annually in an Afromontane forest system in southern Ethiopia. Using an ordinal logistic regression (OLR) approach, change magnitude, calculated based on differences between observed and expected values in a monitoring period, was found to be an essential predictor variable for disturbances. After applying a NDVI change magnitude threshold of -0.065, overall accuracy was estimated to be 78%, and both producer's and user's accuracy of the disturbance class were estimated to be 73%. The method and results presented here are relevant to tropical countries engaged in REDD+ for whom data availability and complex forest change dynamics limit the ability to reliably track forest disturbances over time.

2.1 Introduction

With deforestation in the tropics accounting for upwards of 20% of global CO_2 emissions (Gullison et al., 2007), mitigation efforts against global climate change must include considerations to reduce tropical deforestation and forest degradation. To this end, international climate negotiations include the development of a mechanism aimed at the "Reduction of Emissions from deforestation and degradation and considerations for conservation, enhancement of carbon stocks", commonly known as REDD+. For a results-based mechanism such as REDD+ to be successful, countries are required to establish robust Measuring, Reporting and Verification (MRV) systems with which to report forest changes and impact of REDD+ activities.

A key component of a REDD+ MRV is the assessment of activity data - the area of forest undergoing change processes, including deforestation, forest degradation, and forest regrowth (Penman et al., 2003). To support REDD+ MRV and other efforts to conserve tropical forest resources, participating countries need to establish robust forest monitoring systems to track activity data at regular time-frames (Holmgren & Marklund, 2007). Remote sensing based approaches play a key role in forest monitoring, as they provide the best opportunity for mapping forest area change over large areas (Herold & Johns, 2007; De Sy et al., 2012; DeVries & Herold, 2013; Sanz-Sanchez et al., 2013). To date, only few remote sensing based forest monitoring systems exist in tropical countries, the most advanced of which are the PRODES and DETER systems of the Brazilian Space Agency (INPE), used for annual deforestation mapping and near real-time deforestation monitoring, respectively (INPE, 2014a,b). Considerable advancements in monitoring capacities are needed for other tropical countries to establish similar forest monitoring systems (Romijn et al., 2012).

To track forest change over time, most change detection methods rely on the selection of imagery from key points in time, which necessitates the selection of appropriate imagery from the archive from which to derive change information. These bi-temporal change detection methods range from simple image differencing methods (Coppin et al., 2004) to statistically-based methods such as the Multivariate Alteration Detection method (Nielsen et al., 1998). An important constraint in the selection of imagery for such change detection methods is the loss of data due to a number of contaminations or errors. First, where bi-temporal change detection methods require that the source imagery be cloud-free for a gap-free change product, cloud cover presents a key constraint (Ju & Roy, 2008), especially in the tropics where cloud cover is frequently high (Mitchard et al., 2011). Second, other sensor-specific sources of data loss can present significant constraints to the selection of imagery for detecting change. Notably, the scan-line corrector (SLC) on board the Landsat 7 Enhanced Thematic Mapper (ETM+) failed in March 2003, resulting in the loss of approximately 22% of data from each scene (Zhang et al., 2007). While methods

exist to fill these gaps with data derived from other scenes or even other sensors (Zhu et al., 2012a; Chen et al., 2011), introduction of extraneous data (e.g. from other images) into the data processing chain can introduce additional errors into the processing chain (Bédard et al., 2008; Alexandridis et al., 2013). Introducing gap-filling or other data fusion methods into the preprocessing chain for bi-temporal change detection approaches can also introduce uncertainties related to the actual acquisition date of the source data, which can have implications on quantitative estimates of forest change (Pelletier et al., 2011).

Another potential drawback of using a bi-temporal change detection approach relates to the dynamic behaviour of vegetation over time. Basing change estimates on differencing between images at only two points in time risks interpreting natural phenological change as actual land cover change (Verbesselt et al., 2010; Zhu et al., 2012b). This problem is especially pronounced in tropical regions, where frequent cloud cover can severely limit the choice of imagery available per year, sometimes necessitating the use of non-anniversary imagery in change detection studies. Confusion between forest and non-forest spectral signatures can arise as a result of imagery from different seasons, which can lead to increased errors in the change classification result (Coppin et al., 2004).

With the opening of the U.S. Geological Service (USGS) Landsat data archive, large amounts of medium-resolution optical earth observation data have been made freely available to the public, which combined with continued advances in the field of cloud computing for geo-spatial data (Evangelidis et al., 2014; Lee & Kang, 2013) has allowed for high temporal resolution forest change monitoring at unprecedented spatial scales (Hansen et al., 2013). Similar developments in multi-temporal satellite image analysis have been previously realized in the case of coarse resolution datasets, including AVHRR (Cihlar et al., 1997, 2004; Pinzon & Tucker, 2014; Tucker et al., 2005) and MODIS (Roerink et al., 2000, 2003; Verbesselt et al., 2010; de Jong et al., 2013) time series data, based on their high return rates and rich historical archives. A number of temporal trajectory methods based on Landsat time series data have been developed in recent years to make more extensive use of the temporal domain. Some methods construct regular (e.g. annual) image composites to understand disturbance-recovery dynamics (Kennedy et al., 2010; Huang et al., 2010), while others use all available data to allow for considerations of more complex change dynamics, such as phenology (Zhu et al., 2012b) and transient forest changes (Broich et al., 2011). Despite the number of temporal trajectory change detection approaches recently published in the literature, many of these methods have been developed in temperate forests with relatively high data availability (Zhu et al., 2012b; Zhu & Woodcock, 2014; Kennedy et al., 2010; Huang et al., 2010). There are relatively few studies demonstrating these methods in tropical areas with lower data availability due to persistent cloud cover (Mitchard et al., 2011; Duveiller et al., 2008; Ernst et al., 2013) or excessive gaps in the Landsat archive (Broich et al., 2011).

While the monitoring of tropical deforestation at large spatial scales has been well documented and is largely operational (Achard et al., 2010), methods able to track small-scale deforestation at high temporal resolution are currently lacking. Small-scale deforestation driven by small-holder subsistence agriculture is a prominent forest change process found in sub-Saharan African countries (Fisher, 2010; Potapov et al., 2012; Joseph et al., 2013). Monitoring these small changes is essential for such countries to play a role in climate change mitigation and to implement forest protection measures. Much of the research done on deforestation in tropical Africa has been undertaken in central Africa, where small-scale forest changes have been mapped using multi-temporal segmentation (Duveiller et al., 2008; Ernst et al., 2013), classification of annual Landsat time series (Hirschmugl et al., 2014), or analysis of all available Landsat ETM+ data (Potapov et al., 2012). Persistent small-scale changes in these landscapes (usually related to small-holder agricultural expansion) are a major constraint to the accurate mapping and accounting of deforestation (Tyukavina et al., 2013).

In this paper, we describe a robust and novel approach to monitoring forest disturbance in the tropics using Landsat time series data using the Breaks For Additive Season and Trend (BFAST) Monitor method (Verbesselt et al., 2012). Recent work has been done to demonstrate this algorithm on Landsat times series for tropical forest monitoring using fused Landsat-SAR time series (Reiche et al., 2015a) or Landsat-MODIS time series (Dutrieux et al., 2015). The goal of this study was to investigate the suitability of the BFAST Monitor method to detect forest disturbances using Landsat time series data over a tropical montane forest system in southwestern Ethiopia. To this end, we addressed two objectives: (i) to test the method in an area with lower data density typical of tropical montane forest systems experiencing regular cloud cover; and (ii) to develop an approach to track small-scale forest disturbances characteristic of changes driven by small-holder agriculture expansion in the tropics. The monitoring approach demonstrated in this study and described in this paper can serve a number of purposes, including acting as a key component in REDD+ monitoring systems (Sanz-Sanchez et al., 2013).

2.2 Study Area

2.2.1 Geographic and Biophysical Characteristics

This study was carried out in the UNESCO Kafa Biosphere Reserve (http://www.kafa-biosphere.org), located in the Afromontane forests in Southern Nations Nationalities and People's Region (SNNPR) state of southern Ethiopia. Due to availability of very high resolution (VHR) reference imagery, we focused our research on a subset of the Biosphere Reserve, bound by 7.22°E to 7.84°E and 35.59°N to 37.17°N (Figure 2.1). The Biosphere is comprised of three zones related to forest management: core (protected forest area), buffer

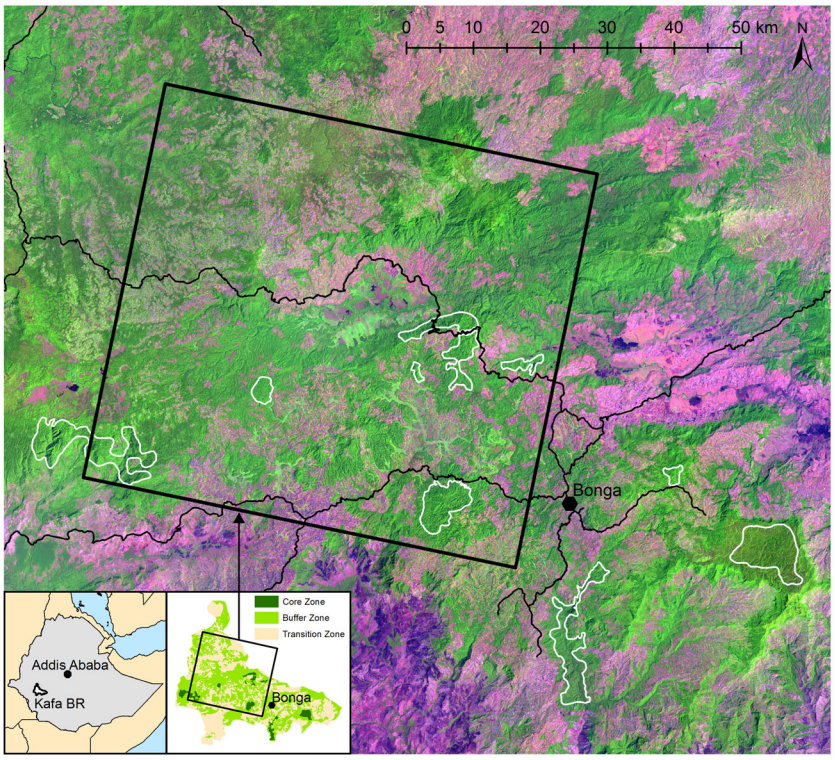

Figure 2.1: Overview of the study area, located in the UNESCO Kafa Biosphere Reserve in southwestern Ethiopia. Core, buffer and transition forest areas are indicated in the bottom inset. The footprint of the SPOT5 time series from K-J coordinates 133-335 is shown as a black rectangle. White outlines indicate core forest protection areas. The base image is a band 5-4-3 composite of an ETM+ image (WRS-2 p170r55) from 2001-02-05.

(forest with mixed land use) and transition (agriculture landscape with forest patches). The area is characterized by vegetated mountains ranging from an altitude of 1400m to 3000m. Approximately half of the area is covered with fragmented moist broadleaf evergreen forests, and the rest of the area is characterized by patchy cropland-forest matrix landscapes. Small-holder agriculture is the major driver of forest loss with coffee being a major crop for both small-holder farmers and investors alike (Schmitt et al., 2010b).

The Kafa Biosphere Reserve experiences a humid tropical climate, with a mean annual temperature in the region of approximately 19°C (Schmitt et al., 2010a). According to daily rainfall data acquired from the Tropical Rainfall Monitoring Mission (TRMM), average annual rainfall between 1998 and 2013 is approximately 1700mm, which is comparable to estimates based on local climate stations (Schmitt et al., 2010a). Rainfall is distributed in a unimodal pattern throughout the year, with one dry and one wet season per year.

2.2.2 Drivers of Deforestation in Southern Ethiopia

Despite the relatively low forest cover, deforestation and forest degradation in Ethiopia is a pressing issue that has implications that reach beyond climate change, threatening endemic biodiversity and valuable genetic resources (Teketay, 1997; Hein & Gatzweiler, 2006). Land use change studies in several sites of Ethiopia have revealed high rates of natural forest cover loss since the 1950's in Southern Ethiopia (Assefa & Bork, 2014; Getahun et al., 2013; Tadesse et al., 2014b), the Blue Nile watershed (Gebrehiwot et al., 2013) and the Central Rift Valley (Garedew et al., 2009). These studies attributed high rates of deforestation and forest degradation to agricultural expansion, decrease in crop yields and rising fuelwood demand stemming from an increasing population. Tadesse et al. (2014b) partially attributed forest loss in the Kafa and Sheka zones of Southwestern Ethiopia to land redistribution and resettlement programmes. In addition to agricultural expansion and fuelwood harvesting, coffee cultivation is an important driver of forest change in Southern Ethiopian forest ecosystems (Aerts et al., 2011), and the increasing intensity of coffee cultivation systems represents a major threat to the remaining native Afromontane forests (Schmitt et al., 2010b; Tadesse et al., 2014a).

2.3 Data and Methods

2.3.1 Data acquisition and preprocessing

An overview of the methods used in this study is shown in Figure 2.2. We downloaded all available Landsat ETM+ with WRS-2 coordinates p170r55 at processing level L1T and cloud cover below 70% from the USGS Glovis repository (http://glovis.usgs.gov). On average, 9 ETM+ scenes were available per year until 2011, with fewer scenes in 1999, 2000 and 2008 in particular (Table 2.1). To convert raw imagery from digital number (DN) to Top of Atmosphere (ToA) Reflectance and Surface Reflectance (SR), we used the LEDAPS method (Masek et al., 2006b), which is based on the 6S radiative transfer method (Vermote et al., 1997). We used the object-oriented FMASK algorithm (Zhu & Woodcock, 2012) to detect clouds and cloud shadows subsequently masked these out of the images. After removing cloud-contaminated and SLC-gap pixels, we estimated the number of clear-sky observations throughout the period 1999 to 2012 for each pixel (Figures 2.3 and 2.A1). An average of 55 clear-sky observations were available per pixel during this time period. Areas in which the least amount of data were available were associated with high-altitude areas with frequent cloud cover.

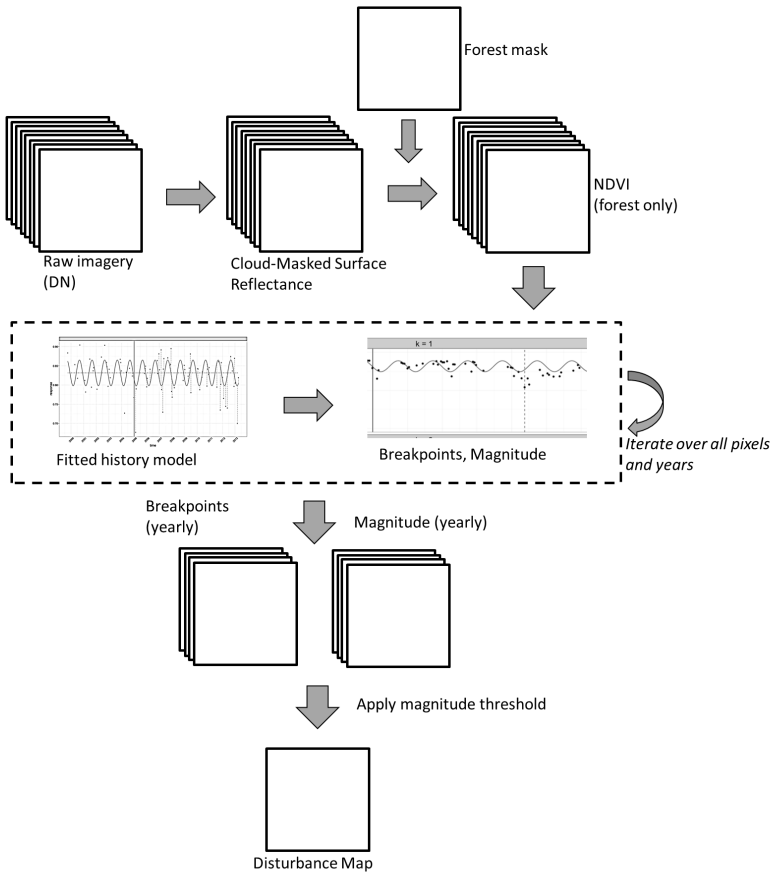

Figure 2.2: Flowchart used in this study. Rectangles represent image layers resulting from processing steps.

2.3.2 Benchmark forest mask

To avoid confusion between forest disturbances and other land cover dynamics (e.g. cropping cycles), we produced a benchmark forest mask for 2005 representing all forested pixels at the beginning of the study period. We selected a base image from the 4$^{\text{th}}$ of March, 2005 and another image from the 1$^{\text{st}}$ of December, 2005 to fill gaps left by the failure of the SLC-corrector (following Zhu et al. (2012a)). We classified the resulting gap-filled image using a supervised maximum likelihood classifier in the ArcGIS 9.2 software package (ESRI, inc.). Our initial land cover map included forest, cropland, wetland, shrubland, bare soil, plantations and urban classes. We aggregated all non-forest classes to produce a binary forest/non-forest mask. To avoid high commission errors arising from patchy mosaic transitional areas (including, for example, cropland demarcated with planted trees), we further refined the forest mask by masking out all pixels with a tree

Table 2.1: Number of scenes and mean and standard deviation clear sky pixel observations across the study area for each year included in this study. Only pixels included in the 2005 benchmark forest mask were included in the means and standard deviations.

year	# scenes	mean obs.	s.d. obs.
1999	2	0.49	0.60
2000	3	1.44	0.77
2001	5	3.68	1.33
2002	9	4.33	1.55
2003	10	4.43	1.70
2004	9	3.89	1.64
2005	9	4.10	1.57
2006	10	3.83	1.82
2007	16	7.39	2.95
2008	6	3.44	1.45
2009	9	3.82	1.76
2010	12	5.56	2.27
2011	12	3.87	2.02
2012	11	4.87	1.72

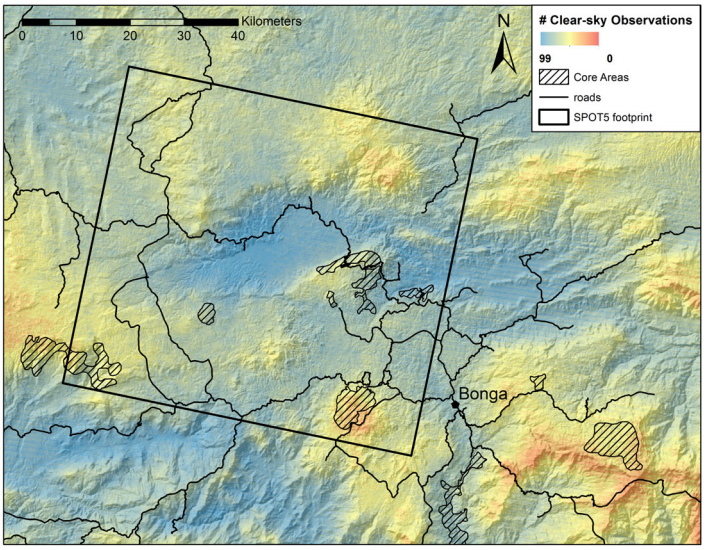

Figure 2.3: The number of clear-sky ETM+ observations between 1999-2012 for each pixel overlaid onto a hill-shade layer derived from an SRTM DEM.

cover of less than 30% according to the corresponding MODIS VCF product for 2005 (MOD44B; Hansen et al. (2003)). Finally, we masked all non-forest pixels according to our 2005 forest mask out of all images in the time series, and produced an NDVI image stack from the resulting imagery.

2.3.3 Breakpoint detection in Landsat time series

To detect forest disturbances, we applied a pixel-wise time series method based on the BFAST monitoring approach described in Verbesselt et al. (2012). Our approach follows three main steps to classifying changes in each of the pixels included in the benchmark forest mask: (1) fitting a harmonic model based on observations within a defined history period; (2) testing observations in the monitoring period directly following the history period for structural breaks from the fitted harmonic model; and (3) calculating the median of the residuals for all expected and actual observations within the monitoring period. These steps are described in more detail below.

1) Fitting the harmonic model. We divided each pixel time series defined by $t_i \ \epsilon \ [t_1, t_N]$ into a history period and a monitoring period. For a monitoring period beginning at time t_n, we defined the history period as the period where $t_1 \leq t_i < t_n$ and the monitoring period as the remainder of the time series, in which $t_n \leq t_i \leq t_N$ (see Figure 2.4 for an illustration of these time variables). We assumed that forested pixels were generally stable in the period leading up to the beginning of the monitoring period (t_n). As such, we fit a harmonic model (Verbesselt et al., 2012) to all observations in the history period:

$$y_t = \alpha + \gamma sin(\frac{2\pi t}{f} + \delta) + \varepsilon_t \tag{2.1}$$

where y_t and t are the response (dependent variable) and time (independent variable), f is the temporal frequency, α is the intercept, γ, and δ are the amplitude and phase of the harmonic component, and ε_t is the residual (noise component). Our time series model differed from that of Verbesselt et al. (2010) and Verbesselt et al. (2012) in two important aspects. First, we employed a simple single-order model (Equation 2.1) given the fact that forest phenology in the study area followed a similar first-order harmonic curve (Figure 2.4). Moreover, complex seasonal patterns were not expected to be detectable with Landsat data alone in our study area, due to the irregularity of clear-sky observations within a given year, and any attempt to model these processes resulted in model over-fitting. Second, we omitted the trend term from the fitted model. Even in cases where forest regrowth in the history period might justify the inclusion of a trend, projecting this trend into the monitoring period resulted in unrealistically high expected NDVI values, generating false breakpoints and inflated change magnitude values.

We fit the harmonic model independently for each pixel time series using Ordinary Least Squares (OLS) to determine the model of best fit, as described in more detail in Verbesselt et al. (2012). Given the short length of the history period, a result of a lack of Landsat data before the launch of ETM+ in 1999, we chose to include all observations in the history period in the model fitting process, in contrast to the stable history model employed by Verbesselt et al. (2012).

2) Detecting change. To detect breakpoints in pixel time series, we used the approach described in Verbesselt et al. (2012) for monitoring structural changes, in which moving sums (MOSUM) are computed using all observations in the monitoring period. Thus for all $t_n \leq t_i \leq t_N$, the MOSUM (MO_t) was determined by:

$$MO_t = \frac{1}{\hat{\sigma}\sqrt{n}} \sum_{s=t-h+1}^{t} (y_s - \hat{y}_s) \tag{2.2}$$

where y and $\hat{y}$ are actual and expected observations, respectively, and $\hat{\sigma}$ is an estimator of the variance (Zeileis et al., 2005). The MOSUM bandwidth, h, is defined as a fraction of the number of observations in the history period (n) (Verbesselt et al., 2012). A breakpoint is signaled when $|MO_t|$ deviates from zero beyond a 95% significance boundary as described in Verbesselt et al. (2012) and Leisch et al. (2000). We assigned a value of $0.25n$ to h throughout this study.

3) Computing change magnitude within the monitoring period. We computed change magnitude (M) by taking the median of residuals within the monitoring, in which $t_n \leq t_i \leq t_N$:

$$M = median\{y_t - \hat{y}_t\} \tag{2.3}$$

where y_t and $\hat{y}_t$ are actual and expected observations, respectively. While this measure is closely related to the criterion used for the MOSUM test (Equation 2.2), the median of the residuals is expected to be less sensitive to noise in the monitoring period than the sum (as in the MOSUM test), and thus provides an added insurance against spurious breakpoints. As the length of the monitoring period is increased, this measure of change magnitude could be affected by an increased number of observations before and after the change event. For this reason, we chose to limit the monitoring period to one year and applied the monitoring method described here in an iterative fashion, using sequentially defined monitoring periods (2005-2006, 2006-2007, and so on). For each monitoring period, we trimmed the time series such that t_N was equal the date of the final observation within the 1-year monitoring period. The sequential monitoring approach we described here is demonstrated in Figure 2.4.

2.3.4 Sample-based reference dataset

We centred our validation approach on changes in 2009 to ensure availability of enough high-resolution observations before and after to assess changes (Table 2.2). We constructed a reference dataset using a stratified random sampling approach from two populations of pixels: (1) those having breakpoints assigned in 2009 (and not in previous monitoring periods, to prevent assessing redundant change pixels); and (2) those having no breakpoints assigned in any monitoring periods up to and including 2009. Both populations were stratified into three magnitude quantiles, resulting in a total of six strata from

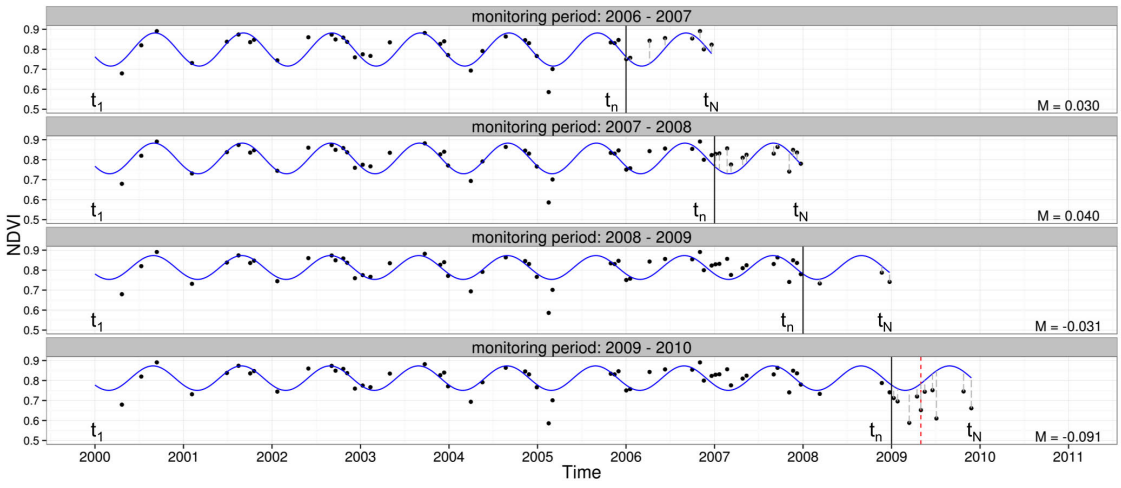

Figure 2.4: Demonstration of the sequential monitoring approach used in this study. In this illustration, results of a series of sequential 1-year monitoring periods from 2006 to 2009 (from top to bottom). The presence or absence of a breakpoint (dotted red line) and magnitude (M) are shown on each plot. The residuals, defined as the difference between observed values (black dots) and expected values (blue line) are shown as broken grey lines in each monitoring period. The solid black line denotes both the beginning of the monitoring period and the end of the history period.

which roughly equal numbers of pixels were selected. After removing 19 pixels lacking enough data to confidently classify disturbances (e.g. due to excessive cloud cover in the high resolution data), the reference dataset consisted of a total of 112 breakpoint pixels and 109 non-breakpoint pixels.

To classify changes in the randomly sampled pixels, we used a combination of Landsat time series and very high resolution (VHR) imagery. First, we viewed time series of Landsat RGB composites (using both bands 3-2-1 and 7-4-5 composites) in 35 x 35 pixel windows following Cohen et al. (2010) to identify potential disturbance events. Second, we complimented the Landsat time series with anniversary 2.5m resolution SPOT5 imagery from 2007 until 2011 inclusive (Table 2.2) to confirm change classes. We chose a relatively cloud-free image from 2009 from the SPOT5 dataset to be co-registered to an orthorectified Landsat image, and registered all other SPOT5 images to that image. Where available, we complemented the SPOT5 time series data with RapidEye imagery from 2012 and 2013, and GoogleEarth imagery from 2012 and 2014 (based on SPOT5 and DigitalGlobe imagery). Cases of deforestation were possible to identify with the Landsat time series and were confirmed with the VHR datasets. In cases of degradation, we flagged potential degradation in the Landsat time series and assigned a visual estimate of canopy cover (a value between 0 and 1) to each of the available SPOT5 images for that location. According to the definition of forest employed in this study, we assigned a degradation label to the pixel when a change was evident but estimated canopy cover from the VHR

Table 2.2: High resolution imagery used for validation of change results.

sensor	scene ID	date
SPOT5	133-335	2007-11-02
		2009-01-12
		2010-01-01
		2011-03-24
	132-334	2011-02-05
	132-335	2011-02-05
RapidEye	3742502	2012-01-05
		2012-10-17
	3642428	2012-12-12
	3642528	2012-12-12
	3642627	2012-12-12

images did not drop below 0.2 (e.g. Figure 2.9).

We calculated total accuracy (TA), user's accuracy (UA; inversely related to commission errors) and producer's accuracy (PA; inversely related to omission errors) using these reference data. Our accuracy estimates were limited to disturbance and non-disturbance classes, where disturbance included both the deforestation and degradation classes described above.

2.3.5 Modeling the effect of breakpoints and magnitude on disturbance probabilities

Since breakpoints are sometimes associated with near-zero or positive magnitudes which are not related to forest disturbances, commission errors are high when the presence or absence of breakpoints is used as the sole criterion for change labeling. Detected breakpoints are therefore not sufficient criteria for classifying change and the magnitude must also be factored into the classification. We used an ordinal logistic regression (OLR) modeling approach (Walker & Duncan, 1967) to further understand the relationship between magnitude and varying degrees of disturbances found in the study area. We used three classes as ordered response variables in the OLR models: deforestation, degradation and no change.

The OLR model takes the general form:

$$P(Y \geq j|X) = \frac{1}{1 + e^{-\alpha_j + X\beta}} \tag{2.4}$$

where $P(Y \geq j|X)$ is the cumulative probability of class j given a measured covariate X,

α_j is the intercept for each class j, and

$$X\beta = \beta_1 X_1 + \ldots + \beta_k X_k \tag{2.5}$$

for k covariates X. By solving for model coefficients β using the Maximum Likelihood (ML) method, a model for likelihood of each class j can be constructed. Rearranging equations 2.4 and 2.5, the model takes on the linear form:

$$logit(Y \geq j|X) = \alpha_j + \beta_1 X_1 + \ldots + \beta_k X_k \tag{2.6}$$

where:

$$logit(Y \geq j|X) = log(\frac{P}{1-P}); P = P(Y \geq j|X) \tag{2.7}$$

We tested two models describing the response of the three ordered classes to several predictor variables. The first model related P (as defined in Equation 2.7) as a function of magnitude (M) and the second model related P as a function of M and breakpoints (C). We compared these models using chi-squared probabilities (compared to a null intercept-only model) and the Akaike Information Criterion (AIC) (Akaike, 1973), which is a measure of goodness of fit and includes a penalization for additional parameters to prevent model over-fitting.

2.4 Results

2.4.1 Robustness of the MOSUM breakpoints test

The MOSUM breakpoint test proved effective in discriminating deforestation events from stable forest trajectories in the presence of noise and data gaps in the time series data. Discrete deforestation events (Figure 2.5B) resulted in a sudden and persistent decrease in NDVI, whereas stable forests were largely free of breakpoints (Figure 2.5A). Forests undergoing degradation intense enough to cause canopy openings also led to breakpoint detection (Figure 2.5C), even though some degree of seasonality due to the remaining forest canopy was still present in the follow-up time series. In regions where low availability of clear-sky observations caused the pixel time series to be irregular, our method was still able to capture forest changes in most cases (Figure 2.6).

2.4.2 Relationship between magnitude and forest change processes

The examples shown in Figure 2.5 demonstrate the differences in magnitude ($\Delta NDVI$) commonly observed between varying degrees of forest change intensity. Here, a stable forest pixel with no breakpoint detected in the monitoring period (A) had a magnitude of

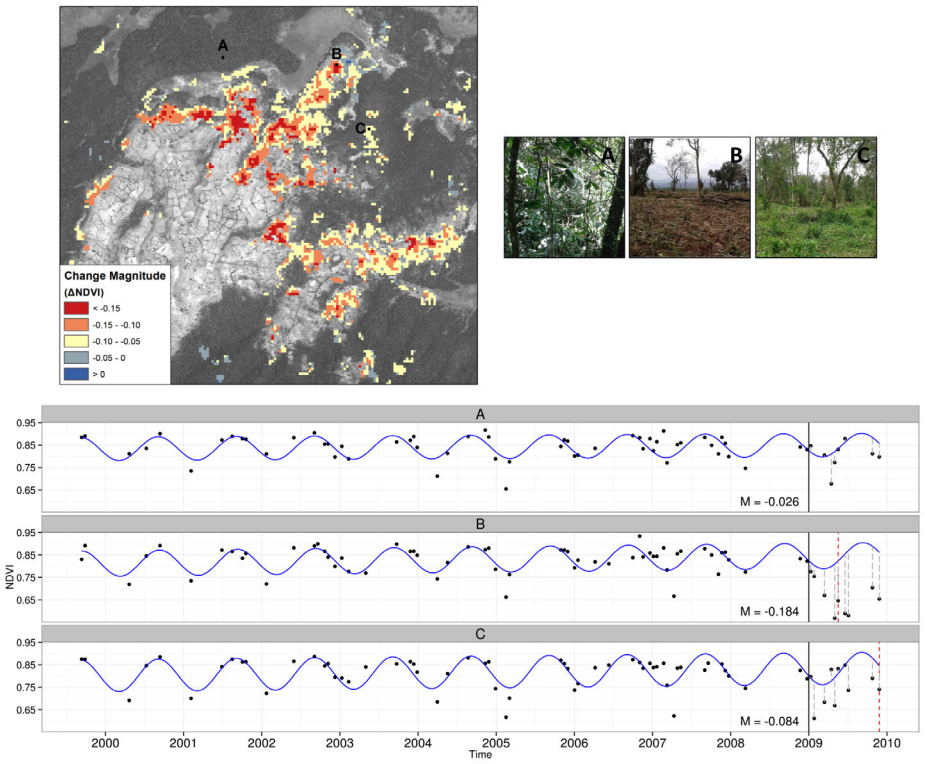

Figure 2.5: Results from the 2009-2010 monitoring period (left panel), chosen to illustrate different change processes. Change magnitude for all pixels with breakpoints are shown overlaid on a greyscale SPOT5 image (band 2) from February 2011. Time series plots for intact forest (A), deforestation and subsequent cropping (B), and progressive canopy clearing (C). Photos taken in April 2013 from areas in the neighbourhoods of each corresponding pixel are also shown.

-0.026, a pixel where a discrete forest clearance event occurred (B) had a breakpoint and a magnitude of -0.18, and a pixel where progressive reduction of canopy cover (C) had a breakpoint and a magnitude of -0.084.

Figure 2.7 shows the magnitudes for sequential monitoring periods (top panel) compared to a SPOT5 time series (bottom panel) corresponding to each monitoring period over an area experiencing progressive forest loss over this time period. In 2008, very few changes were detected in this area and the SPOT5 imagery shows mostly full canopy cover. By 2009, several discrete forest perforations appeared which correspond with high-magnitude pixel clusters in the BFM results. By 2011, most of this entire region had been cleared and converted to cropland, but due to cloud cover in the SPOT5 image from 2010 (not shown), it was not possible to ascertain visually when this change exactly happened. The magnitude shown in the top panel of Figure 2.7 reveals that most of the area surrounding this perforation was cleared within the 2009-2010 monitoring period.

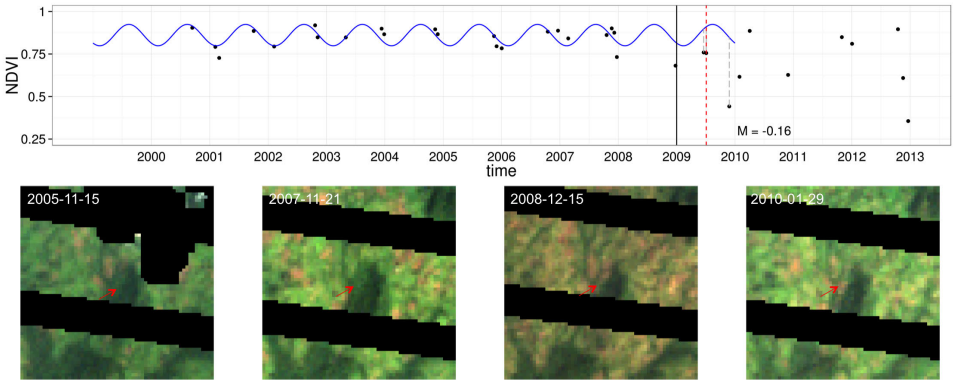

Figure 2.6: Example of a small change correctly identified in the 2009-2010 monitoring period, despite an irregular time series with frequent gaps. Landsat 3-2-1 composites for four key dates are shown below the time series plots. The Landsat pixel for which time series plots are shown is indicated by a red arrow. Pixels masked out using the FMASK product are shown in black.

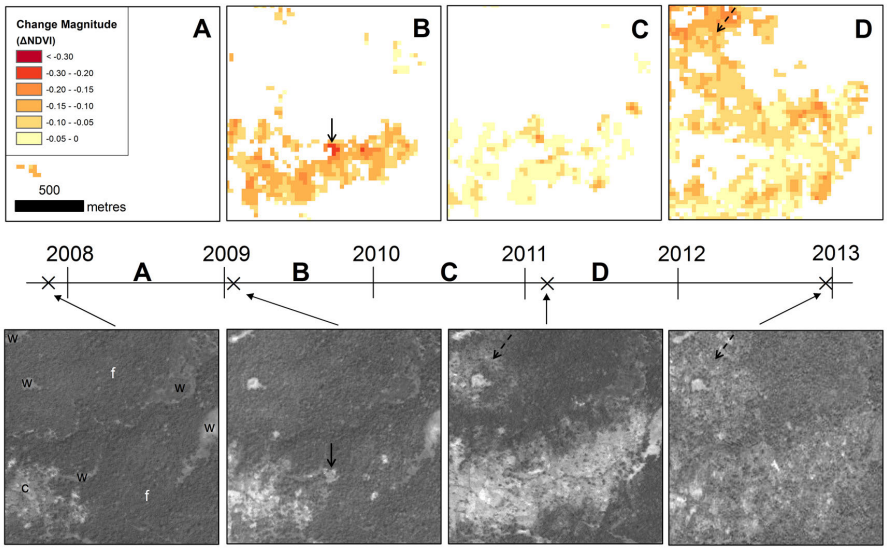

Figure 2.7: Magnitude values for annual monitoring periods between 2008 and 2012 (labeled from A to D, respectively) with SPOT5 images acquired between 2007 and 2011 and one RapidEye image acquired in 2012. The change magnitude in the top panel is only shown for pixels for which a breakpoint with negative magnitude in that monitoring period was detected. Land cover types in the initial SPOT5 image (bottom left) are labeled for forest (f), wetland (w) and cropland (c). An example of discrete deforestation is shown as a solid arrow and an example of gradual clearing is shown as a broken arrow.

2.4.3 Predicting forest disturbances using breakpoints and magnitude

The ordinal logistic models (OLR) relating the cumulative probability (P) of each of the change classes (deforestation, degradation or no-change) as a function of magnitude (M)

Table 2.3: Stepwise comparison of ordinal logistic regression models including magnitude only or breakpoints and magnitude to the null model (intercept only).

regressors	residual d.f.	residual deviance	P(χ^2)	AIC
(null)	201	383.2	–	387.2
magnitude	200	304.7	<0.0001	310.7
magnitude, breakpoint	199	299.7	0.025	307.7

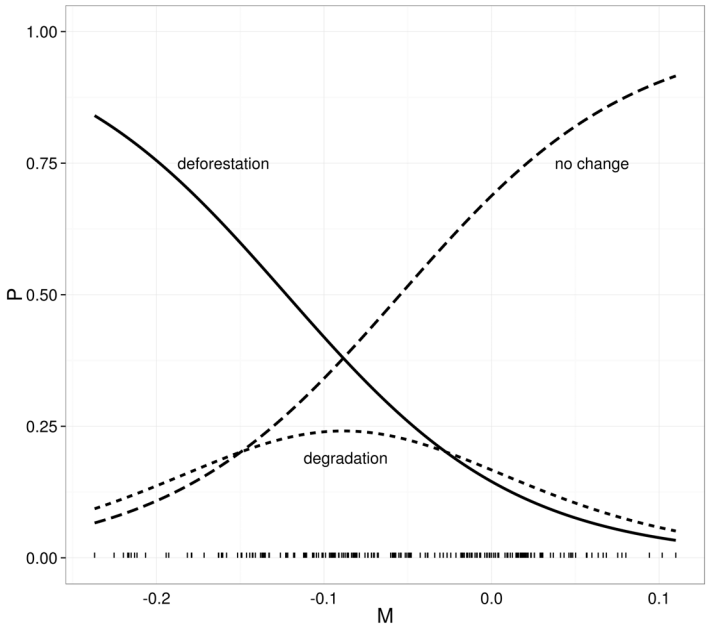

Figure 2.8: Ordinal logistic regression (OLR) model including magnitude and breakpoints for three disturbance classes: "deforestation", "degradation" and "no change". The probability of each class (P) is shown on the y-axis as a function of magnitude (M) on the x-axis. The distribution of reference observations are shown as small segments along the x-axis.

showed that M was a significant predictor of P, both in the presence or absence of a breakpoint (C) as a second binary regressor. Introducing C to the model resulted in a slight decrease in the AIC (from 326.6 to 305.9; Table 2.3), but had otherwise little effect on the fitted model. The probability distribution for each of the disturbance classes (deforested, degraded, no-change) is shown in Figure 2.8. The probability of the deforestation class increased with decreasing magnitude, while the probability of the no-change class increased with decreasing magnitude. The probability of the degradation class showed a weak relationship with magnitude, with a slight peak at approximately $M = -0.1$, but did not exceed probability of the other classes for any values of M.

The total accuracy (TA) and user's and producer's accuracy of the disturbance class (UA and PA, respectively) are shown for a range of magnitude thresholds in Figure 2.10 for disturbances classified using magnitude only (left panel) and magnitude and breakpoints

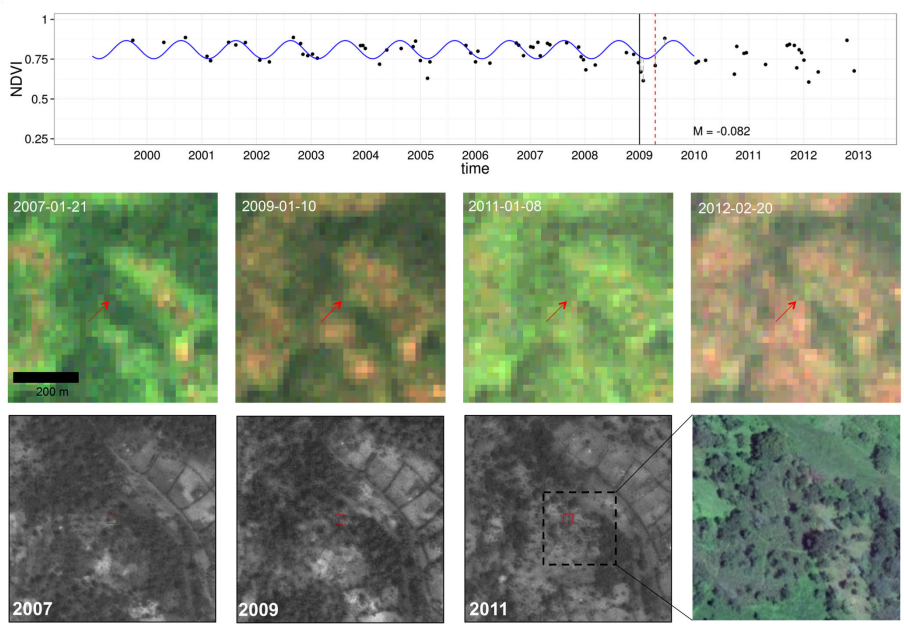

Figure 2.9: Example of degradation, where canopy cover is visibly reduced without complete conversion to non-forest. Landsat images are shown as band 3-2-1 composites in the top panel. SPOT5 images for the same extent are shown in the 2nd row, with a GoogleEarth™ image (DigitalGlobe, 2012) in the last panel. The time series plot (top) is shown for monitoring period 2009-2010.

(right panel). Here, disturbances were defined to include both deforestation and degradation. A maximum TA of 79% was achieved in both cases with a magnitude threshold of -0.080. The UA/PA cross-over point for the magnitude-only case occurred at a threshold between -0.075 and -0.080 and at -0.065 for the magnitude+breakpoint case. In both cases, the UA and PA were 73% at their cross-over points. In the latter case (which was selected as a final disturbance threshold), TA was estimated at 78%. Including breakpoints in the disturbance classification had a noticeable effect for magnitude thresholds approaching zero. Here, the decrease in UA was less severe when breakpoints were included in the disturbance classification and the PA leveled off at 81% instead of rising to 92% as in the magnitude-only case.

The UA and PA for the no-change class (not shown in Figure 2.10) were generally higher than all other accuracies. At the -0.080 threshold, UA and PA for the no-change class were 82% and 83% respectively when only magnitude was considered, and 81% and 85% respectively when breakpoints were included.

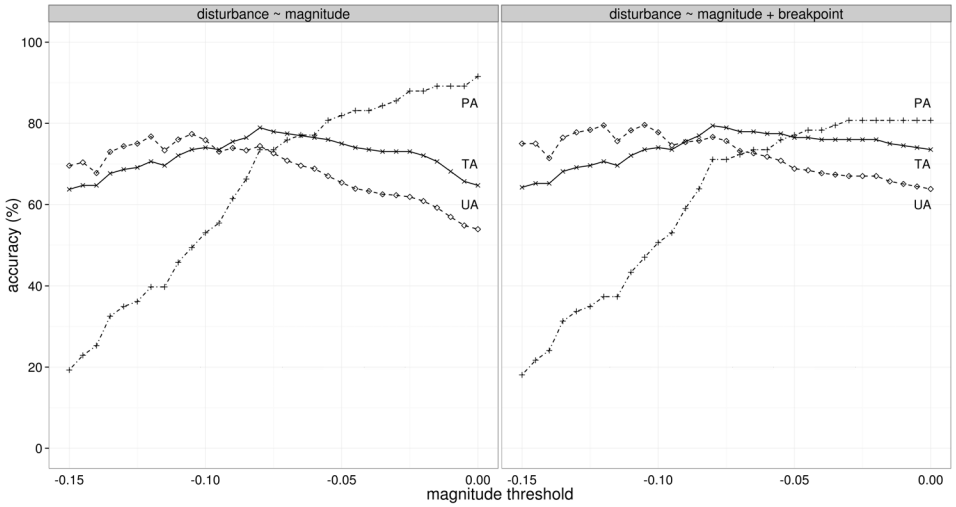

Figure 2.10: Total accuracy (TA) and producer's and user's accuracies for the disturbance class (PA and UA respectively) as a function of magnitude. Disturbance is defined as deforestation and degradation and modeled using magnitude only (left panel) or magnitude and breakpoints (right panel).

2.4.4 Area and spatial distribution of forest disturbances

We chose a magnitude threshold of -0.065 (corresponding to the cross-over point between UA and PA shown in Figure 2.10, right panel) to generate a final disturbance map (Figure 2.12). From this map, the total disturbed forest area was estimated to be over 11,000 hectares throughout the entire 2005-2012 period, representing roughly 3% of the total forest area in the Biosphere Reserve. In total, 0.84% of core zone forest, 2.1% of buffer zone forest, and 1.9% of transition zone forests were disturbed over this time period. Small incremental disturbances permeated the forest areas throughout this period. The mean size of disturbance pixel clusters was 0.6 hectares, with a maximum change cluster of 285 hectares.

2.5 Discussion

2.5.1 Forest change in the Ethiopian Afromontane forests

In this paper we present the first detailed study on forest disturbances in the Ethiopia Afromontane forests, in which we estimate total forest loss of roughly 11,000 hectares between 2005 to 2012 in the UNESCO Kafa Biosphere Reserve, representing approximately 3% of the total forest area. This deforestation rate corresponds to a loss of roughly 0.4% of forest land per year, which is comparable to change rates estimated by Getahun et al. (2013) for a neighbouring Afromontane forest area (0.19% between 1975 and 2007). Sim-

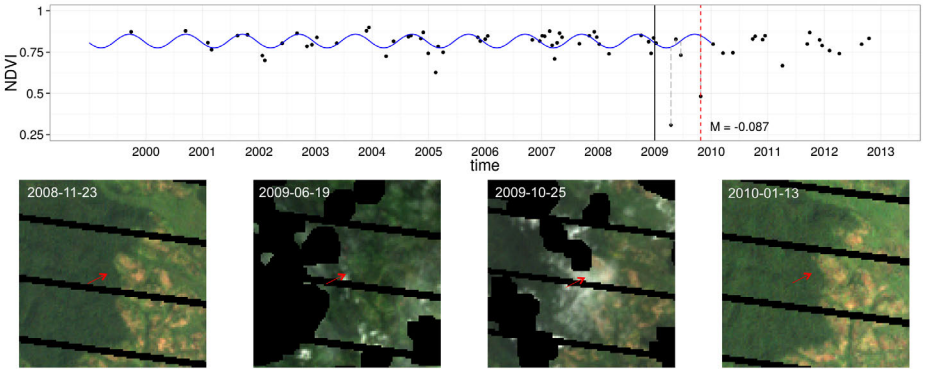

Figure 2.11: Example of a commission error arising from several unmasked clouds within one monitoring period (2009-2010). A Landsat 3-2-1 composite for four key dates are shown below the time series plots. The Landsat pixel for which time series plots are shown is indicated by a red arrow. Pixels masked out using the FMASK product are shown in black.

ilarly to Getahun et al. (2013), we found that forest change was largely small-scale and driven by small-holder agriculture and occurred at higher rates in more remote locations. We additionally note that in-migration of resettlers from other areas in Ethiopia (Figure 2.12A) was largely responsible for abrupt larger-scale changes in these remote areas.

The ability to describe these change processes with high temporal detail highlights the advantage of the time series curve-fitting approach used in this study over more conventional forest change detection studies conducted in Ethiopia (Getahun et al., 2013; Gebrehiwot et al., 2013; Garedew et al., 2009; Assefa & Bork, 2014). By making use of the magnitude parameter, we have shown that forest change does not typically occur as large discrete clearing events, but rather in an incremental manner (Figure 2.7). Discussions with local farmers in the study area revealed that clearing of a forest demarcated for agriculture is a process that can last up to several years, as forest is left standing in the first years and used for cattle grazing and harvest of forest resources (wild coffee and spices). During this time fuel-wood and timber is gradually harvested by hand, and local crops such as sorghum, tef are eventually cultivated in place of the forest.

2.5.2 Forest change tracking with sequential monitoring periods

We employed a sequential monitoring approach based on the BFAST monitoring method Verbesselt et al. (2012), where a harmonic curve was fit to a historical time series and a MOSUM test for monitoring change was applied to the Landsat time series stack using non-overlapping 1-year monitoring periods (Figure 2.4). The reason for defining equal monitoring period length was related to the output magnitude parameter. Magnitude is defined as the median of the residuals within a monitoring period between observations and expected values (based on the history period model; Equation 2.3). It was therefore

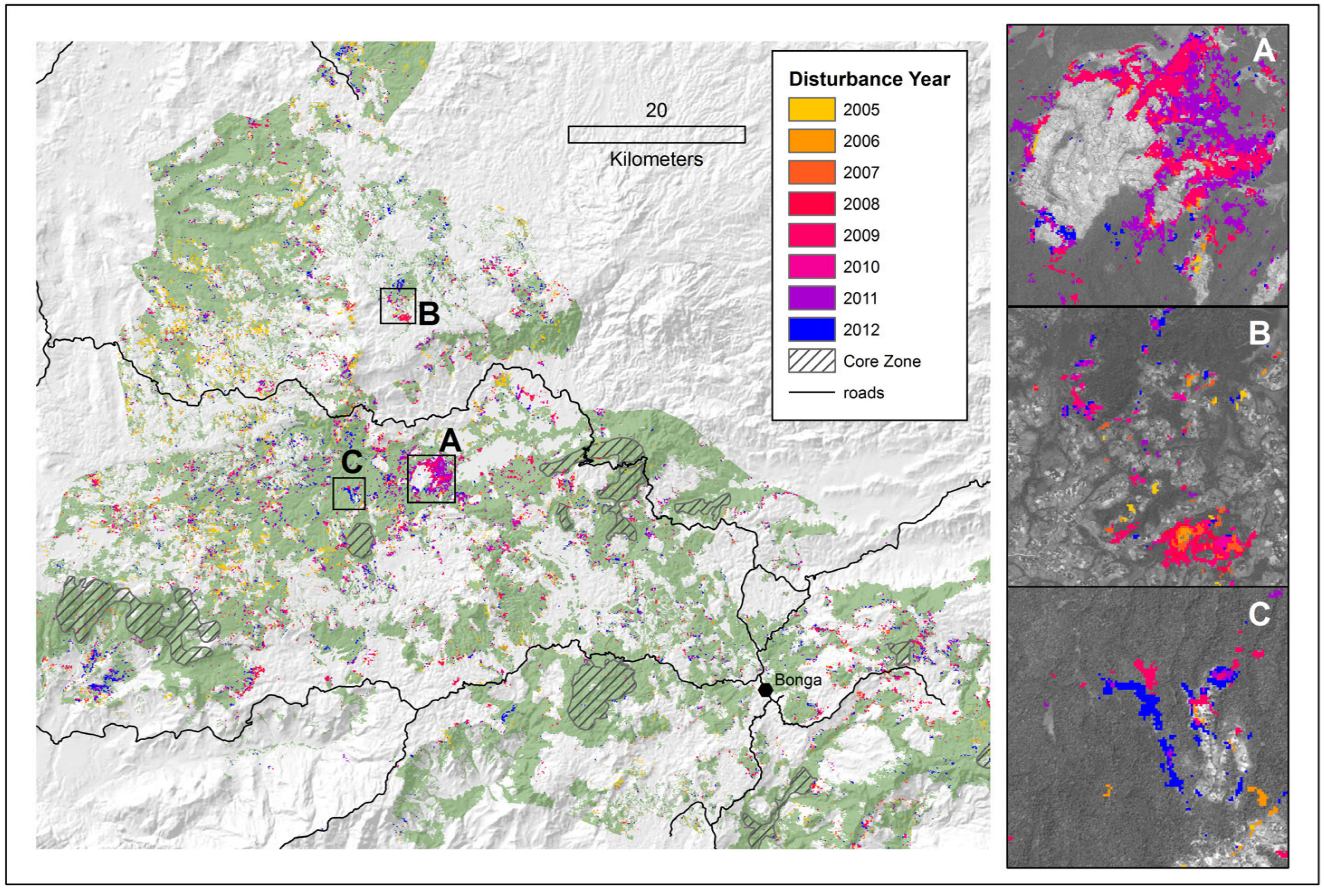

Figure 2.12: Forest change map produced using a magnitude threshold of -0.065. The predicted time of deforestation is shown both in the main panel and insets A to C, and areas of possible degradation are also shown in the insets. The original forest mask from 2005 (green) and core forest areas defined under the UNESCO Kafa Biosphere Reserve (hatched areas) are shown in the main panel. Three examples of different change processes occurring in the study area are shown in the insets (using a SPOT5 image from 2011 as a basemap), including in-migration from other parts of the country (A), gradual reduction of forest cover in forest-agriculture matrix landscapes (B) and construction of a rural road (C).

important to keep a consistent definition of the monitoring period, as change magnitude in longer monitoring periods would be affected by follow-up land use (e.g. seasonal changes due to cropping cycles after deforestation), and the metric would no longer be comparable across change processes. In the case of this study, we assumed that no significant follow-up changes occurred within the 1-year monitoring period, and that the change magnitude could therefore be explained by the specific change being observed in that year (rather than a combination of change and follow-up change processes).

In this study, we found that small-scale forest changes could be tracked using NDVI time series. It has been previously shown that NDVI is affected by saturation effects when forest cover is dense (Carlson & Ripley, 1997) and is less sensitive to forest changes than other metrics based on the short-wave infrared (SWIR) region of the electromagnetic spectrum (Zhu et al., 2012b; Kennedy et al., 2010; Jin & Sader, 2005). Despite these limitations, our approach relies not only on absolute difference between observations, but on structural breaks in the time series (Leisch et al., 2000; Verbesselt et al., 2012). As such, even a saturated NDVI signal followed by an altered seasonal NDVI curve (due to regenerating vegetation or follow-up cropping cycles, for example) would be sufficient for a breakpoint to be detected. The types of forest change encountered in this study resulted in a general decline in NDVI in cases of incomplete forest clearing (Figures 2.5C, 2.7 and 2.9) and a significantly altered harmonic curve in cases of complete conversion from forest to cropland (Figure 2.5B).

2.5.3 Modeling disturbance processes with breakpoints and magnitude

The ordinal logistic regression (OLR) model including breakpoint and magnitude as explanatory variables performed only slightly better than that of the model including only magnitude (Table 2.3). Both the AIC and the accuracies (Figure 2.10) show that addition of breakpoints as an additional predictor variable resulted in a slight improvement in accuracy. Adding breakpoints to the disturbance definition shifted the cross-over point of the UA and PA (Figure 2.10) to a higher magnitude threshold and reduced the commission errors that arise when the magnitude threshold approaches zero. In practice, all breakpoints with negative magnitudes could be defined as disturbances for the forest types featured in this study, but would only achieve accuracies on the order of 60%. We thus conclude that while magnitude alone is sufficient to predict disturbances for the montane forests in Southern Ethiopia, the best prediction is achieved using both magnitude and breakpoints.

The reliance on magnitude to detect disturbances has implications on the reproduction of our method in similar study areas. Rather than applying the curve-fitting and breakpoint detection algorithm in a purely data-driven manner, calibration of a magnitude threshold against reference data are needed to derive a final disturbance label. Similar work in

southern Peru has shown that with relatively large, discrete forest clearances, breakpoints are sufficient to detect disturbances when only negative magnitudes are taken (DeVries et al., 2015). The importance of magnitude in our study is thus related to the scale of disturbances experienced in the study. In areas with small-scale, incremental forest changes (e.g. due to small-holder agricultural expansion), the magnitude of the change is an essential variable for mapping disturbances.

2.5.4 Comparison with other time series curve-fitting methods

The approach we used in this study, based on previous work on MODIS time series (Verbesselt et al., 2010, 2012), joins the ranks of other recent methods using all available Landsat data to detect changes in forest cover (Zhu et al., 2012a; Broich et al., 2011; Ernst et al., 2013; Hansen et al., 2013). Of all the time series methods using all available Landsat observations for forest change detection, our approach is most similar to that of Zhu et al. (2012a). Both approaches use similar model-fitting approaches using historic data from each pixel, and subsequent time series data are checked against the fitted model for deviation from the fitted model. Our approach differs from that of Zhu et al. (2012a) in two aspects. First, our approach flagged potential disturbances using a MOSUM test for monitoring change in the monitoring period while accounting for seasonal variability (Verbesselt et al., 2012; Leisch et al., 2000), whereas Zhu et al. (2012a) flagged disturbances when residuals exceeded a multiple of the RMSE on several consecutive instances. Second, our method also features the calculation of a consistent magnitude metric independent of the presence or absence of breakpoints. In addition to being an essential predictor variable of disturbances in our study area (Table 2.3), the magnitude allowed for mapping of incremental changes over time (Figure 2.7).

2.5.5 Sources of errors

The two major sources of error arising from this study were unmasked clouds or cloud shadows and errors arising from the benchmark forest mask.

Unmasked clouds or cloud shadows

Occasional unmasked clouds or cloud shadows resulted in greatly reduced NDVI values for those pixels. The method used in this study featured two safeguards against these types of noise in the monitoring period. First, a single outlier observation was unlikely to trigger a breakpoint, as the MOSUM value is a sum of all observations within a moving window (Equation 2.2). Second, the magnitude was calculated as the median of all residuals within the monitoring period (Equation 2.3), which is robust against single outliers. These safeguards became less effective with multiple occurrences of unmasked clouds or cloud

shadows within one monitoring period, as demonstrated in Figure 2.11. Persistent cloud cover (e.g. over mountain peaks in our study area, shown in Figures 2.3 and 2.A1) can thus present a significant challenge to the application time series based change detection methods in tropical montane forest systems (Broich et al., 2011).

Benchmark forest mask

Classification errors in the benchmark forest mask propagated through to the curve-fitting and MOSUM breakpoints test, leading to breakpoints resulting from non-forest related dynamics (e.g. cropping cycles). While our revised mask, modified using the the MODIS Vegetation Continuous Field (VCF) product (Hansen et al., 2003), was more conservative than the original Landsat-based classified mask, some of the disturbances shown in the first monitoring period (2005; Figure 2.12) may have arisen from mis-classified non-forest pixels in the benchmark year, causing them to be mis-labeled as deforestation in the initial monitoring period. On the other hand, changes occurring in small forest patches may have been omitted as a result of the application of the MODIS VCF mask, which would contribute to omission errors in the overall change result.

2.5.6 Other limitations

In addition to the error sources noted above, several other limitations encountered in this study warrant attention here.

Historical data availability

A common requirement of curve-fitting time series methods is the need for historical data from which to establish a "stable" reference model (Zhu et al., 2012b; Verbesselt et al., 2012). In many areas in the tropics, including southern Ethiopia, there is a near-complete lack of Landsat 5 observations in the 1990's (Broich et al., 2011). For this reason, the time series data used in this study were limited to Landsat 7 observations acquired after 1999 as in other similar studies in the tropics (Broich et al., 2011; Potapov et al., 2012). For many parts of the study area, there were not enough observations in the 1999-2005 period to monitor for changes in those periods. For example, the 2002-2003 monitoring period would require enough observations from 1999-2001 (inclusive) to fit a history model. The significant data gaps throughout the 1990's in the Landsat archive over our study area, combined with the need for a history period from which to fit the season model, presents a constraint to tracking historic changes, a prerequisite for establishing monitoring baselines for REDD+ (Olander et al., 2008; Kim et al., 2014).

Ability to map degradation

Even though we were able to identify several cases of degradation (e.g. Figure 2.9) and include them in the OLR model, there was a large spread in the relationship between probability of degradation and magnitude (Figure 2.8), both with and without breakpoints. For this reason, we could not conclusively determine a relationship between magnitude and probability of degradation. Several limitations to our approach contributed to uncertainties in degradation detection. First, as noted above, NDVI is known to be less sensitive to forest structure than other spectral indices. In addition to other ratio-based or transformation-based indices used for disturbance monitoring, sub-pixel un-mixing metrics, such as the Normalized Difference Fraction Index (NDFI) have shown promise in mapping degradation due to selective logging in tropical forest systems (Souza et al., 2005). However, the sensitivity of these indices to the types of degradation encountered in this study remains largely unexplored.

Second, the fact that our reference dataset was limited to visual interpretation of optical satellite imagery represents an additional imitation to our ability to assess the ability of our method to detect degradation. Combining the time series approach described in this paper with advances in forest monitoring methods, such as LiDAR (Zhuravleva et al., 2013; Thompson et al., 2013; Ahmed et al., 2014) and field-based monitoring methods (Gonsamo et al., 2013; Pratihast et al., 2014), can provide new opportunities for mapping and validation of low-intensity degradation processes. The integration of these monitoring technologies with Landsat time series for monitoring forest degradation is a topic for future research.

Finally, our inability to conclusively predict degradation was related to the low intensity of degradation processes in our study area, a constraint which has been reported in other areas in sub-Saharan Africa (Zhuravleva et al., 2013). Recent field studies have shown that fuelwood harvesting at the community scale is the dominant driver of forest degradation in Kafa (Pratihast et al., 2014; Dresen et al., 2014). The impact of degradation due to fuelwood harvesting remains invisible to optical satellites until its cumulative effects result in changes to the forest canopy (Pratihast et al., 2014; Herold et al., 2011).

Repeat disturbances

The method we used in this study does not allow for detection of follow-up regrowth and repeat disturbances, a similar limitation to that reported by Zhu et al. (2012b). We instead assumed that the earliest encountered breakpoint with magnitudes lower than the calibrated magnitude threshold represented a permanent change. Other trajectory-based approaches, on the other hand, monitor disturbance and follow-up regrowth in a holistic manner (Huang et al., 2010; Kennedy et al., 2010). To further develop our approach to include disturbance-regrowth dynamics, continued monitoring of forest regrowth and

iterative disturbance monitoring needs to be built into the algorithm (DeVries et al., 2015).

2.5.7 Implications for national monitoring activities

For the method presented in this paper to be applicable to a national-scale MRV and National Forest Monitoring System (NFMS) in Ethiopia, several key questions need to be addressed. The first question relates to the applicability of the method over all forest types in the country. Despite the fact that we have focused our research on the moist Afromontane forests of the south, we expect the method presented here to be applicable over all forest types, as it is robust to noise and data gaps. The second question relates to the impact of errors on overall CO_2 emissions estimates, a key requirement for REDD+ MRV. The accuracies estimated in this study indicate that despite the robustness of our method to noise and data gaps, the nature of forest change in our study area presents key challenges to reliably tracking changes over time. Similar challenges were encountered by Tyukavina et al. (2013), who noted considerable scale-related uncertainties in above-ground carbon stock changes in the Democratic Republic of the Congo due to the small-scale of forest changes there. Similarly, uncertainties arising from small-scale changes in our study area are expected to propagate through to forest area loss and carbon stock change estimates.

2.6 Conclusions

In this paper, we show that the BFAST Monitor method (Verbesselt et al., 2012) for breakpoint detection in time series is applicable to Landsat ETM+ time series data for forest disturbance monitoring for an area in Southwestern Ethiopia characterized by highly fragmented Afromontane forests. Using high resolution time series imagery as reference data, we estimated an overall accuracy of 78%, with associated user's and producer's accuracy of 73% for disturbances. Our results show that magnitude of residuals during the monitoring period is essential for mapping disturbances in the landscape featured in the study area, while MOSUM-based breakpoints slightly improved disturbance results. Applying the algorithm to Landsat time series allows for regular monitoring of the small-scale forest change processes characteristic of Ethiopia and other tropical countries where small-holder agriculture is the main driver of disturbance. Between 2005 and 2012, the mean disturbance cluster size was found to be 0.6 hectares, which demonstrates the scale at which this disturbance driver operates. A major constraint faced in this study was the fact that we could not quantitatively describe degradation processes, due to the small scale of degradation in the study area and limited data availability in the Landsat NDVI time series. The method was shown to be useful in monitoring of forest disturbances,

and given the opening and expansion of the Landsat data archive, could be a key asset to regions and countries developing REDD+ MRV and National Forest Monitoring Systems (NFMS).

Acknowledgements

We would like to thank Dr. Nikolaus Umlauf (University of Innsbruck) and Dr. Achim Zeileis (University of Innsbruck) for assistance with the ordinal logistic regression models, and Michael Schultz (Wageningen University) for assistance in pre-processing the SPOT5 data.

2.A Appendix: Clear-sky Observations

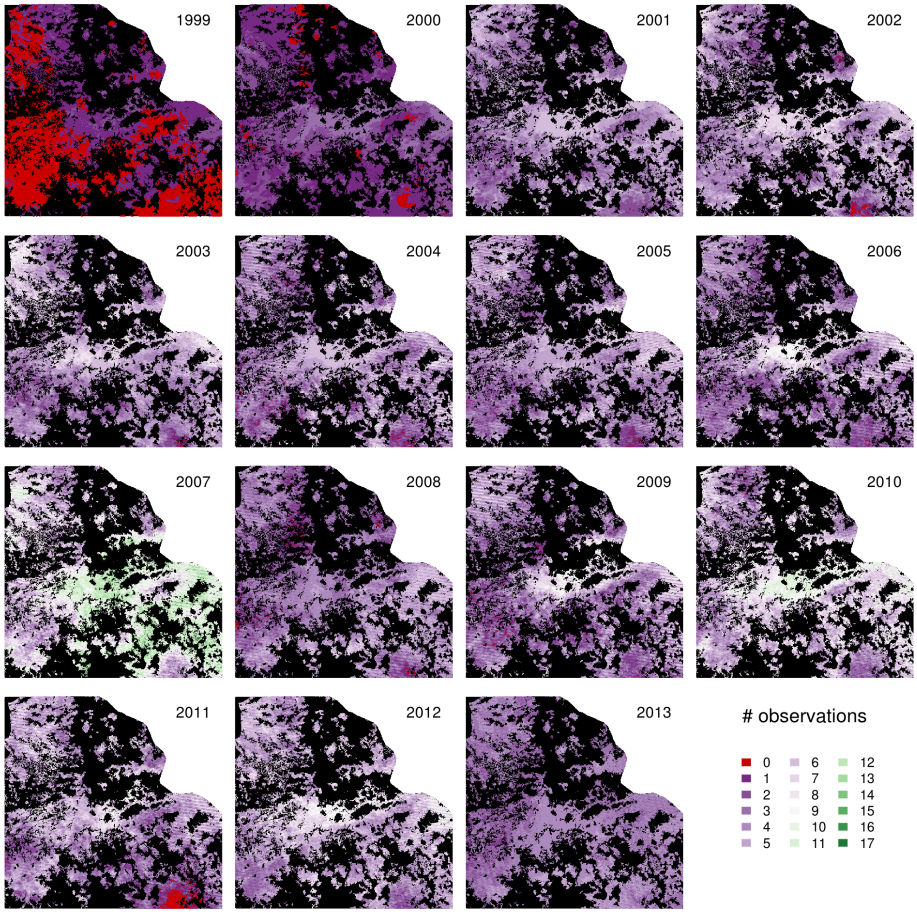

Figure 2.A1: Clear sky observations per year over a subset of the study area. Non-forest pixels according to the 2005 benchmark forest mask are shown in black.

Chapter 3

Tracking post-disturbance regrowth using Landsat time series

This chapter is based on:

DeVries, B., Decuyper, M., Verbesselt, J., Zeileis, A., Herold, M. & Joseph, S. 2015. Tracking disturbance-regrowth dynamics in tropical forests using structural change detection and Landsat time series. *Remote Sensing of Environment*, 169:320-334. doi:10.1016/j.rse.2015.08.020.

Abstract

Increasing attention on tropical deforestation and forest degradation has necessitated more detailed knowledge of forest change dynamics in the tropics. With an increasing amount of satellite data being released to the public free of charge, understanding forest change dynamics in the tropics is gradually becoming a reality. Methods to track forest changes using dense satellite time series allow for description of forest changes at unprecedented spatial, temporal and thematic resolution. We developed a data-driven approach based on structural change monitoring methods to track disturbance-regrowth dynamics using dense Landsat Time Series (LTS) in a tropical forest landscape in Madre de Dios, southern Peru. Whereas most existing post-disturbance regrowth monitoring methods rely on annual or near-annual time series, our method uses all available Landsat data. Using our disturbance-regrowth method, we detected annual disturbance from 1999 to 2013 with a total area-weighted accuracy of 91 $\pm$ 2.3%. Accuracies of the regrowth results were strongly dependent on the timing of the original disturbance. We estimated a total area-weighted regrowth accuracy of 61 $\pm$ 3.9% for pixels where original disturbances were predicted earlier than 2006. While the user's accuracy of the regrowth class for these pixels was high (84 $\pm$ 8.1%), the producer's accuracy was low (56 $\pm$ 9.4%), with markedly lower producer's accuracies when later disturbances were also included. These accuracies indicate that a significant amount of regrowth identified in the reference data was not captured with our method. Most of these omission errors arose from disturbances late in the time series or a lack of sensitivity to long-term regrowth due to lower data densities near the end of the time series. Omission errors notwithstanding, our study represents the first demonstration of a purely data-driven algorithm designed to detect disturbances and post-disturbance regrowth together using all available LTS data. With this method, we propose a continuous disturbance-regrowth monitoring framework, where LTS data are continually monitored for disturbances, post-disturbance regrowth, repeat disturbances, and so on.

3.1 Introduction

Rapid changes in tropical forest ecosystems worldwide in recent decades have had tremendous environmental impacts globally, contributing significantly to climate change (Gullison et al., 2007) and biodiversity loss (Laurance et al., 2012). In response to these threats, international level discussions, frameworks and initiatives have been set up to combat anthropogenic forest loss. One such initiative, the "Reducing Emissions from Deforestation and forest Degradation" (REDD+) programme, features results-based payments to mainly tropical countries who implement activities to stem CO_2 emissions arising from deforestation and forest degradation (Corbera et al., 2010). A key requirement for the successful implementation of REDD+ is the Measuring, Reporting and Verification (MRV) of forest-related emissions and emission reductions (Joseph et al., 2013; DeVries & Herold, 2013; Herold & Skutsch, 2011). The importance of including remote sensing data in MRV for REDD+ has been widely recognized among the scientific community (Goetz & Dubayah, 2011; De Sy et al., 2012).

A range of tropical forest monitoring systems and initiatives have been developed in recent years to support national and international efforts to stem tropical forest loss. With an increase in the availability of free satellite imagery, large-area mapping of forest disturbances has been operationalised in several key instances in the tropics. First, the Brazilian Space Agency (INPE) launched the PRODES and DETER monitoring databases to provide data on annual forest change and near real-time disturbance detection, respectively (INPE, 2014a,b). Second, a global map of annual forest change made at 30m resolution (Hansen et al., 2013) was recently made public under the banner of the Global Forest Watch (World Resources Institute, 2014). These systems represent an important development towards the operational monitoring of forest change, not only in support of REDD+ MRV, but also as a tool to raise public awareness of the scale and rate of tropical forest change.

Change detection methods increasingly make use of Landsat Time Series (LTS) data, signaling a shift away from conventional bi-temporal change detection methods (Coppin et al., 2004). This shift is due in part to the opening of the Landsat archive to the public in 2008, which was followed by the development of methods which make maximal use of the data contained in the Landsat archive (Wulder et al., 2012). Following the opening of the Landsat archive, the pre-processing of imagery to derive surface reflectance and mask clouds became operationalised (Masek et al., 2006b; Zhu & Woodcock, 2012), facilitating the use of these data for a wide range of applications, including change detection. Table 3.1 outlines a selection of some change detection methods based on dense LTS either by creating annual composite time series (e.g. Kennedy et al., 2010; Griffiths et al., 2013; Huang et al., 2010) or by exploiting all data available in the archive (e.g. Broich et al., 2011; Zhu et al., 2012b; DeVries et al., 2015; Dutrieux et al., 2015; Reiche et al.,

2015a).

While a wealth of forest disturbance methods and products based on LTS have been developed in recent years, disturbance-recovery dynamics are less well understood, especially in tropical forest systems. An understanding of the fate of forests after a disturbance is important in order to estimate net changes (Brown & Zarin, 2013) or to elucidate the drivers of forest change (Kissinger et al., 2012). As in the case of disturbance monitoring, LTS data present an opportunity to describe forest dynamics with much more detail and certainty than is possible with bi-temporal comparison methods (Kennedy et al., 2014). A number of studies in temperate and tropical forests have used LTS to describe disturbance-regrowth dynamics, ranging from classification to temporal trajectory based methods. Carreiras et al. (2014) monitored disturbance-regrowth dynamics at several sites in the Brazilian Amazon by classifying near-annual Landsat time series data into forest, secondary forest or non-forest classes, thereby shedding light on age classes and re-clearance rates of the forests. Schmidt et al. (2015) measured regrowth in a forest-savanna landscape in Queensland, Australia by measuring trends in annual minimum NDVI. Czerwinski et al. (2014) monitored sudden and gradual positive and negative trends in a protected forest in Canada by applying the Theil-Sen slope estimator (Fernandes & G. Leblanc, 2005; Sen, 1968) paired with the Contextual Mann-Kendall test (Neeti & Eastman, 2011; Neeti et al., 2012) on annual LTS data. The LandTrendR method (Kennedy et al., 2010), which segments LTS into temporal trajectories, has been demonstrated in a number of contexts to be useful in describing historical forest disturbance-regrowth patterns (Main-Knorn et al., 2013; Powell et al., 2013; Neigh et al., 2014), an approach which has also proven valuable in predicting above-ground biomass using LTS (Pflugmacher et al., 2012; Frazier et al., 2014). The most spatially comprehensive analysis of forest regrowth was undertaken by Hansen et al. (2013), who mined LTS data globally to produce a map of global forest loss and gain over the period 2000 to 2012 using a thresholding and bagged decision tree approach.

The spectral band or index used in the disturbance-regrowth method is an important determinant of the sensitivity of the method to forest change dynamics. The Normalized Difference Vegetation Index (NDVI) is one of the most commonly used indices in vegetation monitoring. While NDVI has been shown to be sensitive to forest change when used in a time series context (DeVries et al., 2015; Reiche et al., 2015a; Dutrieux et al., 2015), it performs poorly as a measure of forest cover and structure (Freitas et al., 2005), and tends to saturate over dense forest (Gamon et al., 1995; Huete et al., 2002). A number of alternative metrics have been proposed in the forest disturbance monitoring literature, including the Normalized Burn Ratio (NBR) (Key & Benson, 2006), the Normalized Difference Moisture Index (NDMI; also known as the Normalized Difference Water Index, NDWI) (a.J. McDonald et al., 1998; Wilson & Sader, 2002; Gao, 1996), and a range of metrics derived from the Tasseled Cap transformation (Crist & Kauth, 1986; Crist & Cicone, 1984; Healey et al., 2005; Ahmed et al., 2014; Kennedy et al., 2010, 2012). Indices

Table 3.1: Selection of forest change detection methods using LTS data.

	Method	Study Area	Reference(s)
1	LandTrendR - temporal segmentation on annual LTS	temperate forests (U.S., Europe)	Kennedy et al. (2010); Griffiths et al. (2013)
2	CMFDA - temporal trajectory-based method for all available LTS data based on modeled historical time series	Eastern U.S.	Zhu et al. (2012b); Zhu & Woodcock (2014)
3	VCT - change detection on annual Integrated Forest Z-scores (IFZ) derived from LTS data	U.S.	Huang et al. (2010)
4	BFAST Monitor - temporal trajectory based method for all available LTS data based on monitoring structural changes in a monitoring period	tropical forests	DeVries et al. (2015); Dutrieux et al. (2015); Reiche et al. (2015a); Verbesselt et al. (2012)
5	Global forest change mapping using thresholding and bagged decision tree classifiers	Global	Hansen et al. (2013)
6	Time series of forest probabilities for forest change monitoring	Indonesia	Broich et al. (2011)

exploiting difference in reflectance between the SWIR and near infra-red (NIR) regions of the electromagnetic spectrum (e.g. NDMI or Tasseled Cap Wetness) have been found to be particularly useful in discriminating forest age classes (Fiorella & Ripple, 1993) due to their sensitivity to canopy moisture content (Hardisky et al., 1983; Hunt Jr & Rock, 1989; Jin & Sader, 2005).

Most regrowth monitoring algorithms rely on annual or near-annual time series constructed either by selecting a representative image or composite of images for each time period (Carreiras et al., 2014; Kennedy et al., 2012; Czerwinski et al., 2014). As with disturbance monitoring, the reduction of the temporal resolution of the data can lead to losses of information as off-season images are excluded from the analysis (Zhu et al., 2012b). The inclusion of all available data in a time series, on the other hand, gives a clear advantage for specific monitoring objectives, including near real-time disturbance monitoring, for example (Verbesselt et al., 2012; Reiche et al., 2015a; Zhu et al., 2012b). Other monitoring objectives such as post-disturbance regrowth can similarly benefit from the inclusion of all available data. Temporally dense time series with multiple observations per season can shed light on phenological dynamics in forests (Schmidt et al., 2015; Verbesselt et al., 2010), potentially reducing the need for training data in separating permanent land use change (e.g. forest to cropland) from transient changes (e.g. forest harvest cycles).

Structural change monitoring methods rooted in the econometrics discipline have been shown to be useful in describing time series data in rich detail (Zeileis et al., 2005; Leisch et al., 2000; Chu et al., 1992). Structural change monitoring is based on the presumption that current observations in a stable time series should approximately follow historically defined behaviours (e.g. existing seasonal patterns or linear trends). A structural breakpoint is defined as the moment at which time series observations deviate significantly from a previously established model, similar to the change detection methods based on statistical quality control charts (Brooks et al., 2014). Structural change monitoring has been demonstrated more recently on remote sensing time series in the form of the Breaks for Additive Season and Trend (BFAST) family of methods (Verbesselt et al., 2010, 2012). These algorithms are based on the decomposition of pixel time series into trend, season and noise components, and have been shown to be robust against sensor noise in 16-day MODIS composite time series (Verbesselt et al., 2010, 2012) as well as in irregular LTS (DeVries et al., 2015). However, there are few comparably robust methods that can monitor post-disturbance forest regrowth. Structural change monitoring can additionally allow for a more data-driven approach to regrowth monitoring, whereby post-disturbance time series profiles are continually compared to historical stable forest profiles. By applying the reverse logic of the breakpoint monitoring functionality of the structural change monitoring methods, the stability of time series data after a disturbance could conceivably be monitored by observing the moving sum (MOSUM) of the residuals against a statistically defined stability boundary (Leisch et al., 2000).

The overall aim of this study is to develop and test a robust data-driven method for describing disturbance-regrowth dynamics in a tropical forest system. Here, we interpret "data-driven" to imply that minimal user input is needed to derive an output. A robust data-driven method is thus able to ingest all available observations and is reasonably insensitive to noisy observations. To this end, we addressed the following specific objectives:

1. Map disturbances over the period 2000-2013 using all available LTS data.
2. Test the ability of structural change monitoring methods to identify post-disturbance regrowth using all available LTS data.

We addressed these objectives using a two-staged disturbance-regrowth monitoring approach. First, we monitored forest disturbances at an annual timescale using BFAST Monitor (Verbesselt et al., 2012) applied using sequential 1-year monitoring periods (DeVries et al., 2015). We then developed a data-driven method based on moving sums (MOSUM) and structural change monitoring methods (Zeileis et al., 2005; Chu et al., 1992) to track post-disturbance regrowth processes. We applied these methods Landsat NDMI time series to test how close the canopy reflectance trajectory matches that of the historical forest signature. We tested this approach over a tropical forest system in Madre de Dios, southeastern Peru, and assessed the accuracy of the results using a human-interpreter approach (Cohen et al., 2010).

3.2 Study Area

Our study was conducted in Madre de Dios (MDD), a province in southeastern Peru. The study area is defined by the Landsat scenes found in WRS-II path/row 2/68 and 2/69 and is bound approximately by 11.480°S, 69.568°W and 12.795°S, 68.889°W (Figure 3.1). Mean annual precipitation from 2000 to 2014 for the area estimated from data from Tropical Rainfall Monitoring Mission (TRMM) is approximately 2039 mm/y. Rainfall has a unimodal distribution through the year, with the peak of the wet season occurring around January, and the dry season in July, with average minimum and maximum monthly rainfall estimated at 28mm/month and 371mm/month, respectively.

MDD holds a significant portion of Peru's share of the Amazon forest system. The Amazon forest is the largest tropical forest system in the world and boasts some of the worlds largest and most important stores of terrestrial carbon (Baccini et al., 2012; Saatchi et al., 2011) and biodiversity (Malhi et al., 2008). For its share, MDD is part of the Tropical Andes biodiversity hotspot (Myers et al., 2000) and is home to some of the last remaining un-contacted human groups (Shepard et al., 2010).

Few studies have been undertaken in MDD to quantify forest change. Joshi et al. (2015)

estimated a disturbance rate of approximately 2.3% between 2007 and 2010 over a similar study area to that described in this study. Post-disturbance regrowth, on the other hand, has only been qualitatively described (Joshi et al., 2015), and besides national and global maps of forest gains and losses (Potapov et al., 2014; Hansen et al., 2013), no quantitative estimates of net forest changes over MDD exist, to the best of our knowledge.

Forest loss in the Amazon has been mainly driven by cattle ranching, conversion to croplands, logging and road construction (Nepstad & Carvalho, 2001; Walker et al., 2009; Arima et al., 2008; Chavez, 2013). Crop- or pasture-driven deforestation experienced in the Amazon basin is sometimes followed by regrowth, resulting in high forest change dynamics and an abundance of secondary forests (Caviglia-Harris et al., 2014; Feldpausch et al., 2007; Joshi et al., 2015). The construction of roads in Madre de Dios after the 1960's has led to rapid changes in the once pristine forest landscape (Scullion et al., 2014). Specifically, the implementation of the Inter-Oceanic Highway between Brazil and Peru, designed to facilitate transport and trade between Brazil and the Pacific coast of Peru, has been of particular concern to the status of forests in the area (Dourojeanni, 2006). In addition to these drivers, a significant rise in gold mining activities as a result of the global financial crisis in 2008 and a rise in gold prices has fueled an increase in deforestation close the Madre de Dios River and its tributaries (Asner et al., 2013; Alvarez-Berríos & Mitchell Aide, 2015). A series of national-scale REDD+ activities have been initiated in Peru (Peru: Ministerio del Ambiente, 2011; Potapov et al., 2014), including several local REDD+ initiatives in MDD (Hajek et al., 2011) aimed at addressing these drivers of forest change.

3.3 Methods

A general overview of the methods used in this study is shown in Figure 3.2. Each of the steps taken in the study are described in detail below.

3.3.1 Data acquisition and preprocessing

We downloaded all available level-1 terrain-corrected (L1T) Landsat scenes at WRS-II path/row 2/68 and 2/69 (Figure 3.1), for which surface reflectance and cloud masks had already been produced using the LEDAPS (Vermote et al., 1997; Masek et al., 2006b) and FMASK (Zhu & Woodcock, 2012) algorithms, respectively. After applying the available cloud masks to each individual scene to mask out clouds and cloud shadows, we computed the proportion of no-data pixels per scene and removed all scenes with greater than 80% no-data pixels. As a result of the failure of the Scan Line Corrector (SLC) on board Landsat 7 ETM+ in 2003, we found that cloud pixels adjacent to masked SLC-off gaps were frequently missed by the cloud mask. For this reason, we applied a 5-pixel sieve

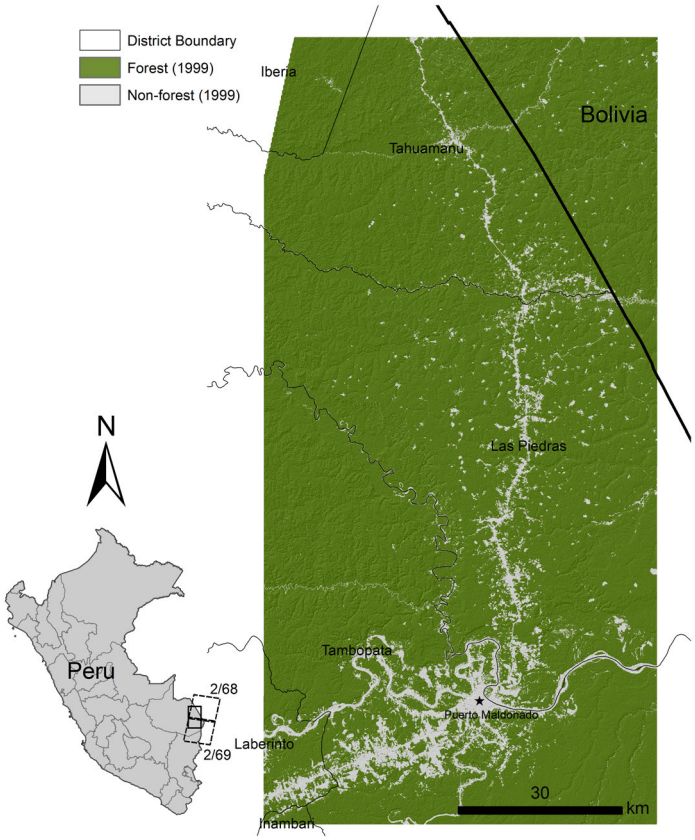

Figure 3.1: Study area located in Madre de Dios province in south-eastern Peru. Forest and non-forest classes from the 1999 benchmark mask are shown as green and grey, respectively. Landsat scene footprints at WRS-II path/row 2/68 and 2/69 are also indicated in the inset.

on each remaining scene, which succeeded in removing these outliers. Finally, 15 scenes having serious mis-registration issues were removed from the dataset.

Statistics for the number of clear-sky observations available per year are shown in the Supplementary Data. After screening of all images, the available data were still reasonably dense compared to LTS datasets from other areas of the tropics (DeVries et al., 2015; Reiche et al., 2015a), forming a continuous time series from 1990 to present. After 2003, the failure of the SLC on board Landsat 7 was largely compensated by a large number of TM scenes following 2003. The decommissioning of Landsat 5 at the end of 2011, however, caused a marked decrease in data availability in 2012 and 2013. An average of 72% and 69% of the total observations per pixel were valid clear-sky observations (no cloud, cloud shadows or SLC-off gaps) for path/row 2/68 and 2/69, respectively.

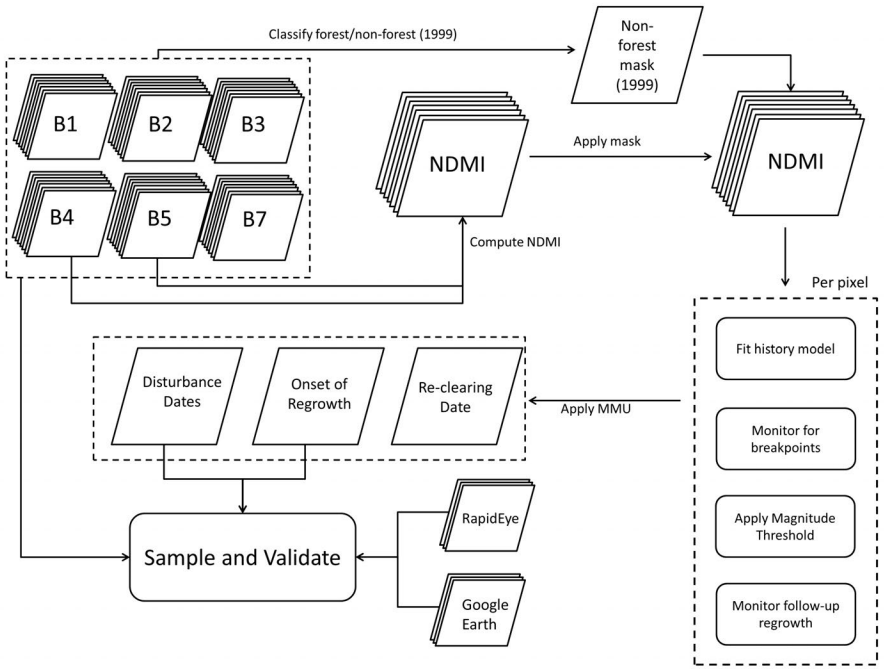

Figure 3.2: Flowchart outlining the main steps implemented in this study.

With the remaining scenes, we computed the Normalized Difference Moisture Index (NDMI), from the short-wave infrared (SWIR) and near infrared (NIR) bands as follows (Gao, 1996):

$$NDMI = \frac{NIR - SWIR}{NIR + SWIR} \tag{3.1}$$

where the NIR and SWIR bands are the fourth and fifth bands, respectively, of the Landsat TM and ETM+ sensors. We compared disturbance and regrowth results for NDVI, NDMI and Band 5 and found that NDMI and band 5 gave comparable results for disturbance detection and NDMI gave the best results for monitoring regrowth (Figure 3.A1). We thus chose NDMI for both disturbance and regrowth monitoring for the remainder of the study.

3.3.2 Benchmark non-forest mask

Since our approach to monitoring forest disturbance requires a history period from which a stable forest time series can be modeled, it is important to begin with a benchmark non-forest mask to limit the algorithm to pixels which are known to have been forested at the beginning of the first monitoring period. For this reason, we produced a benchmark non-forest mask for 1999 using two cloud-free images for path/row 2/68 and 2/69, both acquired on the 10^{th} of August 1999. We classified the images using the interactive supervised classification included in the ArcGIS 10.1 (ESRI, inc.) software package. Initial

land cover classes included bare soil, pasture, urban and water, which were fused into the non-forest classes. Primary and secondary forest classes were fused into a single forest class.

3.3.3 Monitoring for disturbances

In this study, we define "disturbance" to include negative changes to the forest canopy induced by human activity (deforestation or degradation) or natural disturbances. To monitor disturbance, we followed the approach of DeVries et al. (2015), who applied the BFAST Monitor algorithm (Verbesselt et al., 2012) on sequential monitoring periods. Given the relatively high data density from 1990 to present, we began disturbance monitoring in the year 1999 and defined 1-year monitoring periods continuing to 2014. Since the BFAST Monitor algorithm is described in detail in DeVries et al. (2015) and Verbesselt et al. (2012), only a brief overview is given here. For each sequential monitoring period, a first-order harmonic seasonal model is derived from all available data prior to the onset of the monitoring period and projected into the monitoring period. All data in the monitoring period are then checked for consistency with this model by way of a Moving Sums (MOSUM) of the residuals (Zeileis et al., 2005; Verbesselt et al., 2012). The MOSUM is defined for each time point (t) in a monitoring period as follows:

$$MO_t = \frac{1}{\hat{\sigma}\sqrt{n}} \sum_{s=t-h+1}^{t} (y_s - \hat{y}_s) \tag{3.2}$$

where $\hat{\sigma}$ is the predicted variance estimated on the history period, n is the number of observations in the sample, $y - \hat{y}$ are the residuals in the MOSUM window, and h is the MOSUM bandwidth, which defined as a fraction of the number of observations in the sample. Following previous studies using the BFAST Monitor method (Verbesselt et al., 2012; DeVries et al., 2015), we assigned a value of $0.25n$ to h for the disturbance monitoring component of this study. A structural breakpoint is declared when the null hypothesis of structural stability (i.e. stability of the seasonality pattern) is rejected (Verbesselt et al., 2012; Zeileis et al., 2005). The decision to reject this null hypothesis is based on a boundary condition which is set according to a 5% probability level following the Functional Central Limit Theorem (see Leisch et al. (2000) for more information on how this boundary function is computed). In other words, if the time series pattern is stable compared to the historical data, all residuals and hence also their MOSUM values should fluctuate closely around zero. However, if there is a breakpoint in that particular monitoring period, the MOSUM values will deviate significantly from zero.

3.3.4 Calibrating a disturbance magnitude threshold

In addition to breakpoints, the disturbance magnitude was computed by taking the median of all the residuals within each monitoring period. Even though the breakpoints detected by the BFAST Monitor method are considered robust against noise and other variability in the time series (Verbesselt et al., 2012), a magnitude threshold can help to distinguish between positive and negative breakpoints, and between actual forest change and spurious breakpoints due to outliers in the monitoring period (DeVries et al., 2015). These outliers can trigger a breakpoint if the residual (numerator in Equation 3.2) overcomes the $\hat{\sigma}$ term in the denominator of Equation 3.2.

From a reference dataset consisting of randomly sampled pixels with breakpoints in years 2005, 2009 and 2012, we found a strong effect of magnitude on the probability of detecting disturbance (described further in the Supplementary Data). We derived a magnitude threshold using a Binomial Logistic Regression (BLR) approach. We chose a magnitude threshold where the probability of detected actual disturbances was approximately 50%. A magnitude threshold of -0.006 achieved a 50% probability of actual disturbance. Using a qualitative assessment of various thresholds on the final mapped disturbance, we revised the final threshold to -0.01, as this threshold was found to further reduce noise in the disturbance maps. We eliminated all breakpoints with magnitudes exceeding the selected threshold and took the earliest remaining breakpoint for each pixel as the "final" change label. We flagged all disturbance pixels for follow-up regrowth monitoring starting at their final disturbance dates.

3.3.5 Monitoring for post-disturbance regrowth

For all pixels where a disturbance was detected, we continued monitoring for post-disturbance regrowth. Here, we define "regrowth" to be the establishment of a secondary forest canopy following a disturbance. We chose NDMI to monitor this process due to two associated phenomena known to have a visible impact on the short-wave region of the electro-magnetic spectrum. First, exposed soil reflectance causes high reflectance in this region, similarly to the red visible band. Re-establishment of a canopy reduces exposure of the soil and decreases soil reflectance. Second, and most importantly, reflectance in the short-wave infrared region has been previously shown to be impacted by differences in canopy moisture contents (Jin & Sader, 2005). The goal of this step was thus to gauge whether post-disturbance NDMI trajectories reflected moisture and soil reflectance properties comparable to that of the stable forest model derived in the history period.

Our approach to monitoring post-disturbance regrowth follows a similar logic to the disturbance monitoring method described above. In short, we are interested in knowing whether values following a disturbance in a time series return to the previously defined stable state or not. If such a return to stability occurs, we are also interested in knowing

after how much time this signal recovery occurs. While MOSUM values at a breakpoint deviate significantly from zero (crossing a certain critical boundary, as described above), forest regrowth is expected to result in MOSUM values returning to near-zero (i.e., crossing back below the same critical boundary). It is important to note that a return to stability in the time series does not imply that the conditions of the regrowth forest match that of the previously intact forest. For this reason, our method returns a regrowth class label but does not quantitatively describe the post-disturbance forest state.

Figure 3.3 outlines our general approach to regrowth monitoring. We set the beginning of the regrowth monitoring period to the beginning of the disturbance year and defined the history period based on the stable portion of all data prior to this date (Bai & Perron, 2003; Verbesselt et al., 2010). The definition of the history period differs from that of the disturbance monitoring part of our method (which employs all historical observations to derive a model) because regrowth monitoring was found to be much more sensitive to noise in the history period (discussed further in Section 3.5.3). Using the model derived from these data as described in Section 3.3.3, we took the minimum critical value returned by the boundary function as the critical boundary for regrowth (shown as a green dotted line in Figure 3.3). This critical boundary is not a sufficient definition of forest regrowth, however, since naïvely assigning a regrowth label at the moment when the first MOSUM value crosses below the critical boundary can result in erroneous flagging of regrowth. To align the statistical regrowth definition with an ecologically sound definition of forest regrowth, we imposed a number of additional conditions to be met for a regrowth flag to be assigned. Thus, for a post-disturbance time series at times $t_B \leq t < t_N$, a regrowth flag is assigned at time t_R if:

1. $(t_R - t_B)$ is greater than or equal to 3 years (shown as w in Figure 3.3);
2. the period after t_R in which MOSUM values remained below the critical boundary is greater than or equal to 1 year (shown as s in Figure 3.3); and
3. at least some of the MOSUM values at times $t_B \leq t < t_R$ exceed the critical boundary (i.e. not all pre-regrowth values are lower than the critical boundary).

The third condition is especially important in cases where noise in the history period affect the MOSUM process in the monitoring period. Noise in the history period is represented by a high $\hat{\sigma}$ in the denominator of the MOSUM equation (Equation 3.2), resulting in particularly low MOSUM values. In some cases, these values may never rise above the critical boundary and would therefore be erroneously interpreted as regrowth.

The size of the monitoring window used in the MOSUM calculation is expressed as h in Equation 3.2), and the effect of varying h is shown in Figure 3.4. We chose a value of $0.5n$ for h for the regrowth monitoring component of this study, as lower values tended to signal regrowth too early (e.g. $h = 0.25n$ in Figure 3.4), and the maximum value of

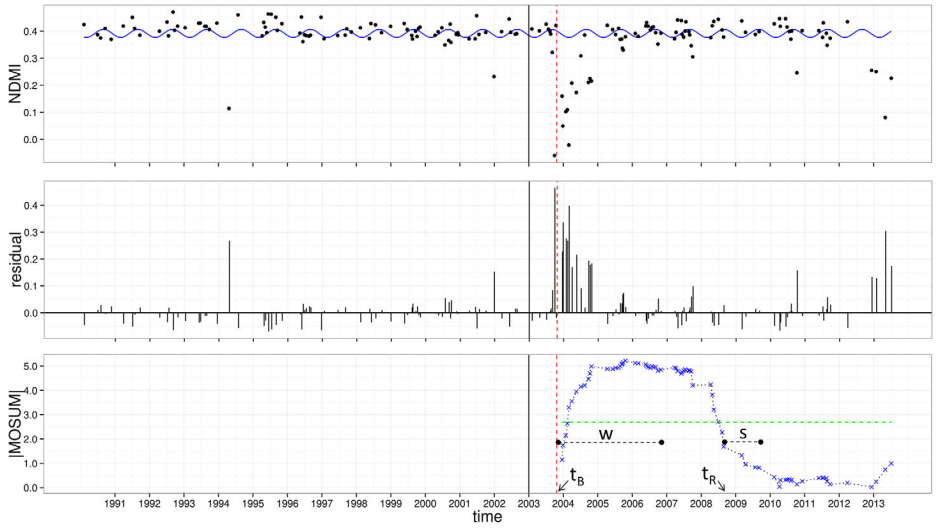

Figure 3.3: Demonstration of the MOSUM-based regrowth test. MOSUM values (bottom plot) after a disturbance (t_B) are evaluated against a statistically defined stability boundary (green line). A regrowth label is assigned at t_R if MOSUM values return below the boundary at least w years after the initial disturbance and remain below the boundary for an additional s years.

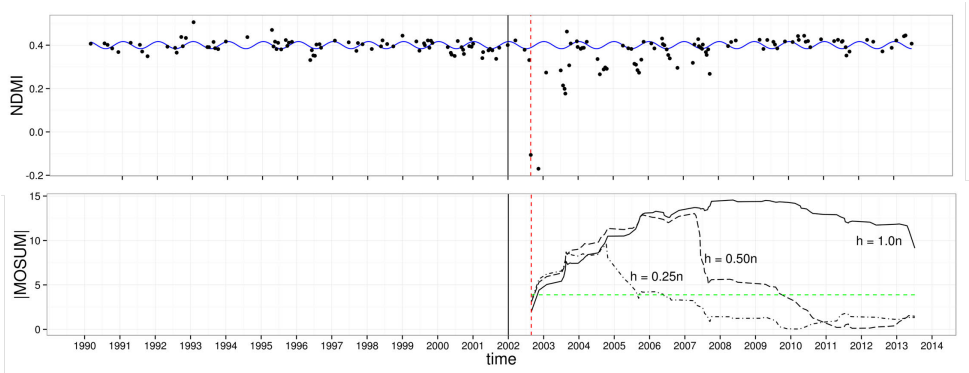

Figure 3.4: Demonstration of the effect of varying MOSUM window sizes (h) on the response of MOSUM values during post-disturbance regrowth.

$1.0n$ tended to omit much of the regrowth due to the extended response time.

For pixels where a final regrowth flag was assigned, we monitored for repeat disturbances by applying BFAST Monitor to the entire time series with the data between the original breakpoint (t_B) and onset of regrowth (t_R) removed. We set the monitoring period directly after the regrowth flag, and if a breakpoint was detected, the pixel was assigned a "re-clearance" label, indicating a repeat disturbance.

We conducted all analyses using the "bfast", "bfastSpatial" and "strucchange" packages in R (R Core Team, 2014; Zeileis et al., 2002; Verbesselt et al., 2012).

3.3.6 Accuracy Assessment

We assessed the accuracy of the disturbance and regrowth results following a two-stage sampling design. First, we selected a random sample of pixel clusters with disturbance labels, with or without follow-up regrowth. We then randomly selected one pixel from each of the sampled clusters. Additionally, we selected random samples from all non-disturbance forest pixels with the aim of assessing the omission errors. Given the relatively large size of the non-disturbance class (e.g. with disturbance across 5% of a forest landscape, 95% of the pixels would belong to the non-disturbance class), a reliable sample-based estimate of omission errors is very difficult. To aid in the estimation of omission errors, we assumed that the probability of forest disturbance is highly affected by the presence of roads (Pfaff, 1999). We thus stratified the non-disturbance class based on a 4 km buffer around the roads in the study area. Half of the non-disturbance samples were selected from within this buffer, and the other half from the rest of the non-disturbance class. All samples were selected from a spatial subset spanning both path/rows having a sufficiently high density of very high resolution (VHR) RapidEye or GoogleEarth imagery.

After rejecting sample pixels where interpretation was not possible (e.g. due to lack of sufficient VHR data), our final reference dataset consisted of 617 pixels derived from the following strata: 218 pixels from the disturbance class, 188 from the buffered no-change class and 211 pixels from the no-change class. We removed all disturbance commission errors and selected the remaining disturbance pixels for follow-up regrowth. After adding additional similarly sampled disturbance pixels with and without predicted regrowth, the number of samples assessed for follow-up regrowth was 216. We assessed the sampled pixels using the human interpreter approach described in the calibration method above and in Cohen et al. (2010) and DeVries et al. (2015) to derive a reference label for each pixels. Specifically, we identified disturbances by interpreting the LTS data. While small disturbances can also be identified using this approach (DeVries et al., 2015), a lack of VHR or ground data for earlier dates limited our ability to verify some small diffuse changes. In pixels where we identified disturbances, we used the VHR data to confirm or reject the presence of a secondary forest canopy following disturbance.

We produced area-weighted confusion matrices and accuracy estimates following Stehman et al. (2004) and Olofsson et al. (2013) and computed inclusion probabilities for samples from the disturbance stratum ($\pi_{s,d}$) as follows:

$$\pi_{s,d} = \frac{n_{cl}}{N_{cl} N_{p,x}} \tag{3.3}$$

for sample s on pixel cluster x, where n_{cl} is the number of sampled pixel clusters, N_{cl} is the total number of pixel clusters in output map and $N_{p,x}$ is the total number of pixels

Table 3.2: Count-based confusion matrix for randomly sampled pixels assessed for forest disturbances. Classes are defined as disturbance (1), no-change within the 4-km roads buffer (2) and no-change outside the 4-km roads buffer (3).

		Reference						
		1	2	3	$\sum$	UA	PA	TA
Predicted	1	183	19	12	214	0.86	0.85	
	2	25	169	0	194	0.87	0.90	0.89
	3	10	0	199	209	0.95	0.94	
	$\sum$	218	188	211	617	–	–	–

within x. We computed inclusion probabilities of non-disturbance pixels from both the buffered and non-buffered strata ($\pi_{s,nc}$) as follows:

$$\pi_{s,nc} = \frac{n_s}{N_s} \tag{3.4}$$

for sample s, where n_s and N_s are the number of sampled and total pixels, respectively, in each stratum. We then weighted all samples by the inverse of their respective inclusion probabilities as described in detail in Stehman et al. (2004). From the resulting area-weighted confusion matrix, we calculated the total accuracy (TA), producer's accuracy (PA; inversely related to omission errors) and user's accuracy (UA; inversely related to commission errors) for the disturbance, regrowth and no-change classes.

3.4 Results

3.4.1 Accuracies of the disturbance and regrowth classes

The count-based confusion matrix for the sampled disturbance pixels is shown in Table 3.2 and the area-weighted confusion matrix is shown in Table 3.3. From the area-weighted confusion matrix, we estimated a total accuracy (TA) for the disturbance class of 91 ± 2.3% ($\alpha = 0.05$). User's accuracy (UA) and producer's accuracy (PA) of the disturbance class were 84 ± 5.5% and 74 ± 5.7% respectively. The count-based confusion matrix for the regrowth class is shown in Table 3.4 and the area-weighted confusion matrix for the regrowth class is shown in Table 3.5. Here, we estimated a total accuracy of 48 ± 3.9%, with estimated UA and PA for the regrowth class of 83 ± 7.0% and 25 ± 7.0% respectively.

To investigate whether these low accuracies were affected by timing of original disturbance, we post-stratified the samples into "early" and "late" disturbances, using the original predicted disturbance date as a cut-off. The resulting accuracies for regrowth following

Table 3.3: Area-weighted confusion matrix for samples shown in Table 3.2

		Reference						
		1	2	3	$\sum$	UA	PA	TA
Predicted	1	0.16	0.026	0.0047	0.19	0.84 ± 0.055	0.74 ± 0.057	
	2	0.032	0.21	0	0.24	0.87 ± 0.063	0.89 ± 0.064	0.91 ± 0.023
	3	0.027	0	0.54	0.56	0.95 ± 0.070	0.99 ± 0.070	
	$\sum$	0.22	0.24	0.54	1	–	–	–

Table 3.4: Count-based confusion matrix for randomly sampled pixels assessed for forest regrowth. Only sample pixels where disturbances were correctly identified are included.

		Reference					
		regrowth	no-regrowth	$\sum$	UA	PA	TA
Predicted	regrowth	102	21	123	0.83	0.64	0.64
	no-regrowth	57	36	93	0.39	0.63	
	$\sum$	159	57	216	–	–	–

Table 3.5: Area-weighted confusion matrix for all samples ($n = 216$) shown in Table 3.4.

		Reference					
		regrowth	no-regrowth	$\sum$	UA	PA	TA
Predicted	regrowth	0.16	0.034	0.20	0.83 ± 0.070	0.25 ± 0.070	0.48 ± 0.069
	no-regrowth	0.49	0.31	0.80	0.39 ± 0.10	0.90 ± 0.040	
	$\sum$	0.66	0.34	1	–	–	–

Table 3.6: User's accuracy (UA), producer's accuracy (PA) and total accuracy (TA) of the regrowth class for samples with original disturbances predicted prior to a given cut-off year.

cut-off	UA	PA	TA	n
2002	0.89 ± 0.085	0.88 ± 0.089	0.82 ± 0.092	78
2003	0.86 ± 0.091	0.83 ± 0.10	0.78 ± 0.095	85
2004	0.85 ± 0.083	0.70 ± 0.10	0.69 ± 0.091	111
2005	0.85 ± 0.078	0.66 ± 0.099	0.67 ± 0.085	129
2006	0.84 ± 0.074	0.56 ± 0.094	0.61 ± 0.081	153
2007	0.83 ± 0.074	0.47 ± 0.090	0.56 ± 0.077	173
2008	0.83 ± 0.073	0.40 ± 0.085	0.54 ± 0.074	188
2009	0.83 ± 0.071	0.31 ± 0.076	0.50 ± 0.070	212

Table 3.7: Area-weighted confusion matrix for samples shown in Table 3.4 with original predicted disturbances prior to 2006 ($n = 153$).

		Reference					
		regrowth	no-regrowth	$\sum$	UA	PA	TA
Predicted	regrowth	0.40	0.076	0.48	0.84 ± 0.074	0.56 ± 0.094	0.61 ± 0.081
	no-regrowth	0.32	0.21	0.52	0.39 ± 0.15	0.73 ± 0.16	
	$\sum$	0.72	0.28	1	–	–	–

"early" disturbances are shown in Table 3.6. The area-weighted confusion matrix for regrowth following disturbances predicted before 2006 ($n = 153$) is shown in Table 3.7. In this case, we estimated a total area-weighted accuracy of 61 ± 8.1%, with user's and producer's accuracies of the regrowth class of 84 ± 7.4% and 56 ± 9.4%, respectively.

3.4.2 Disturbed area and follow-up regrowth

The final map of disturbances and regrowth from 1999 to 2013 is shown in Figure 3.5. The right panel shows the onset of regrowth as determined by our regrowth monitoring algorithm.

The area disturbed per year is shown in Figure 3.6, which also includes the disturbed area undergoing post-disturbance regrowth. The mean disturbed area per year (including areas with and without follow-up regrowth) was 4587 hectares, representing approximately 0.5% of the total forest area in 1999.

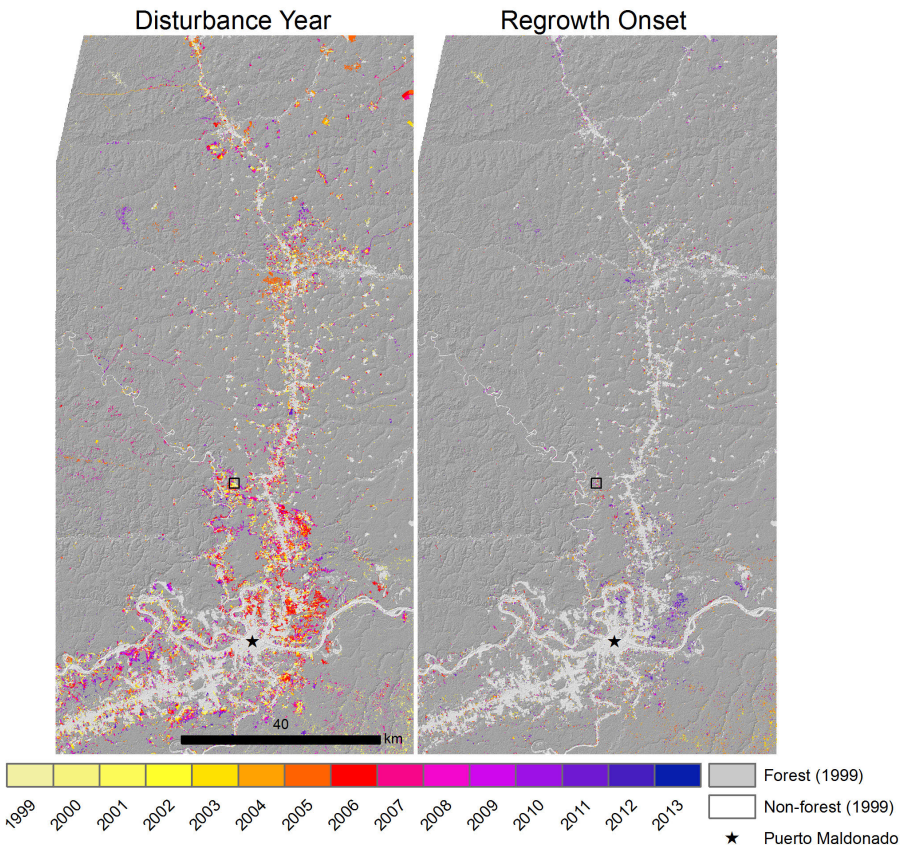

Figure 3.5: Disturbances (left panel) and follow-up regrowth (right panel) between 1999 and 2014 over the whole study area. The example area shown in Figure 3.7 is shown as a black box.

3.5 Discussion

3.5.1 Forest disturbance rates in Madre de Dios

The first objective of this study was to map forest disturbances from 2000 to 2013 in the study area using LTS. Our estimates show that forest disturbances peaked in 2006 and 2008, after which there was a decline in forest disturbances (Figure 3.6). The disturbed area in which forest regrowth was subsequently detected is shown as a lighter shade in Figure 3.6. Subtracting the disturbed forest area where regrowth eventually occurred from the total gross disturbed area, we estimated a net change between 1999 and 2014 of approximately 5.6% of the total initial forest area. While a conclusion of change dynamics cannot be made by a direct comparison with 2.44% national-scale disturbance rate estimated by Potapov et al. (2014) over the same time period, we do note that our rate could be higher due to high omission errors in the regrowth class. These errors result in a higher proportion of net disturbances when area under regrowth is subtracted from

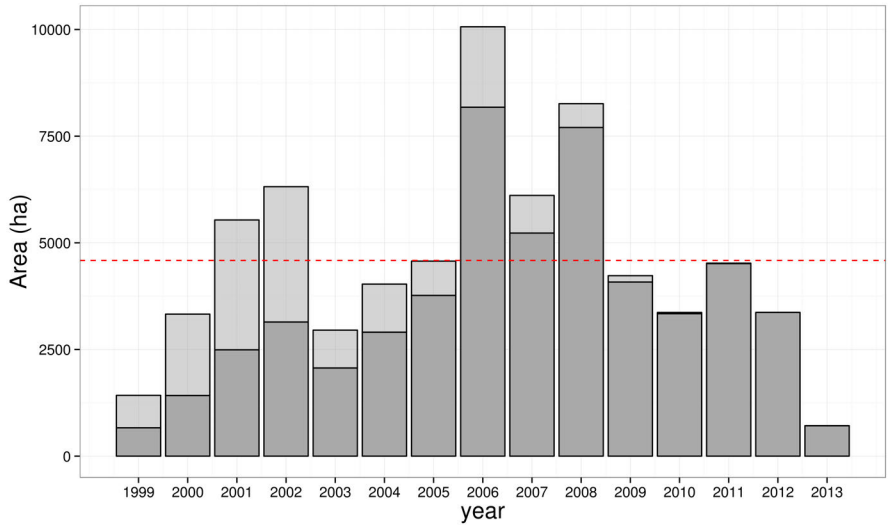

Figure 3.6: Disturbed forest area per year from 1999 to 2014. The proportion of disturbed area where regrowth eventually occurred is shown as a lighter shade. The mean disturbed area per year is shown as a red dotted line.

the disturbance class. Updating these results as more data become available will result in more of the disturbances detected in these years assigned to the regrowth class and lower net disturbance rates.

Joshi et al. (2015) reported a disturbance rate of 0.78% per year for the years 2007, 2008 and 2009 over a very similar study area, which is close to our estimated disturbance rate of 0.65% per year over the same time period. This comparison indicates that our estimates of disturbed area compare well with independent estimates based on radar satellite data (Joshi et al., 2015).

3.5.2 Robustness of the disturbance-regrowth monitoring algorithm

A number of studies have demonstrated the ability of the BFAST Monitor algorithm (Verbesselt et al., 2012) to detect disturbances in tropical forest landscapes with varying accuracies (Reiche et al., 2015a; DeVries et al., 2015; Dutrieux et al., 2015). In this study, we have shown that given a reasonably dense LTS dataset for MDD, Peru, this algorithm can detect disturbances with high accuracy. A major advantage of the BFAST Monitor method is the inclusion of the noise term ($\hat{\sigma}$ in Equation 3.2) in the MOSUM computation. Incorporation of this term effectively allows for consideration of remaining contamination, either from unmasked clouds, cloud shadows, or other sensor-derived noise, and results in a method which is largely robust against commission errors. In other words, presence of some noise in the history period means that a single noise value in the monitoring period would not be expected to trigger a breakpoint.

The second objective of this study was to extend the principle of "robustness against noise" to the monitoring of post-disturbance regrowth, whereby the same MOSUM values used to monitoring for breakpoints are then used to monitor for a return to time series stability. In following this principle, our study represents the first attempt at monitoring post-disturbance regrowth using a purely data-driven approach using all available LTS data. The examples shown in Figures 3.7 and 3.8 demonstrate how a such a data-driven approach can discriminate between permanent land use change and post-disturbance regrowth. In the case of permanent land use change (Figures 3.7A and 3.8A), a new seasonal profile is visible in the post-disturbance time series and MOSUM values do not return to below the critical boundary. In the case of regrowth (Figures 3.7B and 3.8B), on the other hand, the post-disturbance time series eventually returns to a profile that somewhat resembles the historical time series, and the MOSUM values accordingly return below the critical boundary. In this case, it is apparent that even though the time series profile does not exactly resemble that of the historical time series, most likely due to differences in the NDMI reflectance profiles between old-growth and young secondary forests (Jin & Sader, 2005), the MOSUM values are sufficient to signal a general return to "stability", interpreted here as forest regrowth.

The demonstrations outlined above highlight some key differences between the disturbance-regrowth monitoring method described in this paper features and other methods based on temporal composites (Huang et al., 2010; Kennedy et al., 2010). While annual composites are useful in detecting long-term changes, including forest regrowth (Kennedy et al., 2010; Czerwinski et al., 2014), using all observations in an LTS conveys a number of distinct advantages in disturbance-regrowth monitoring. First, multiple observations within a year can reveal different temporal patterns, allowing for the distinction between actual regrowth processes and permanent land use transitions as described above. Second, forest disturbances are often associated with discrete events in time, and the timing of a disturbance event can be captured with greater temporal resolution using multiple observations per year. On the other hand, the reliance on discrete breakpoints for monitoring disturbances in our study likely results in a loss in sensitivity to gradual forest decline due to degradation or other long-term disturbance agents, for which other trajectory-based approaches such as LandTrendR are well suited (Kennedy et al., 2010). Recent research in a tropical montane forest system has shown that measuring change magnitude alongside breakpoints can bolster sensitivity to small-scale changes, although further research is needed to expand this approach to degradation monitoring (DeVries et al., 2015).

3.5.3 Sources of omission and commission errors in regrowth monitoring

For the regrowth class, we estimated a UA of 83%, indicating that commission errors were reasonably low. However, a PA of 25% for the regrowth class indicates a very high

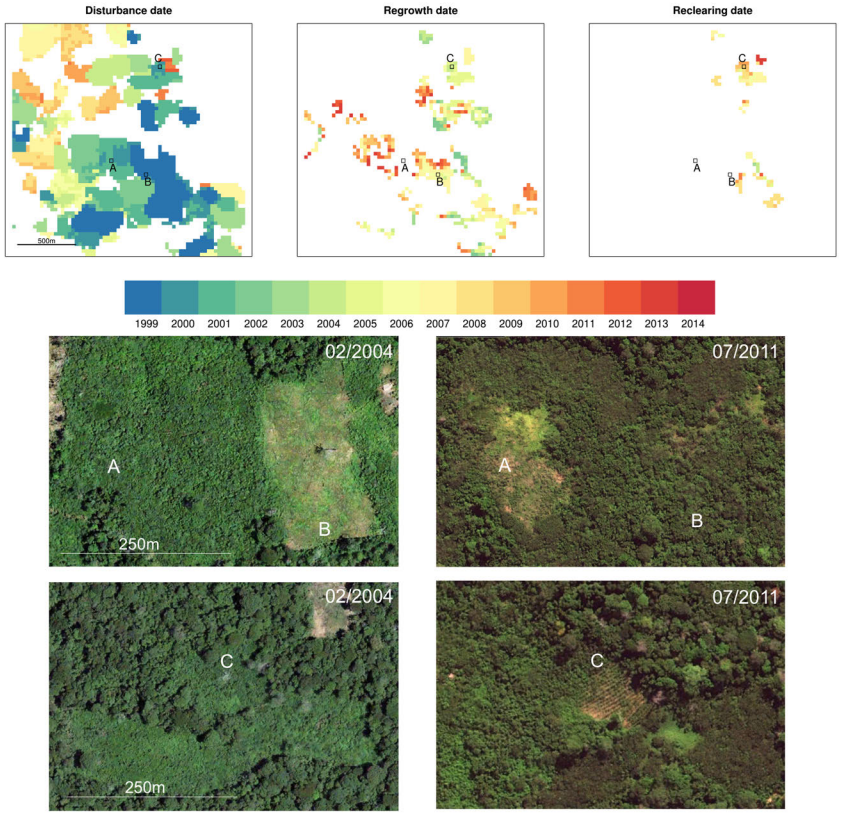

Figure 3.7: Dates of disturbance (top left), regrowth (top centre) and re-clearing (top right) for a small area. Images from GoogleEarth^{TM} in 2004 and 2011 are shown for three pixels of interest (labeled A, B and C). Pixel time series for points A, B and C are shown in Figure 3.8.

incidence of omission errors, which warrants further investigation here. Post-stratification of the sample revealed that PA has a strong dependence on the timing of the original disturbance, ranging from 88% for disturbance prior to 2002 to 31% for disturbances prior to 2009 (Table 3.6). This trend indicates that in most cases, even though regrowth had been occurring over a number of years, the MOSUM values had simply not reached the critical boundary yet (Figure 3.9), but may have done so with more observations following the disturbance. In the example shown in Figure 3.9, a reduction in data density at the end of the time series, partly due to the lack of TM data after 2011 (also shown in Table S1 in the Supplementary Materials), resulted in a more slowly descending MOSUM, and hence a delayed regrowth flag. It is debatable whether these can be considered actual omission errors, since the regrowth algorithm would eventually have assigned a regrowth label to these pixels, barring any repeat disturbance. An alternative interpretation of these cases is that the regrowth monitoring algorithm is not sensitive enough for fast detection of regrowth processes. If earlier detection of regrowth onset is desired, this can be accomplished by assigning a smaller value for the monitoring window (h in Equation 3.2 and Figure 3.4) or by relaxing some of the additional criteria (e.g. w

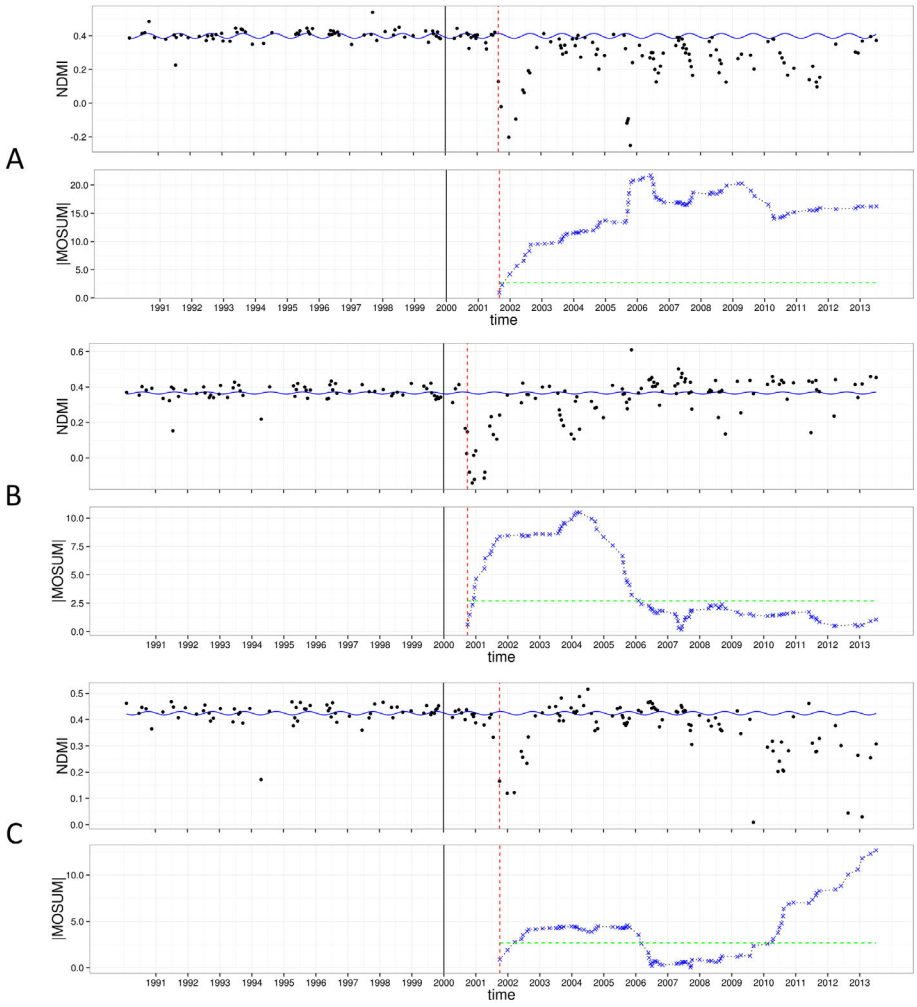

Figure 3.8: NDMI time series with fitted history model (top panel) and corresponding post-disturbance MOSUM time series (bottom panel) for the three pixels shown in Figure 3.7. The monitoring period is shown as a vertical black line, breakpoints are shown as vertical red lines, and the MOSUM stability boundary is shown as a green line.

or s in Figure 3.3). Additionally, forest areas could be stratified based on areas where rapid recovery of the spectral signal is expected, whereby different values are assigned h based on these strata.

According to our estimates, commission errors in the regrowth class were markedly lower than omission errors. One source of commission errors observed in the validation process was related to the effect of a noisy history period on MOSUM values in the monitoring period. Figure 3.10A shows an example of a commission error, where a disturbance in the history period (circa 1991) resulted in a high noise term ($\hat{\sigma}$) and accordingly low MOSUM values. The implication of the low MOSUM values in this case is that while the

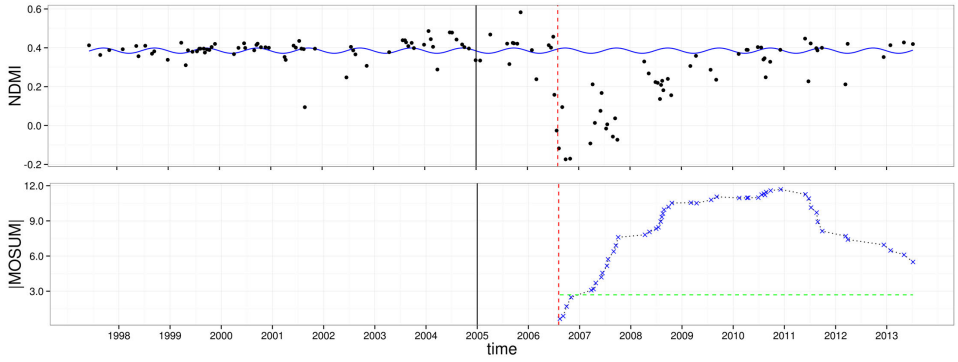

Figure 3.9: Example of an omission error due to gradual post-disturbance recovery with insufficient data in the post-disturbance period to confirm regrowth.

first disturbance in the monitoring period (2000-2001) was correctly identified, the second disturbance (2004-2005) failed to bring MOSUM values back above the critical boundary. Removing the all data prior to 1992 in this example resulted in a correctly detected disturbance without regrowth (Figure 3.10B), indicating that this historical disturbance had a critical impact on the regrowth monitoring process in this example. The history period used in the regrowth monitoring process was defined based on a statistical estimate of stability (Bai & Perron, 2003; Verbesselt et al., 2010), rather than using all historical data as in the disturbance monitoring method, which succeeded in excluding such disturbances in most cases. With an estimated UA of 83% for the regrowth class, we conclude that this phenomenon is relatively uncommon, but serves to demonstrate the effect of noise in the history period on the MOSUM tests.

3.5.4 Validation of forest change products by human interpretation

Validation of high temporal resolution forest change products is a significant challenge, given the paucity of historical change reference data. Visualization tools using LTS, such as TimeSync (Cohen et al., 2010), have been developed to address this gap. By using a similar approach, we were able to derive reference data for our disturbance and regrowth products. Disturbance samples were generally straightforward to validate, since most disturbances were a result of clear-cutting (e.g. conversion to cropland or pasture, or forest clearing due to mining operations), and thus resulted in a discrete change signal in the RGB images. The post-disturbance regrowth product, on the other hand, absolutely required high resolution data to confirm the presence of a secondary forest canopy after disturbance. Without these data, it was impossible to confirm whether an increase in NDMI in the LTS was a result of forest regrowth or the presence of other vegetation. One drawback of the reliance on high resolution data was the presence of a large gap in these datasets: RapidEye data were only available from 2010 to 2013, and GoogleEarth data were only available for 2004 and from 2011 to 2013. We derived regrowth refer-

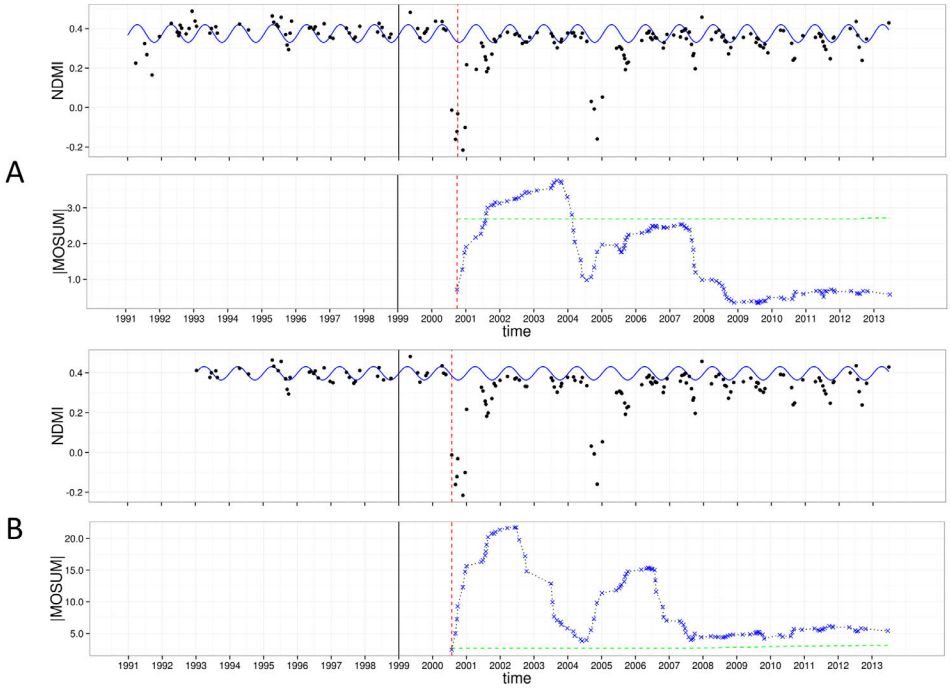

Figure 3.10: Example of a regrowth commission error, where a disturbance in the history period affects the MOSUM values used to monitoring regrowth (A). Removing the historical disturbance from the history period (B) causes an increase in MOSUM values in the monitoring period, and eliminates the regrowth flag.

ence data by confirming the presence or absence of a forest canopy in the period where high-resolution were available, and were not able to address the issue of timing of forest regrowth. Applying our disturbance-regrowth method in an area where reference datasets including disturbance dates and stand age of regrowth forests are available will allow for further fine-tuning of the parameters used in our method to detect forest regrowth.

3.5.5 Towards a continuous monitoring framework for net changes

In this study, we monitored and mapped historical disturbance-regrowth dynamics using a novel data-driven approach. With the ability to track these change dynamics using LTS, we propose a framework for continuous monitoring of forest disturbance and regrowth. While we used 1-year monitoring periods to track disturbances in this study, an approach using single, newly available observations in near real-time (Verbesselt et al., 2012) is easily envisioned. Within this framework, disturbance or regrowth monitoring algorithms are employed for each pixel depending on the current forest status of the pixel. For forested pixels, disturbances are tracked using the BFAST Monitor algorithm, while for previously disturbed (but not yet recovered) pixels, the regrowth algorithm described in this paper

is evoked. At the moment a breakpoint is detected in the forested pixels, a disturbance label is assigned. Conversely, when post-disturbance MOSUM values return below the critical boundary and satisfy the conditions set for regrowth monitoring (Figure 3.3), a regrowth label is assigned and the pixel is once again considered to be forested. This framework can be extended to REDD+ MRV and other forest monitoring systems for the purpose of accounting for net changes in forest landscapes.

Acknowledgements

We would like to thank Christopher Martius and Louis V. Verchot of CIFOR for their support in carrying out this study, and Nandika Tsendbazar for helpful comments on the manuscript.

3.A Appendix

To derive a magnitude threshold, we first randomly sampled unique change pixels from several monitoring periods. For each pixel, we checked whether deforestation had occurred and noted the timing following the TimeSync approach (Cohen et al., 2010), adapted as in DeVries et al. (2015) to include 6.5m resolution RapidEye time series from 2010 to 2013 and GoogleEarth^{TM} imagery from 2004 and 2011 to 2013. Using the reference change labels, we constructed a Binary Logistic Regression (BLR) model using magnitude as a regressor and the reference binary change label as the response variable. As such, we modeled the probability of correctly identifying deforestation according to the form:

$$P(Y = 1|X) = \frac{1}{1 + e^{-X\beta}} \tag{3.5}$$

where Y is the response variable (binary change/no-change label), X is the continuous regressor (magnitude) and β is a regression coefficient. The result of the BLR model is shown in Figure 3.A1. We chose a magnitude threshold such that $P(Y = 1|X)$ was approximately equal to 0.5 (shown as a red dotted line in Figure 3.A1) and eliminated all breakpoints with magnitudes exceeding that threshold.

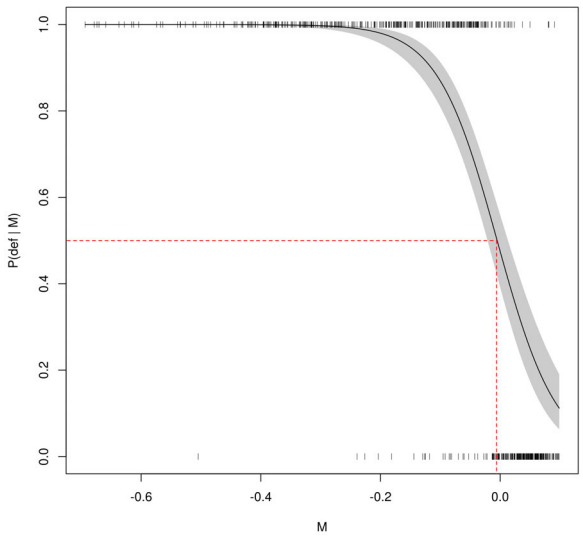

Figure 3.A1: Results of the binomial logistic regression (BLR) for all reference disturbance pixels sampled from breakpoints in 2005, 2009 and 2012 monitoring periods. Change magnitude (M) is shown on the x-axis and the probability of detecting deforestation ($P(def|M)$) is shown on the y-axis. A threshold at which $P(def) = 0.5$ is shown as a red hatched line. The shaded area represents the 95% confidence interval. Change labels assigned by a human interpreter are shown as hatches where 1 = deforested and 0 = no-change.

Chapter 4

Combining satellite data and community-based observations

This chapter is based on:

Pratihast, A.K., DeVries, B., Avitabile, V., de Bruin, S., Kooistra, L. & Herold, M. 2014. Combining satellite data and community-based observations for forest monitoring. *Forests*, 5:2464-2489.

Abstract

Within the Reducing Emissions from Deforestation and Degradation (REDD+) framework, the involvement of local communities in national forest monitoring activities has the potential to enhance monitoring efficiency at lower costs while simultaneously promoting transparency and better forest management. We assessed the consistency of forest monitoring data (mostly activity data related to forest change) collected by local experts in the UNESCO Kafa Biosphere Reserve, Ethiopia. Professional ground measurements and high resolution satellite images were used as validation data to assess over 700 forest change observations collected by the local experts. Furthermore, we examined the complementary use of local datasets and remote sensing by assessing spatial, temporal and thematic data quality factors. Based on this complementarity, we propose a framework to integrate local expert monitoring data with satellite-based monitoring data into a National Forest Monitoring System (NFMS) in support of REDD+ Measuring, Reporting and Verifying (MRV) and near real-time forest change monitoring.

4.1 Introduction

Forests cover approximately 30% of the Earth's land surface (Hansen et al., 2013) and are of immense value to humankind, as they provide habitats for a wide variety of species and play an important role in the global carbon cycle. However, a loss of approximately 2101 square kilometers of tropical forests per year (Hansen et al., 2013) has made a significant contribution to the increase of greenhouse gases (GHGs) in the atmosphere, resulting in accelerated global warming (Gullison et al., 2007). To mitigate this effect, the United Nations Framework Convention on Climate Change (UNFCCC) has proposed an international mechanism called Reducing Emissions from Deforestation and Degradation (REDD+) in developing countries (Gullison et al., 2007; UNFCCC, 2009a). The REDD+ mechanism includes reducing deforestation and forest degradation, forest enhancement, sustainable forest management and conservation (UNFCCC, 2010). Recently, the 19th Conference of Parties (COP) of the UNFCCC in Warsaw, November, 2013, agreed on a collection of seven decisions on REDD+ (UNFCCC, 2013). Together with the REDD+ decisions adopted at previous COPs, these decisions provide international policy guidance (the Rulebook on REDD+) on how countries should deal with REDD+ in the framework of the UNFCCC (UNFCCC, 2013). Besides reduction of carbon emissions, the REDD+ mechanism also includes establishment of national institutions, ensuring co-benefits and safeguards and, above all, creating performance-based financing mechanisms (Gullison et al., 2007; Danielsen et al., 2011).

A country participating in REDD+ requires a reliable, transparent and credible national-level forest monitoring system (NFMS) for Measuring, Reporting and Verifying (MRV) activity data and emission factors (GOFC-GOLD, 2010; Sanz-Sanchez et al., 2013; Herold & Skutsch, 2011). Activity data is defined as the magnitude of human activity resulting in emissions or removals. In the case of forest-related emissions and removals, activity data refers to forest area change (generally measured in hectares), whereas the emission factor is related to the rate of emission of a given GHG from a given source, relative to units of activity (generally measured in tons of carbon per hectare) (Penman et al., 2003). Given that forest change is a dynamic process, monitoring needs to be carried out on a regular basis to support national MRV requirements. Establishing such monitoring systems is presumed to be expensive for developing countries (GOFC-GOLD, 2010; Romijn et al., 2012; Visseren-Hamakers et al., 2012; Bucki et al., 2012). An activity monitoring system should be based on four broad monitoring objectives related to the location, area, time and drivers of forest change. These objectives should be properly integrated with monitoring and MRV systems at the national level. Current schemes for monitoring these activities are based on remote sensing and field measurements mainly from national forest inventories.

Remote sensing has proven to be very useful for deforestation monitoring at the global,

national and subnational scale (Hansen et al., 2013; De Sy et al., 2012; Achard et al., 2010; DeVries & Herold, 2013). However, remote sensing based monitoring of forest degradation and regrowth still remains problematic (Achard et al., 2006; Defries et al., 2007; Vargas et al., 2013), due to cloud cover, seasonality and the limited spatial and temporal resolution of remote sensing observations. Enhancing the interpretation of remote sensing analyses requires substantial ground verification and validation (Strahler et al., 2006). Accomplishing these tasks through national forest inventory data is expensive, time-consuming and difficult to implement across large spatial scales (Gibbs & Herold, 2007; Tomppo et al., 2010).

Community-based monitoring (CBM) is an emerging alternative method for forest change monitoring that promises to be cheaper than conventional monitoring methods (Danielsen et al., 2011; Skutsch et al., 2014a, 2011; Pratihast et al., 2013). CBM methodologies can be organized into two main categories: (i) forest carbon stock measurements for emission factors; and (ii) forest change monitoring for activity data. Results from well-designed forest carbon measurement studies (Danielsen et al., 2013; Topp-Jørgensen et al., 2005; Shrestha, 2010; Pratihast et al., 2012) have demonstrated that local datasets are comparable to professional measurements, while being cheaper to obtain. Furthermore, CBM can be considered as a tool to empower the local communities and raise awareness towards better forest management (Palmer Fry, 2011; Lawlor et al., 2013).

While CBM-based forest carbon stock measurement has been shown to be feasible (Danielsen et al., 2013; Topp-Jørgensen et al., 2005), monitoring of forest change through CBM has not been thoroughly investigated yet. Forest change monitoring is a continuous process, which requires continuous data acquisition, and local communities may act as active in situ sensors (Goodchild, 2007). Their local knowledge could be especially valuable in signaling forest change activities (deforestation, forest degradation or reforestation) and providing valuable information, such as location, time, size, type and proximate drivers of the change events on a near real-time basis (Skutsch et al., 2011). The impacts of these activities are rarely captured comprehensively in national forest inventories or from remote sensing (Danielsen et al., 2011; GOFC-GOLD, 2010; Pratihast et al., 2013). The recent development of hand-held technologies continues to improve and has significantly enhanced the local capacity in data collection procedures (Pratihast et al., 2012). Data acquired by communities can therefore play an essential role in enhancing the efficiency and lowering the cost of monitoring activities, while simultaneously promoting transparency and better management of forests. Thus, local participation within monitoring programmes holds promise for national REDD+ MRV implementation.

Despite the potentials of CBM, the main challenge of using locally collected data lies in the lack of confidence in data collection procedures (Palmer Fry, 2011). The accuracy and reliability of such datasets are often questionable due to inconsistencies arising from the fact that local participants collect data independently of each other. This can further

result in incomplete data collection and a biased representation of changes in a study area (Danielsen et al., 2010). Therefore, data credibility and trustworthiness are major obstacles to the integration of CBM data in NFMS (Conrad & Hilchey, 2011; Skarlatidou et al., 2011). This fact has triggered us to rectify the current shortcomings and expand the current state of knowledge in community-based forest monitoring and its utility in NFMS. Specifically, we aim to check the consistency of local datasets and investigate their complementary use to remote sensing. The purpose of this research is to discover new perspectives and insights into community-based observations. The aims of this paper are to: (i) present the details of a local expert-based forest monitoring system; (ii) assess the spatial, temporal and thematic accuracy of local expert data against independent field-based measurements and high resolution SPOT and RapidEye satellite imagery; and (iii) explore the complementarity of local expert data with remote sensing data. While the UNESCO Kafa Biosphere Reserve in Southwestern Ethiopia is shown here as a case study, the concepts presented in this study are applicable to a broader geographic scope and can be scaled up to the national level in support of NFMS and REDD+ MRV.

4.2 Materials and Methods

4.2.1 Study Area Description

The study area is situated in the Kafa Zone, Southern Nations Nationalities and People's Region (SNNPR), in Southwestern Ethiopia (Figure 4.1). The Kafa Zone is over 700,000 ha in size and was recognized as a Biosphere Reserve by UNESCO's Man and the Biosphere (MaB) programme in March, 2011. This region is characterized by Afromontane cloud forest, with approximately 50% of the land cover still forested. Average annual precipitation in the area is approximately 1700mm, and average annual air temperature is approximately 19°C (Schmitt et al., 2010a). The topography of the Kafa Biosphere consists of mountains and undulating hills, with elevations ranging between 400 to 3100 m. The forest ecosystem provides an important contribution to the livelihoods of the people in the area, including wild coffee, valuable spices and honey from wild bees. It also represents a significant store of forest carbon as above-ground biomass.

4.2.2 Description of the Forest Monitoring System

According to REDD+ monitoring and implementation guidelines, it is important to involve local community groups and indigenous societies to carry out forest monitoring, in particular if there is any prospect of payment and credits for environmental services (UNFCCC, 2013; Lawlor et al., 2013; Stickler et al., 2009). A variety of practical experiences from developing countries, such as Nepal, Tanzania, Cameroon, India, Mexico, Indonesia,

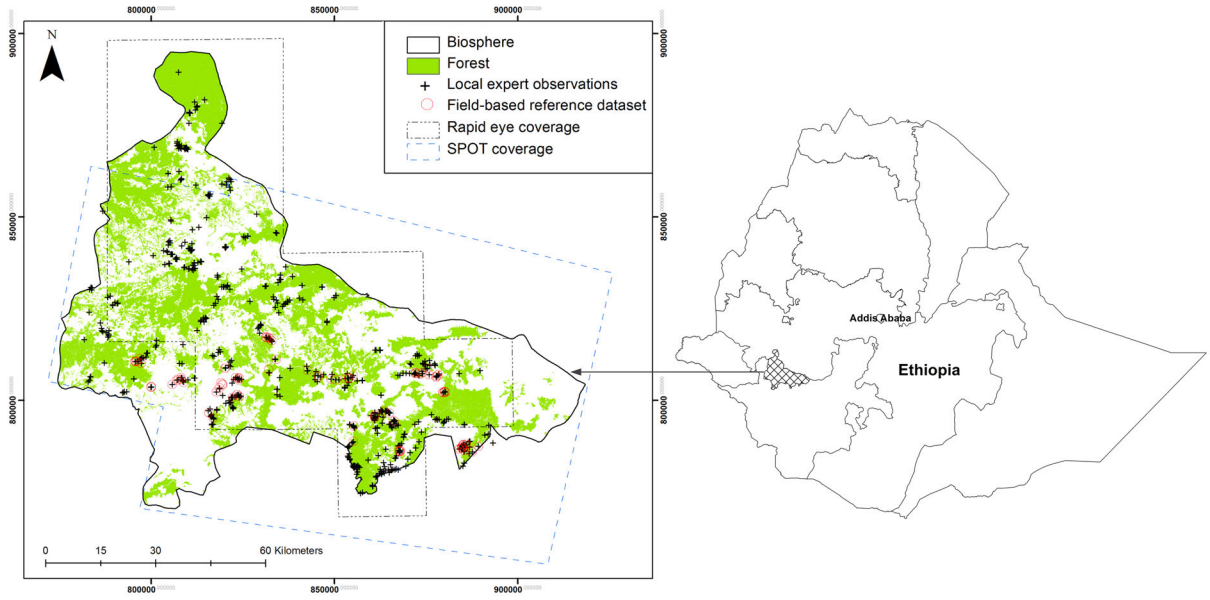

Figure 4.1: Study area in the UNESCO Kafa Biosphere Reserve, Southwestern Ethiopia; local expert observations (black crosses) were compared with a field-based reference dataset (red circles) and high resolution remote sensing data from the SPOT (footprint shown as a blue dotted line) and RapidEye (footprint shown as a black dotted line) sensors.

China, Laos, Cambodia and Vietnam, have demonstrated that local communities can play an essential role in forest monitoring and management programmes (Danielsen et al., 2011, 2013; Topp-Jørgensen et al., 2005; Shrestha, 2010; Pratihast et al., 2012; Ratner & Terry, 2012). However, most of these experiences are limited to carbon stock measurements in support of REDD+ MRV, with few prescribed field methods for establishing activity monitoring (forest change) on the ground (Skutsch et al., 2011; Pratihast et al., 2012). In this study, we present a ground-based system to monitor activity data because of their increasing importance in the context of REDD+. The following setup was designed to contribute an efficient and continuous forest monitoring system for the Kafa Biosphere Reserve.

Selection of local experts. Selection and recruitment of local experts acts as the backbone for a forest monitoring system, as the success of these CBM systems largely depends on the knowledge, commitment, feeling of ownership and competencies of these individuals (Danielsen et al., 2005). The selection process featured in this study is based on a scheme of collaborative design of monitoring with external interpretation of the data, one of five schemes of local involvement in monitoring proposed by Danielsen et al. (2009). A total of 30 local experts were recruited within the frame of the project called "Climate Protection and Primary Forest Preservation - A Management Model using the Wild Coffee Forests in Ethiopia as an Example" under the Nature and Biodiversity Conservation Union (NABU). The recruitment was done through the Kafa Zone Bureau of Agriculture

and Rural Development (BoARD). The selection was done in such a way that it represents on average three experts from each of the 10 woredas (administrative units in Ethiopia). All chosen local experts had at least a secondary level of education and some fundamental understanding of forest management. This selection procedure was seen as a step towards greater community involvement in monitoring activities with the representatives involved from all woredas, assuring the potential for significant enhancement of the monitoring capacity of the project. Apart from monitoring, these experts also bear responsibilities for other project activities, such as the development of ecotourism, reforestation, community plantations, the distribution of energy saving stoves and awareness raising for the sustainable use of forest resources (e.g., honey and wild coffee).

Data acquisition. Two methods of data acquisition were implemented and tested in this study. In the first method, paper-based forest disturbance forms with GPS devices were used by local experts to acquire forest monitoring data. The data collection forms were designed primarily with project monitoring objectives in mind, but also were compliant with REDD+ MRV requirements. This form focused on capturing forest changes, including small-scale forest degradation, deforestation and reforestation. In the second method, mobile devices with integrated GPS and camera functionality were used to increase the ease and simplicity in collection, entering and managing locally acquired data. For this purpose, a decision-based data collection form (Figure 4.2) was designed in XML and was deployed on mobile devices using the Open Data Kit (ODK) Collect application (Anokwa et al., 2009). This form contains optional input constraints, flows that depend on previous input, icon-based user-friendly graphics and local language support. Mobile devices stored the data asynchronously and transferred data to data servers over GPRS, Wi-Fi or USB, as connectivity was available. An online database management system based on ODK Aggregate, postgreSQL and PhP was designed for the proper storage, analysis and visualization of the acquired data. Further details of the adopted proposed data acquisition method can be found in Pratihast et al. (2012). A paper-based data acquisition system was used in 2012, whereas mobile devices were used to collect the data in 2013. Even though the tools used to acquire data were different, the overall form of the design was consistent, with a few key differences in terms of multimedia features.

Training and capacity building program. User friendly training materials were produced for the developed technology and data collection methodology. A series of training events was conducted before and during the implementation of the monitoring activities. The main purpose of training was to enhance the capacity of local experts and to develop approaches and strategies for programme implementation.

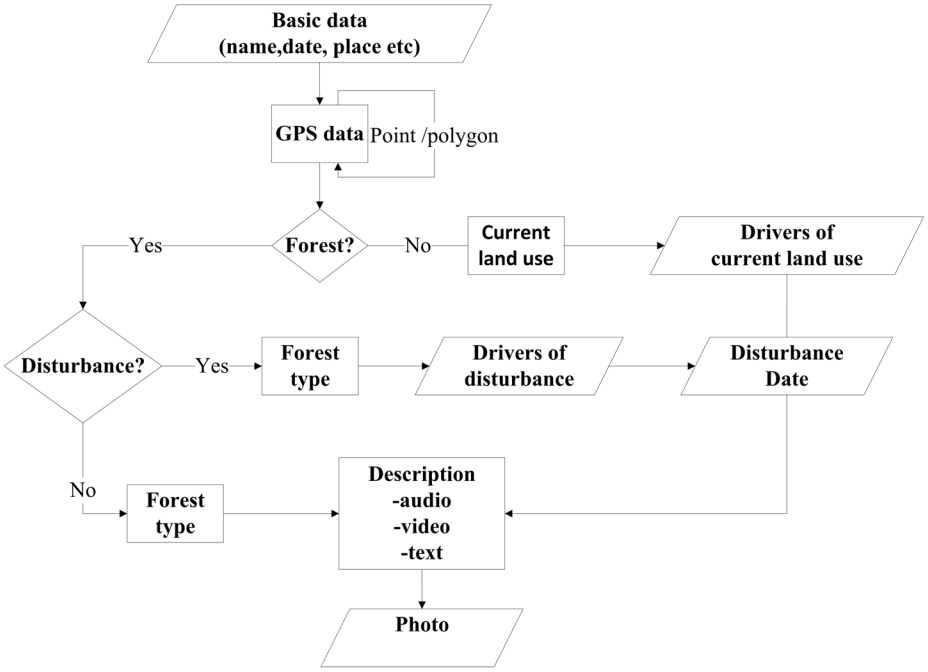

Figure 4.2: Decision-based data acquisition form for local experts; the questions that are posed in the forms depend on answers given to preceding questions; such a design ensures that the questions are relevant to the land cover change being described.

4.2.3 Reference Datasets

Local experts are capable of reporting forest change process at a high temporal frequency. Finding suitable reference data that can thoroughly assess the spatial, temporal and thematic accuracy of these data is difficult, however. In this study, two types of accurate reference datasets were acquired to evaluate the accuracy of these local expert data: field-based reference dataset (FRD) and remote sensing (RS).

Field-based reference dataset (FRD). We conducted a field visit in order to validate the ground data collected by local experts. Due to cost constraints, it was not possible to visit all locations reported by local experts. We selected six accessible woredas owing to practical considerations. These woredas contain more than 65% of the local expert data. Within these woredas, 140 locations (Figure 4.1) were randomly selected and were revisited during November and December, 2013, by a team of professionals. The decision-based data acquisition form on the mobile devices (Figure 4.2) was used by the team of professionals to measure location, size, time, drivers and photographs of change events.

Table 4.1: Summary of the SPOT and RapidEye scenes used in this study.

Sensor	Ground resolution	Year of acquisition	Number of scenes
SPOT4	10m	2005-2006	6
SPOT5	2.5m	2007-2011	8
RapidEye	6.5m	2012-2013	27

Table 4.2: Specific approaches used to assess the spatial, temporal and thematic accuracy of local expert data.

Category	Measured variable local expert data	Reference data	Measures of accuracy
	Location variables (Qualitative)		
Spatial Accuracy	GPS accuracy	Field based	Confidence interval (95%)
	Size of forest change		
Temporal Accuracy	Time of change	Remote sensing	Time lag
	Presence of forest		
Thematic Accuracy	Forest change type	Field based	Error matrix
	Driver of forest change		

Remote sensing (RS). A time series of high resolution remote sensing images acquired between 2005 and 2013 (including pan-sharpened SPOT and RapidEye images) were available for the analysis of reference data (Table 4.1) in the study area (Figure 4.1). The SPOT 4 and SPOT 5 imagery have a ground resolution of 10 m and 2.5 m, respectively, whereas RapidEye has a ground resolution of 6.5 m. Locally-reported forest monitoring locations were visually interpreted based on an approach described by Pohl and Van Genderen (Pohl & Van Genderen, 1998). Following this approach, images were systematically examined and pixels representing forest change areas were manually digitized as polygons. The forest change areas were estimated by calculating the polygon area.

4.2.4 Accuracy Assessment

Several metrics have been proposed by researchers to describe the quality of geographic data (Haklay, 2010; Devillers et al., 2007; Castro et al., 2013). However, no specific list of elements with a consistent definition has yet been agreed upon. The latest attempt to standardize data quality elements was in 2001 with ISO 19113 in 2002 (ISO/TC211, 2002), which proposes the following five elements: completeness, logical consistency, positional accuracy, temporal accuracy and thematic accuracy. In this study, we limited the quality assessment to three of these major categories, namely spatial, temporal and thematic accuracy, since these are essential aspects of forest monitoring datasets (GOFC-GOLD, 2010). The details of the accuracy measures employed in this study are listed in Table 4.2.

Spatial accuracy

In this study, three aspects of the spatial accuracy of the local expert data were assessed, including categorical location information, GPS location information and the estimated size of forest change. The categorical location information included categories for representing the administrative units, like woreda, kebele (administrative sub-unit of a woreda) and a spatial category representing distance to core forest, nearest village and roads (i.e., less than 1 km, 1-2 km, 2-3 km and more than 3 km). To estimate the accuracy of these responses, comparisons were made between the local expert data and the FRD. From this sample, the fraction of correct observations in the total population of local expert reports was estimated using the hypergeometric distribution (Johnson et al., 1992), a discrete probability distribution that describes the probability of obtaining a correct response from a finite population size without replacement. The 95% confidence interval was calculated by using the 0.025 and 0.975 quantiles of this distribution.

In addition to the categorical location descriptors, local experts provided GPS readings for each report. Each reading was associated with a measurement error reported by the GPS receiver. The GPS measurement errors in the local expert dataset were compared with measurement errors in the FRD using a t-distribution (Johnson et al., 1992). Using this distribution, the mean bias (with 95% confidence interval) and the standard deviation between the local expert and FRD GPS errors were calculated.

Finally, the size of forest change polygons mapped by local experts were compared with change polygons digitized from visually interpreted high resolution SPOT and orthorectified RapidEye time series imagery. Forty deforestation polygons falling within the spatial extent of the SPOT and RapidEye time series were selected. The relationship between the size of field-delineated change areas and polygons digitized from high-resolution imagery was evaluated using a t-distribution.

Temporal accuracy

Recording the timing of forest change is essential for the implementation of a robust forest monitoring system. Assessing the temporal accuracy of local monitoring data remains a challenge due to a lack of reference time series imagery of sufficient temporal density and spatial resolution that can describe disturbances in near real-time (Kennedy et al., 2007; Cohen et al., 2010; Schroeder et al., 2011). To overcome this limitation, only the area for which time series images of SPOT and RapidEye were available (Table 4.1) was used for this analysis. Here, a visual interpretation of the time series of satellite images for each local data set was carried out, and the time of forest disturbance was estimated for each data set. Furthermore, a temporal lag between the reference satellite datasets and local expert datasets was calculated to determine the average time delay or temporal lag of

deforestation:

$$L = T_{dist,RS} - T_{dist,LE} \tag{4.1}$$

where L is the temporal lag (in years) and $T_{dist,RS}$ and $T_{dist,LE}$ are the disturbance times detected by remote sensing and local experts, respectively.

Thematic accuracy

Attributes, such as the presence or absence of forest, forest change type and drivers of forest change were included in the assessment of thematic accuracy. The accuracy of these variables was assessed by comparing local expert dataset with the field-based reference dataset. An error matrix was produced for each category and used to derive producer's accuracy, user's accuracy and the overall accuracy (Foody & Boyd, 2002).

4.3 Results

4.3.1 Characteristics of Local Monitoring Data

Attributes of the local expert monitoring data

In this study, we focused on deforestation and forest degradation processes to illustrate the major attributes of the data collected by local people (Figure 4.3, Table 4.3. The results show that local experts have documented forest change processes, which include spatial (location and size), temporal (time of change events) and thematic (type of change, driver of change and photograph from the North, East, West and South directions) information. Furthermore, deforestation, the conversion from forest to non-forest land (GOFC-GOLD, 2010), and forest degradation, negative changes in forest biomass without conversion to another land cover type, could be mapped separately using data provided by local experts (Figure 4.3). In this case, local experts tried to delineate exact deforestation areas from the ground by recording multiple GPS location around the boundary (Figure 4.3a). On the other hand, forest degradation is a gradual process without a fixed boundary (GOFC-GOLD, 2010) and could therefore not be mapped with such precision. In such cases, local experts provided the central location and approximate area affected rather than an exact change polygon (Figure 4.3b).

Monitoring frequency

During the period of January, 2012, to December, 2013, a total of 755 locations were observed (Figure 4.4). Of these, 46% were labelled as forest degradation, 25% as defor-

estation and 30% as reforestation. All data in 2012 were acquired using paper forms with hand-held GPS devices, whereas in 2013, data were acquired using mobile devices. In general, local observations were spread equally over the whole Biosphere Reserve (Figure 4.1). However, monitoring efforts were not consistent throughout the year (Figure 4.4). Irregularities in monitoring activities were influenced by a wide range of factors, including the timing of training and capacity building programmes and adverse weather conditions. The number of received monitoring forms (in 2012) and digital observations (in 2013) increased during training and capacity building programme (January to March), while it decreased during the rainy season (July to September).

Drivers of forest change

Drivers of forest change were mostly associated with agriculture expansion and settlement expansion, followed by charcoal and firewood extraction, intensive coffee cultivation, timber harvesting and natural disasters, which mainly included landslides erosion and windfall. Many of the drivers were found to co-occur at a single location (Table 4.4). In the case of agricultural expansion, 34 of the events were attributed to agriculture expansion alone, whereas 185 events were attributed to agriculture expansion together with charcoal and fire wood collection, and 61 of those changes were found to be due to the co-occurrence of agriculture expansion and timber harvesting. This observation is logical considering that agriculture expansion in Kafa Biosphere Reserves is in fact a gradual process coupled with forest degradation. After demarcation of a portion of forest area for agricultural development, a farmer commonly keeps much of the forest for the first couple of years to harvest coffee, spices, fuel wood, charcoal and timber, before the forest is fully cleared to make way for agricultural activities.

4.3.2 Results of accuracy assessment

Spatial accuracy

A breakdown of the estimated fraction correct of assigned spatial categories with a 95% confidence interval is shown in Table 4.5. The spatial accuracy varied considerably across the various spatial categories included in the monitoring forms. The woreda was recorded with the highest mean fraction correct of 0.92, whereas the estimated distance to core forest was found to have the lowest mean fraction correct of 0.71.

A comparison of GPS errors reported by local experts with those reported in the FRD showed a slight systematic error of 0.65 m between the two datasets (Table 4.6). A similarly slight bias was found between forest change areas as reported by the local experts and forest change areas derived from high resolution remote sensing imagery, in cases where these areas did not exceed 2 ha (Table 4.6). In larger change areas (exceeding

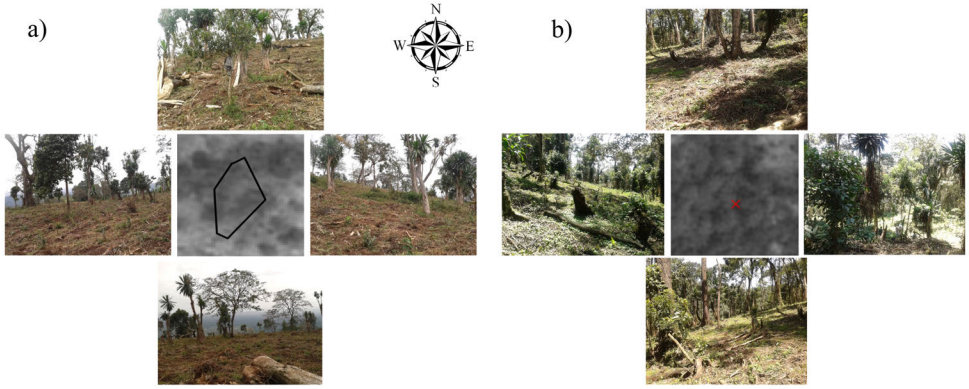

Figure 4.3: Examples of (a) deforestation monitoring and (b) forest degradation monitoring by local experts. Observations were mapped either as polygons (a) or point (b) features, depending on the process being described; each form was accompanied by four photos representing the north, east, south and west perspectives. The attribute tables associated with these observations are shown in Table 4.3.

Table 4.3: Attribute tables derived from local expert observations of deforestation and forest degradation (shown in Figure 4.3a and b, respectively).

Category	Measured Variables	Value of Deforestation (Figure 4.3a)	Value of Forest Degradation (Figure 4.3b)
Spatial	Woreda	Gewata	Gewata
	Kebele	Ganity	Ona
	Distance to Road	More than 3km	1-2km
	Distance to Nearest Village	1-2km	1-2km
	Distance to Core Forest	More than 3km	More than 3km
	GPS coordinates (Lat, Lon)	(7.53, 35.84)	(7.54, 35.81)
Temporal	Disturbance Date	03-18-2013	03-18-2005
	Disturbance Type	Deforestation	Forest degradation
Thematic	Driver of Disturbance	Agricultural expansion, timber harvesting and fuelwood	Coffee cultivation, timber harvesting and fuelwood
	Size of Disturbance	2 ha	4 ha

2 ha), however, the absolute bias increased to 1.06, implying that local experts had systematically underestimated the area of large change polygons.

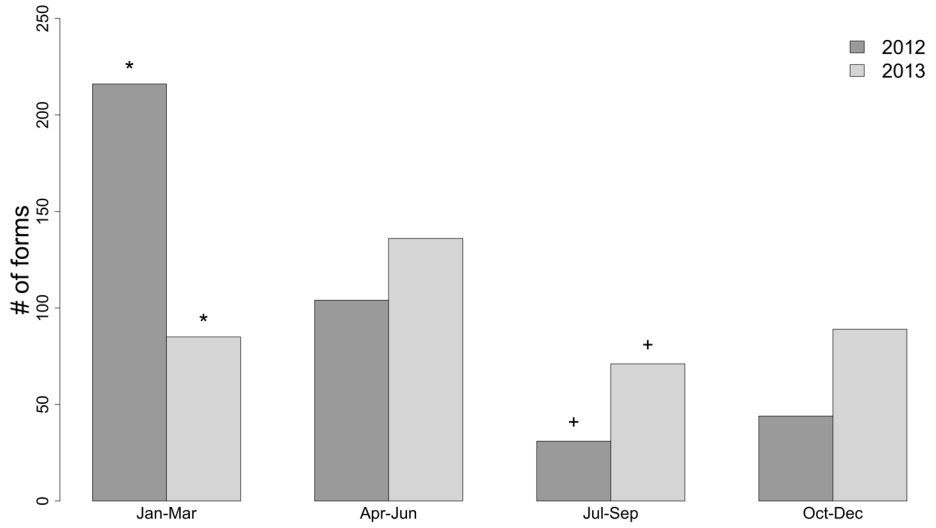

Figure 4.4: Number of observations collected by local experts in 2012 and 2013; all observations in 2012 were acquired using an analogue (paper-based) system, whereas observations acquired in 2013 were collected using either analogue or digital (smart phone-based) methods. Periods following training and capacity building activities (*) and rainy periods (+) are indicated on the plot.

Table 4.4: Number of instances of the co-occurrence of forest change drivers. Numbers along the diagonal indicate the number of instances that a particular driver was reported alone. AE: Agricultural expansion. SE: settlement expansion. CF: Charcoal and fuelwood. IC: Intensive coffee cultivation. TH: Timber harvesting. ND: Natural disaster.

	AE	SE	CF	IC	TH	ND
AE	34					
SE	48	42				
CF	112	75	57			
IC	0	55	76	19		
TH	61	70	44	10	15	
ND	13	17	2	1	2	2

Table 4.5: Fraction correct of local data assignment to spatial categories.

Spatial category	Fraction correct
Woreda	0.92 ± 0.04
Kebele	0.78 ± 0.06
Distance to nearest village	0.77 ± 0.06
Distance to nearest road	0.75 ± 0.06
Distance to core forest	0.71 ± 0.06

Table 4.6: Positional accuracy of local expert data.

Measure	Mean bias	Standard deviation
GPS error (m)	0.65 ± 0.03	1.79
Size of forest change (<2ha)	0.16 ± 0.03	0.29
Size of forest change (>2ha)	-1.06 ± 0.12	1.26

Temporal accuracy

Each forest change event was recorded by local experts with a time stamp that represents the time at which the process of change took place. In total, 40 deforestation and 60 degradation locations were visually assessed from high resolution remote sensing (SPOT and RapidEye) imagery. An example of the visual interpretation of high resolution time series of SPOT5 (2008-2010) and RapidEye imagery (2012-2013) is shown in Figure 4.5. The locally mapped polygon is displayed at the center of each subset of image. The interpretation shows that the forest cover was significantly reduced after 2012.

The histogram of the temporal accuracy of locally determined change dates compared to high resolution imagery for deforestation and forest degradation is shown in Figure 4.6. Here, a positive temporal lag indicates that local experts indicated a change date earlier than that determined using remote sensing data, and a negative time lag indicates the reverse situation. The results reveal that 33% of deforestation events reported by local experts corresponded accurately to the dates observed in the remote sensing data. In other cases, 25% and 20% of total deforestation events as observed from remote sensing were detected one and two years earlier than the local reported time, respectively (Figure 4.6). On the other hand, the comparison of dates associated with forest degradation as reported by local experts shows that the majority of these signals were recorded one (32%) to two (22%) years earlier than dates detected by remote sensing.

Thematic accuracy

Thematic information is one of the added values of the local expert dataset compared to remote sensing. Summaries of the accuracy assessment of three thematic elements (the presence of forest, forest change type and drivers of forest change) are shown in Table 4.7.

The results show an overall accuracy of 82% for thematic elements compared to the field-based reference dataset. The presence of forest was found to have a producer's accuracy of 92%, a user's accuracy of 93% and an overall accuracy of 94%. The drivers of forest change had a comparatively lower producer's accuracy of 71%, a user's accuracy of 68% and an overall accuracy of 69%.

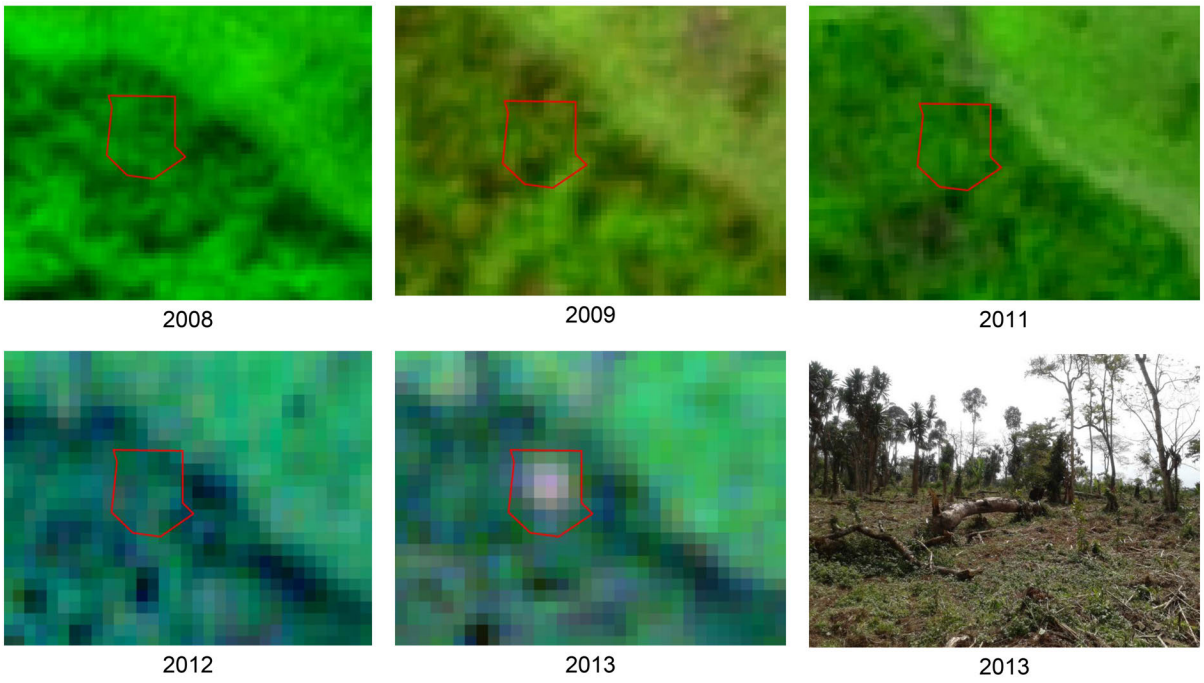

Figure 4.5: Example of visual interpretation to assess the temporal accuracy of the local expert dataset; the image subset is based on SPOT5 data from 2008 to 2011 (red = Band 3, green = Band 1, blue = Band 2) and two RapidEye images from 2012 and 2013 (red = Band 3, green = Band 2, blue = Band 1); a ground photograph taken by a local expert in 2013 is also shown; the red polygon is the forest change mapped by a local expert; the forest change occurred between 2012 and 2013.

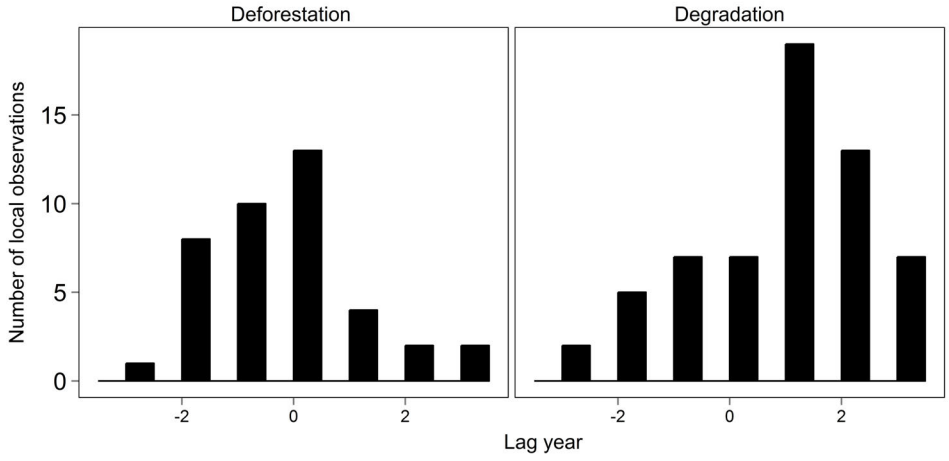

Figure 4.6: Histogram of time lags in capturing deforestation (left) and forest degradation by remote sensing (SPOT and RapidEye) imagery (right); a time lag is defined as the difference between change dates observed from remote sensing image interpretation and those dates recorded by local experts.

Table 4.7: Accuracy assessment of local expert data compared to field-based reference dataset in the thematic domain.

Elements	User's accuracy	Producer's accuracy	Overall accuracy
Presence of forest	93%	92%	94%
Forest change type	83%	84%	83%
Driver of forest change	71%	68%	69%

4.4 Discussion

4.4.1 Local Expert-Based Forest Monitoring System

The establishment of robust and reliable NFMS in developing countries is an expensive and challenging task. Several studies have shown that CBM has the potential to increase the saliency, credibility and legitimacy of such forest monitoring systems (Danielsen et al., 2011, 2013; Topp-Jørgensen et al., 2005; Shrestha, 2010; Danielsen et al., 2014). However, current studies do not clearly describe the following aspects of forest change monitoring (related to activity data): (1) the long-term operational procedures of community involvement; (2) technology selection; (3) consistency of local datasets; and (4) complementarity with remote sensing data. In this regard, we demonstrate an operational forest monitoring system that includes local expert activity monitoring data in the UNESCO Kafa Biosphere Reserve, Southern Nations, Nationalities and People's Region (SNNPR), Ethiopia. In general, our monitoring setup allows local experts to collect forest change variables, such as geo-location, size of forest change, time of forest change and proximate drivers behind the change, in more detail. Similar to previous studies (Pratihast et al., 2012; Bowler et al., 2012), we also found that the use of mobile devices has a clear advantage over a paper-based system in capturing photographs and multimedia information from the ground and improves the local capacity in data collection, transmission and visualization procedures (Figure 4.3 and Table 4.3). Furthermore, our results show that these datasets are fully structured in terms of spatial, temporal and thematic detail and capable of describing the forest change process well. While our results are based on a local case study, these monitoring activities have the potential to be scaled up to the national level and integrated with an NFMS.

The local expert-based forest monitoring system in this study faced some critical barriers, such as systematic coverage and consistency in monitoring frequency. Our results show that 53% of the local data were collected within 1 km of the local road network, hindering systematic coverage of the study area. This restriction is a result of poor road infrastructure or a lack of transportation means. A recent study in Southwestern Ethiopia has shown that most forest change occurs in remote locations far from urban areas (Getahun et al., 2013), suggesting that much of these changes could not be fully captured by local

experts alone. This mobility barrier could be overcome by engaging local communities who live near the forest areas of interest.

We also observed that the frequency of local data collection depends largely on weather conditions and motivations towards monitoring activities. A decrease in data acquisition was seen during the rainy season, indicating that weather has a significant impact on the mobility of local people. This reduction in data frequency may also be due to a decrease in disturbance activities by farmers during this time. The motivation can be triggered by providing local experts with adequate incentives for conducting monitoring activities even during adverse weather conditions and also providing them with the necessary accessories and travel means. Regular training and capacity building programmes should also be conducted to keep the local experts updated. While such initiatives in motivating the local experts towards efficient monitoring may not fill the data gap completely, they could help to substantially increase the commitment and long-term engagement of local people towards monitoring.

4.4.2 Critical Review of the Accuracy of Local Datasets

In this study, we assessed the spatial, temporal and thematic accuracy of the local expert dataset. Identifying the factors influencing these accuracies is important to understanding the role that this dataset can play in a forest monitoring system. The main influencing factors are explained in detail below.

Spatial accuracy

Spatial accuracy was influenced by three main factors: interpretation of administrative boundaries, GPS errors and failure to map full polygons. First, the administrative boundaries are not always visible on the ground. Local experts may incorrectly interpret these boundaries when they are away from their own villages. This error might be solved by providing base maps prepared by an Ethiopian mapping agency and regional governments during field work, which may contain the updated information regarding these administrative layers.

Second, GPS location error arises due to the weak signal caused by dense forests and high slopes. Mobile devices used in this study achieve maximum GPS accuracy by taking the average measurement from all available satellites reached in a given time. GPS accuracy could be improved by using averaging positional measurements over a longer period of time (Sigrist et al., 1999).

Third, the area of change estimated by local experts was found to be biased due to difficulties in mapping large change polygons in the field. When an insufficient number of polygon vertices was mapped by the local experts, resulting polygons were smaller

than those delineated by visual interpretation from remote sensing imagery, giving rise to a negative bias in field-based area estimations. These errors could be avoided by implementing a visualization feature in the mobile device-based forms, whereby local experts can see the polygon they have mapped while in the field. Based on observed errors that arise in the mapping process, these can be corrected by the local experts.

Temporal accuracy

To assess temporal accuracy of the local dataset, temporal lag was calculated based on forest disturbance dates determined using remote sensing time series data. The temporal lag in detecting deforestation and degradation (Figure 4.5) is not necessarily a direct result of inaccuracies in the local dataset, but rather highlights differences in the interpretation of change between ground-based and satellite-based methods in the case of deforestation and forest degradation.

Evidence from our study indicates that deforestation is detected earlier using higher resolution SPOT and RapidEye imagery compared to local expert observations. This time lag in deforestation detection is likely due to differences in the interpretation of change events. Since optical remote sensing observes changes in the canopy cover of forests, changes delineated by visual interpretation of remote sensing time series were directly related to land cover changes. Local experts, on the other hand, reported changes in land use (e.g., the conversion of forest land to agricultural land; Verburg et al., 2011). The difference between the land cover and land use-based definition of deforestation is important in this case, because actual land use change typically follows several years of gradual canopy cover change. Whereas deforestation was understood by local experts to mean the conversion of forest land to cropland, changes in the canopy cover in the years preceding this change were often interpreted as land cover change (deforestation) by the remote sensing analyst, thus giving rise to the temporal lag observed in this study (Figure 4.6).

Interestingly, a reverse temporal lag was found in the case of forest degradation reported by local experts. Optical remote sensing data are known to have limitations with regards to the detection of low-level degradation, especially when driven by fuelwood collection (Skutsch et al., 2011), as was found in this study (Table 4.4). This low level degradation generally takes place underneath the forest canopy and is thus not detectable using remote sensing data until degradation rates are such that canopy openings begin to appear. For this reason, a delay in degradation detection by remote sensing was found in this study. In many cases, low-level degradation is not at all detectable with optical remote sensing data when degradation fails to result in canopy openings. In this case, local datasets convey a clear advantage when combined with remote sensing data to achieve a comprehensive description of the degradation processes.

Thematic accuracy

While analysis of the thematic accuracy of the local expert dataset showed a high overall accuracy (82%), the drivers of forest change were reported with a relatively lower accuracy (69%). One possible explanation for this lower accuracy could be due to differences in perceiving the proximal drivers of forest change by local experts and the team of professionals who were involved in collecting FRD. Another explanation for this lower accuracy could be the complexity of multiple drivers and dynamic nature of land use changes, which make categorization of forest change drivers difficult. In the case of Ethiopia, multiple drivers, such as fuelwood extraction, grazing, timber harvesting and agriculture expansion, operate together, and choosing the most prominent driver for such a situation is difficult (Table 4.4). The reporting of drivers could be improved through improved form design (e.g., using simplified classes and iconography).

4.4.3 Role of Local Datasets in an Integrated Monitoring System

Complementarity with remote sensing analysis

The local data stream presented in this paper is not an investigation to replace or compete with remote sensing-based monitoring data, which is conventionally used in forest area change analyses, but is rather envisioned to be complementary to these data. The complementarity between remote sensing and community-observations is described below in the context of several key REDD+ MRV questions (Figure 4.7).

The first question for REDD+ MRV is the location of change. Remote sensing approaches are highly suitable for answering this question. The value of remote sensing data and their successful implementation to monitor forest change on various scales (global, regional, national, etc.) and at various resolutions is well established (Hansen et al., 2013; Achard et al., 2010). The advantages of these methods include consistent data acquisitions, automated data processing and large area coverage (De Sy et al., 2012; Roy et al., 2014; Hansen & Loveland, 2012). A main shortcoming is the need for spatially-explicit ground (in situ) data to enhance the reliability of these remote sensing products (Li et al., 2013). There is always a lack of spatially-explicit and statistically representative ground data, because this information is expensive and time consuming to acquire. To address this deficiency, local data streams proposed in this study may provide a useful way to complement remote sensing data. The spatial accuracy results of the local expert data (Tables 5 and 6) show that local datasets can be used to better understand information related to local administration (e.g., the name of the district and village) or geographical characteristics (distance to roads, nearest village and core forest). Similarly, remote sensing may help to add value to local data streams by providing wall-to-wall coverage, which can be used to validate local data streams. The synergies of both methods may lead to a more efficient

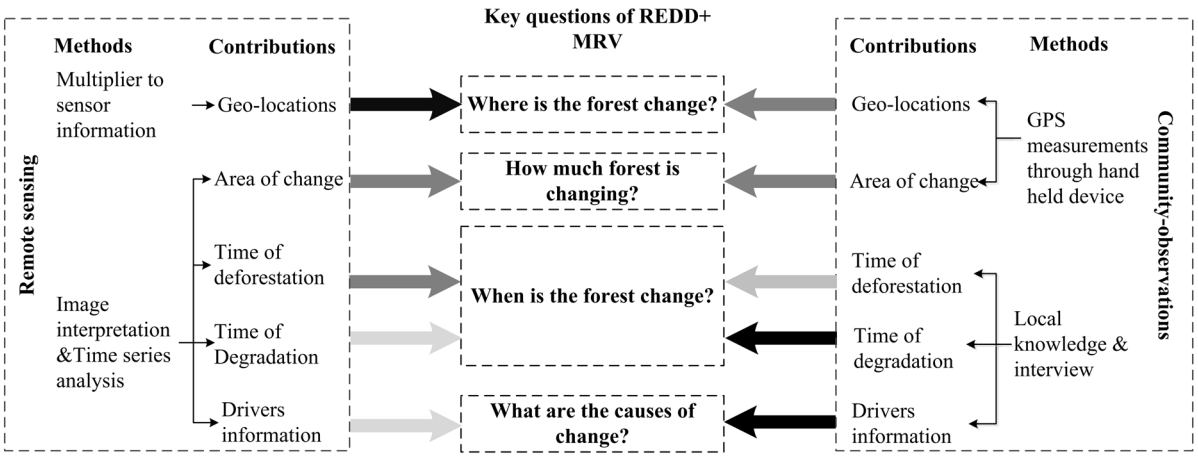

Figure 4.7: Contributions of remote sensing and community-observation for REDD+ MRV monitoring objectives related to location, size, timing and drivers of forest change; black arrows indicate a very strong contribution; dark grey arrows indicate a reasonably strong contribution; and light grey arrows indicate a limited contribution to these monitoring objectives.

monitoring system for data acquisition and to rendering reliable information.

The second REDD+ MRV question is the area of forest change. Both remote sensing and local datasets have their own difficulties when used to map the area of forest change. In general, remote sensing plays a promising role for mapping larger areas, because of its ability to map wall-to-wall changes (Achard et al., 2010). However, the trade-offs between the spatial and temporal capabilities of remote sensing limits their use to monitoring small-scale forest change (De Sy et al., 2012). Since we have shown that local datasets are sufficiently accurate to track small forest changes, the overall mapping of forest change area can be enhanced by exploiting the synergy between these datasets.

The third REDD+ MRV question is related to the timing of forest change. Historical archives of remote sensing imagery and the prospect of a continuous data stream based on new satellites, such as Landsat 8 and Sentinel-2, offer a possibility to analyze the temporal patterns of forest change and the impact of human activities (Hansen & Loveland, 2012; Drusch et al., 2012). However, the temporal accuracy of detected changes based on this imagery depends on: (1) the availability of cloud-free observations; (2) the seasonality and climate trends; and (3) the spatial scales of land cover change phenomena. In areas with high persistent cloud cover, the detection of actual changes can be delayed due to missing observations, and the seasonality of vegetation can obscure actual changes. Climate events, such as major droughts, can result in temporal signals that resemble actual change, thus contributing to errors. Finally, the scale of change can influence the time at which a change is detected from space. Specifically, we have seen in this study that higher resolution SPOT and RapidEye imagery detect deforestation earlier than local experts, whereas the detection of forest degradation using remote sensing data is

delayed compared to that of local experts. Reports of small-scale deforestation and forest degradation from local experts can therefore contribute to an improved understanding of change processes, and the integration of both methods should lead to a more efficient system to signal new changes in near real-time.

The final REDD+ MRV question is related to the driver of forest change. NFMS for REDD+ needs to be designed to track and completely document the drivers of forest change processes (UNFCCC, 2013). Drivers vary across regions (Hosonuma et al., 2012), leading to different dominant forest change processes and different approaches needed to tackle these drivers (Skutsch et al., 2011). In general, remote sensing has limited capabilities to track forest change drivers, whereas community-observations are very accurate in reporting these drivers. These drivers of change can be better understood with an intimate knowledge of forest change processes, and this information has the potential to enhance the pertinence of the remote sensing data analysis. Information on drivers collected by local experts thus presents new opportunities for monitoring forest change events.

Link to the National Forest Monitoring System: "Up-Scaling"

The UNFCCC encourages developing countries to establish an NFMS in support of REDD+ MRV (UNFCCC, 2013). The NFMS needs to monitor forest carbon and changes in compliance with the five IPCC principles: consistency, transparency, comparability, completeness and accuracy (Herold & Skutsch, 2011; Penman et al., 2003). However, most developing countries have a low monitoring capacity, and the development of these capacities will take considerable time and resources (Romijn et al., 2012). In this research, we found that local communities can monitor forest changes in a cost-effective way. By scaling up CBM activities to the national level, these capacity gaps can be addressed in an efficient and cost-effective way. Developing countries should therefore give priority to CBM in developing their NFMS and MRV systems.

The UNFCCC REDD+ also offers an opportunity for safeguards, biodiversity conservation and other ecosystem services beyond carbon sequestration (Dickson & Kapos, 2012; Chhatre et al., 2012; Torres & Skutsch, 2012). Monitoring all of these elements within REDD+ is a challenge. Our proposed local monitoring system is based on well-established monitoring principles and experiences. The main advantage of the system is the flexibility in design. The data acquisition side of the system can be easily modified, and it can incorporate other types of environmental monitoring variables. Thus, the integration of other environmental monitoring variables may lead to long-term benefits (Defries et al., 2007) and shape the future of REDD+ monitoring and implementation efforts (Visseren-Hamakers et al., 2012).

4.4.4 Future Research Directions

Although our study is founded on the argument that considerable progress can be made towards community-based forest monitoring in REDD+, there is a clear need for improvements to the monitoring set-up. The first area of improvement is the engagement of local communities that have an impact on the success of the proposed monitoring setup. In our study, local experts were employed and the acquaintance of the local people with their local area was a clear advantage in monitoring local changes. Moreover, the feeling of ownership that local people have for their locale has a strong influence on the motivation to participate. Local capacities should therefore be developed through extensive training. The second area of improvement is related to data entry errors. Advancements in hand-held devices, such as smart phones and PDA devices, will improve local participation within monitoring programmes. The application of mobile devices can improve the local participation and reduce data entry error within monitoring programmes (Pratihast et al., 2012). However, further improvement is needed in terms of user-friendly form design. Specifically, drop-down selection options and multimedia (photos, video and audio) are preferable to manual text entry, which is prone to entry errors. Finally, there is a need to integrate near real-time data streams from both satellites and CBM. Recently, efforts have been made towards improving near real-time forest monitoring using remote sensing data (Achard et al., 2010; Verbesselt et al., 2012). However, the efficacy of near real-time monitoring from ground-based sources, such as CBM, has not yet been investigated. Addressing these gaps in CBM is an important next step in the arena of REDD+ MRV and NFMS.

4.5 Conclusions

Community-based monitoring is gaining popularity, and large volumes of ground observations that can potentially enhance forest monitoring are being generated. To tap into this potential, we need a better understanding of local data contributions, in particular their consistency and complementarity with remote sensing.

In this article, we present a novel approach to monitor forest change through local experts and evaluate the accuracy and complementarity of local datasets over field-based reference measurements and high resolution satellite imagery from SPOT and RapidEye. We demonstrate the application of the approach by implementing a CBM case study with 30 local experts in the Kafa Biosphere Reserve in Ethiopia. The proposed approach helps us to understand the characteristics and competencies of local datasets. The results show that the local experts are accurate compared to field-based observations and high resolution remote sensing in providing the spatial, temporal and thematic details of the forest change process. Local monitoring data also offer a way to complement and enhance

remote sensing-based forest change analysis. In future research, we foresee new ways to integrate local expert monitoring data with satellite-based monitoring data into NFMS in support of REDD+ MRV and near real-time forest change monitoring.

Chapter 5

Integrating Landsat time series and community-based monitoring data to characterize forest changes

This chapter is based on:

DeVries, B., Pratihast, A.K., Verbesselt, J., Kooistra, L. & Herold, M. 2015. Characterizing forest change using community-based monitoring data and Landsat time series. *PLoS ONE Forests*, under review.

Abstract

Increasing awareness of the issue of deforestation and degradation in the tropics has resulted in efforts to monitor forest resources in tropical countries. Advances in satellite-based remote sensing and ground-based technologies have allowed for monitoring of forests with high spatial, temporal and thematic detail. Despite these advances, there is a need to engage communities in monitoring activities and include these stakeholders in national forest monitoring systems. In this study, we analyzed activity data (deforestation and forest degradation) collected by local forest experts over a 3-year period in an Afro-montane forest area in southwestern Ethiopia and corresponding Landsat Time Series (LTS). Local expert data included forest change attributes, geo-location and photo evidence recorded using mobile phones with integrated GPS and photo capabilities. We also assembled LTS using all available data from all spectral bands and a suite of additional indices and temporal metrics based on time series trajectory analysis. We predicted deforestation, degradation or stable forests using random forest models trained with data from local experts and LTS spectral-temporal metrics as model covariates. Resulting models predicted deforestation and degradation with an out of bag (OOB) error estimate of 29% overall, and 26% and 31% for the deforestation and degradation classes, respectively. By dividing the local expert data into training and operational phases corresponding to local monitoring activities, we found that forest change models improved as more local expert data were used. Finally, we produced maps of deforestation and degradation using the most important spectral bands. The results in this study represent some of the first to combine local expert based forest change data and dense LTS, demonstrating the complementary value of both continuous data streams. Our results underpin the utility of both datasets and provide a useful foundation for integrated forest monitoring systems relying on data streams from diverse sources.

5.1 Introduction

Recent years have seen a dramatic increase in the attention being given to the plight of tropical forests. This attention is due to the importance that these ecosystems have with regards to global climate change (Gullison et al., 2007; van der Werf et al., 2009), biodiversity loss (Laurance et al., 2012; DeFries et al., 2005) and ecosystem services (Aerts et al., 2015). In recognition of the considerable impact human activities are having on tropical forest systems worldwide, a range of initiatives have been launched to mitigate against the adverse effects of tropical forest loss. One such programme - the Reducing Emissions from Deforestation and Degradation (REDD+) - is designed to provide incentives to developing countries to reduce deforestation and forest degradation rates and strengthen conservation measurements (Angelsen, 2009; Herold & Skutsch, 2011).

Countries wishing to engage in REDD+ are required to undertake monitoring measures enshrined in the Measuring, Reporting and Verification (MRV) framework (DeVries & Herold, 2013; Herold & Skutsch, 2011). Estimates of forest area changes in baseline and reporting periods - termed "Activity Data" - comprise an important component of REDD+ MRV (Penman et al., 2003). While the choice of methods and technologies used to fulfill MRV requirements are left up to individual participant countries, satellite remote sensing data have been widely recognized as essential data sources for comprehensive mapping and quantification of forest area change (De Sy et al., 2012). In addition to the various change detection approaches already existing (Coppin et al., 2004), MRV-related capacity gaps among participant countries (Romijn et al., 2012) have resulted in a surge of new forest change monitoring methods and case studies in the tropics. While deforestation monitoring is operational in many cases, forest degradation is still poorly understood in many areas of the tropics (DeVries et al., 2015; Tyukavina et al., 2013; Thompson et al., 2013). This gap is due to the nature of degradation processes, including complex governance structures and drivers, as well as technical challenges related to degradation monitoring, and thus remains a bottleneck to the implementation of effective MRV systems (Mertz et al., 2012).

Recent years have seen a paradigm shift in satellite-based forest monitoring, with dense time series increasingly being used in favour of conventional bi-temporal image comparison approaches (Banskota et al., 2014). This shift is largely due to open data policies, such as the decision to release the entire Landsat archive to the public in 2008, which has spurred considerable development in Landsat time series (LTS) based monitoring methods (Wulder et al., 2012). These methods have allowed for forest change monitoring with gains in both resolution and accuracy in the temporal domain (Zhu et al., 2012b; Reiche et al., 2015a; DeVries et al., 2015; Dutrieux et al., 2015). Furthermore, a number of operational forest monitoring systems based on dense satellite time series have emerged in the tropics, such as the PRODES and DETER systems of the Brazilian Space Agency (INPE,

2014b,a), the Monitoring of the Andean Amazon Project (MAAP; Amazon Conservation Association, 2015), the Global Forest Watch (World Resources Institute, 2014; Hansen et al., 2013) and others.

Not only do forest monitoring methods based on LTS allow for rapid detection of forest disturbance, but they also allow for descriptions of forest change trajectories well beyond what is possible with conventional methods (Kennedy et al., 2010; Huang et al., 2010). Change trajectory analysis usually involves the segmentation and/or reduction of a time series to describe the change history at a particular location. Several segmentation methods have been described in the literature. The Breaks For Additive Season and Trend (BFAST) method detects abrupt and gradual changes in time series decomposed into season, trend and noise components (Verbesselt et al., 2010). The Detecting Breakpoints and Estimating Segments in Trend (DBEST) method similarly segments time series to measure timing, type and magnitude of changes (Jamali et al., 2015), but without considerations for seasonal variations as in BFAST. The Landsat-based detection of Trends in Disturbance and Recovery (LandTrendR) method segments annual or composited Landsat time series using a series of parameters describing segment length, inter-segment angle and other characteristics of time series trajectories (Kennedy et al., 2010). While these and other time series segmentation algorithms have been proven to be useful in describing changes or other state variables using satellite time series, they have all been developed for regularly timed observations such as MODIS 16-day composites (Verbesselt et al., 2010), AVHRR GIMMS3g data (Jamali et al., 2015) or annual Landsat composites (Kennedy et al., 2010). Few studies have applied analogous techniques to time series with missing data ("irregular" time series) such as LTS data using all available observations (Zhu & Woodcock, 2014).

Even with increasingly sophisticated tools for quantifying and describing forest changes using satellite image time series, the involvement of local people in monitoring activities (such as in Community-Based Forestry projects) is necessary to ensure sustainability (Conrad & Hilchey, 2011; Boissière et al., 2014) and equity (Skutsch et al., 2014b) in forest management programmes such as REDD+. Community involvement in monitoring activities has also been shown to reduce overall monitoring costs with negligible trade-offs in data quality for certain monitoring applications (Pratihast et al., 2012). Use of community-based monitoring (CBM) data or volunteered geo-information (VGI) data have been previously shown to be promising in such applications as land cover validation (Foody & Boyd, 2013), climate change impact studies (Delbart et al., 2015) or forest carbon stock estimation (Pratihast et al., 2012; Brofeldt et al., 2014). Emerging technologies such as smart phones (Pratihast et al., 2012; Ferster & Coops, 2015) improve the quality and consistency of these data through functionalities such as integrated photos and geo-tagging capabilities (Bigagli et al., 2015).

Another area where CBM or VGI data could add considerable value is in the training and

validation of forest change detection methods, since the validation of historical change estimates is often severely limited by a lack of reliable historical reference data (Cohen et al., 2010). However, very few studies have been undertaken to demonstrate the utility of local monitoring data in such a context. Pratihast et al. (2014) showed that local forestry experts in southern Ethiopia can describe forest changes with much higher thematic details than is possible with satellite time series, but some trade-offs were encountered with regards to spatial coverage and temporal accuracy. Notably, this study found that local experts were particularly adept at describing locations and drivers of low-level degradation (Pratihast et al., 2014), a great deal of which is not adequately captured by satellite-based methods (DeVries et al., 2015). There is currently a need for more research on approaches to integrate CBM or VGI data with satellite time series data to improve the spatial, temporal and thematic quality of forest change estimates.

The objective of this study was to investigate the utility of local expert data combined with LTS-based trajectory analysis to characterize forest change processes. To this end, we investigated three overall research questions:

1. How well can we differentiate between deforestation and forest degradation using local expert data and Landsat time series?
2. What impact does a continuous stream of local expert data have on predictions of forest change types?
3. How are deforestation and degradation processes related in space?

To address these research questions, we used forest disturbance reports collected from 2012 to 2015 by a team of 30 forest rangers in a montane forest area in southwestern Ethiopia and compared them with LTS trajectories. Using all available LTS data, we first derived a series of temporal trajectory metrics from time series of each spectral band and index using an adapted version of the BFAST algorithm (Verbesselt et al., 2010). We derived these metrics to describe changes in trend and seasonal amplitudes between time series segments as well as overall time series trend and intercepts. We then combined all local disturbance reports and time series metrics to train random forest models designed to predict deforestation, degradation or stable forest (no change). To address the second research question above, we divided the local expert data into training and operational phases and measured the accuracies of predicted models as new training data were added to the models. Finally, to explore the third research question, we used the most important spectral-temporal covariates to map deforested and degraded forests based on LTS as of March 2015.

5.2 Methods

5.2.1 Study Area and Project Context

This study was carried out in the UNESCO Kafa Biosphere Reserve (hereafter referred to as "Kafa BR") in southwestern Ethiopia. The Kafa BR comprises an Afro-montane forest system consisting mostly of highly fragmented moist evergreen forests, forest-cropland matrix landscapes, coffee forests, tree plantations and wetlands. A detailed description of the study area as well as the drivers of deforestation and forest degradation is provided in DeVries et al. (2015).

The research in this study was carried out in the frame of a large project implemented by the German Nature and Biodiveristy Conservation Union (NABU), in partnership with the Kafa Zone Bureau of Agriculture, the zonal office of the Ethiopian Ministry of Agriculture. This project aimed to reduce carbon emissions from deforestation and forest degradation in the Kafa BR and to promote conservation and sustainable management of remaining forest resources in the area. In line with the projects goals, the region was inaugurated as a Biosphere Reserve in 2011 under the UNESCO Man and the Biosphere (MAB) programme and was zoned according to land use (Figure 5.1).

As part of these initiatives, 30 forest rangers (hereafter referred to as "local experts") were recruited to implement forest management, monitoring and community outreach activities in each of the 10 local districts (woredas) within the Kafa BR. As part of their monitoring mandate, local experts were trained in methods and tools to report and describe forest changes, including disturbances (deforestation and degradation) and positive changes (afforestation and reforestation). Figure 5.1 shows the geo-location of the disturbance reports provided by local experts between 2012 and 2015 which were used in this study. The details of these reports are described below, and have also been described in detail in a previous study in the area (Pratihast et al., 2014). The overall goal of the current study was to develop an integrated monitoring system using the knowledge of the local experts in combination with Landsat time series and very high resolution (VHR) time series (Pratihast et al., 2014) to track forest change throughout the Kafa BR. Pratihast et al. (2015) describe the setup of this integrated monitoring system under which the research described in this paper falls.

5.2.2 Definition of Change Classes

In order to address our first research question, a definition of deforestation and forest degradation is needed. This definition can take on several criteria related to area change, canopy cover change, or other dimensions of the change (Lambin, 1999; Mertz et al., 2012; Hirschmugl et al., 2014; Morales-Barquero et al., 2014). For example, the IPCC defines

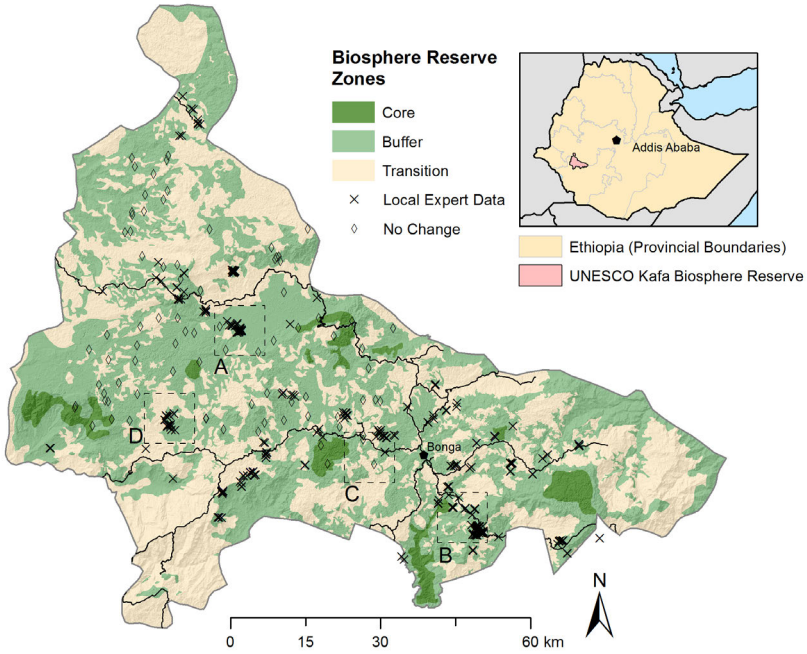

Figure 5.1: Study area located in the UNESCO Kafa Biosphere Reserve in the Southern Nations, Nationalities and Peoples Republic (SNNPR) state of southwestern Ethiopia. Biosphere Reserve zones and location of local expert disturbance reports (deforestation and degradation) and additional reference data (no-change) are shown. The locations of map tiles from Figure 5.9 are shown as boxes labeled A to D.

degradation as changes negatively affecting carbon stocks in forests which remain forests, where a forest is defined based on area, height and canopy cover thresholds (Penman et al., 2003). Degradation can thus occur when a forest is completely cleared, but the total area cleared is less than the area threshold (e.g. 0.5 hectares). Degradation can alternatively occur when a larger area of forest experiences negative changes in forest canopy cover, but the canopy fraction still remains above a defined forest threshold (e.g. 20%).

In this study, we limited the definitions of deforestation and degradation to the tree canopy dimension described above. In other words, if the forest canopy was reduced to below our forest definition canopy cover threshold of 20% at the pixel or plot level, we assigned a "deforestation" label, regardless of the total contiguous area cleared. Any negative changes evident that still resulted in a canopy cover of above 20% thus resulted in a label of "degradation". We neglected the area-based definition in this study for two reasons. First, it was often difficult to determine with certainty the total area affected from local expert disturbance reports, but canopy condition could be verified using plot photos submitted by local experts. Second, we sought to derive relationships between temporal metrics derived from LTS and change classes derived from local expert disturbance data, and spatial context was thus not considered here.

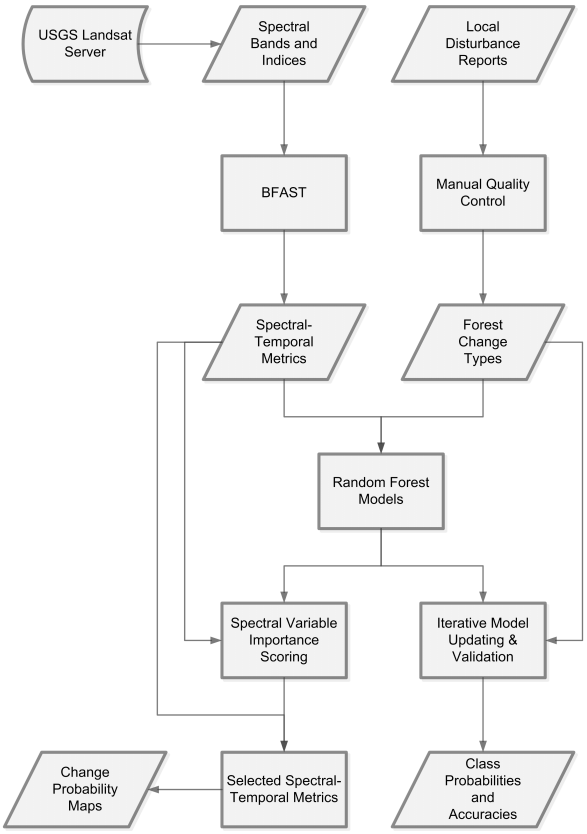

Figure 5.2: Flowchart of methods used in this study. Processes are shown as rectangles and data and results are shown as parallelograms.

A summary of our methods is provided in Figure 5.2. We describe the datasets and individual steps taken in detail below.

5.2.3 Local Expert Disturbance Monitoring Data

Ground based forest monitoring data were provided by local experts employed by the Kafa Zone Bureau of Agriculture. The design of the local disturbance monitoring forms are described in detail in Pratihast et al. (2014). These forms were designed as reporting tools for local experts to report disturbances (deforestation or forest degradation) or positive forest changes (afforestation or reforestation). We used Open Data Kit (ODK) (Anokwa et al., 2009) to integrate these forms with GPS and multimedia (photo, audio). As such, each form contains a range of attributes describing forest status and history and is associated with at least one coordinate pair, five photos (facing north, east, south, west and upwards) and a narrative plot description (input by hand or recorded as audio by the local expert).

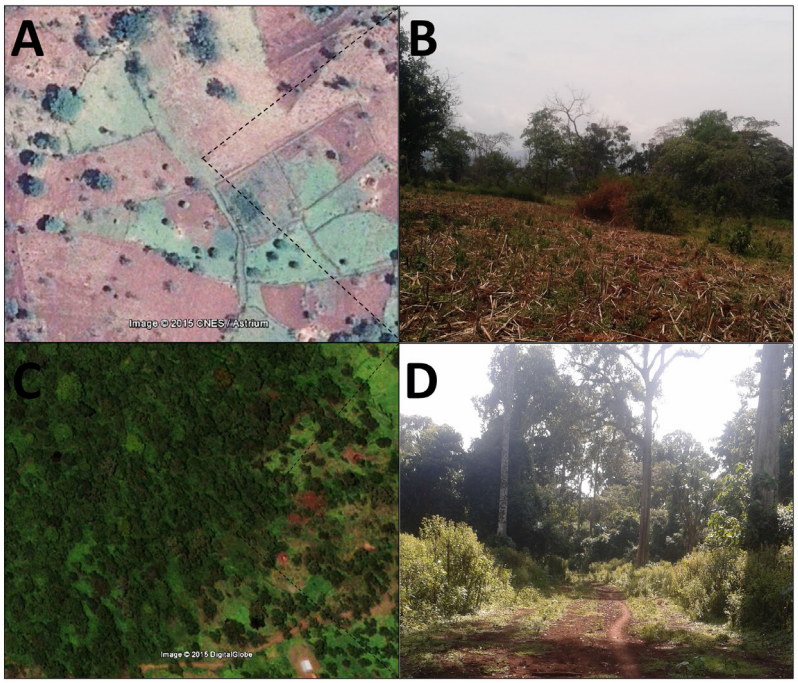

Figure 5.3: Comparison of photo evidence from local disturbance reports with very-high resolution remote sensing data. GoogleEarth imagery for a deforested site (A) and degraded site (C) with photos from local disturbance report from the same sites (B and D, respectively). The location shown in panels A and B corresponds to the time series shown in Figure 5.4. The location shown in panels C and D corresponds to the time series shown in Figure 5.5.

We filtered and classified the local disturbance reports into forest change types as shown in Figure 5.A1. We first assigned a provisional class label (hatched circles in Figure 5.A1) to the reports automatically, based on the current status of the forest and evidence of previous or ongoing disturbance. For these data to be used in an automated workflow, it was necessary to control for the reliability and consistency of the data (Comber et al., 2013). We thus modified the provisional class label where appropriate based on photo evidence, general narrative description of the plot and very high resolution (VHR) imagery from GoogleEarth^{TM}. After visually validating each form, we assigned the definitive labels of "deforestation", "degradation", "no change" or "non-forest". Given the fact that most reports described deforestation or degradation processes, we finally excluded forms from the other two classes from subsequent analysis. We supplemented the final local expert dataset with randomly sampled and validated no-change pixels from a previous study in the region (DeVries et al., 2015) to ensure both change and no-change classes were sufficiently represented in the dataset used to train the forest change models.

5.2.4 LTS Pre-processing

We downloaded all available Landsat imagery from the Landsat5-TM, Landsat7-ETM+ and Landsat8-OLI sensors with cloud cover below 80% per scene and processing level L1T from the USGS Earth Explorer system. We selected all available spectral bands except for the thermal band (shown in Table 5.1). All scenes were already processed to surface reflectance level using the Landsat Ecosystem Disturbance Adaptive Processing System (LEDAPS) atmospheric and topographic correction algorithm (Vermote et al., 1997). We applied a cloud mask derived from the Function of Mask (FMASK) algorithm (Zhu & Woodcock, 2012) to each of the scenes, masking out clouds, cloud shadows and gaps due to the malfunctioning scan-line corrector (SLC) of the ETM+ sensor. Since there were virtually no image acquisitions over our study area during the 1990's, leaving a large gap in the Landsat archive, we limited our time series to all data after and including 1999, coinciding with the launch of the ETM+ sensor.

Using the pre-processed surface reflectance layers shown in Table 5.1, we computed a selection of spectral indices based shown in Table 5.2. These indices have been shown in previous research to be sensitive to vegetation characteristics, states or change dynamics (Tucker, 1979; Wilson & Sader, 2002; Jin & Sader, 2005; Key & Benson, 2006; Crist & Cicone, 1984; Crist, 1985; Gómez et al., 2014; Ahmed et al., 2014). Coefficients for the three basic tasseled cap indices (brightness, greenness and wetness) are shown as b, g and w, respectively, in Table 5.2. Since data from all sensors were pre-preprocessed to surface reflectance products, we used the same surface reflectance derived tasseled cap coefficients across all sensors (Kennedy et al., 2010; Crist, 1985), which are shown in Table 5.A1 in the Appendix.

Since we used all spectral bands and derived indices in our forest change models, we refer to the combination of bands and indices as "spectral bands" for the remainder of this study.

Table 5.1: Spectral bands on the Landsat TM, ETM+ and OLI sensors.

Band	Abbreviation	λ(TM)	λ(ETM+)	λ(OLI)
1 (TM/ETM+), 2 (OLI)	B	0.45-0.52µm	0.45-0.52µm	0.45-0.51µm
2 (TM/ETM+), 3 (OLI)	G*	0.52-0.60µm	0.52-0.60µm	0.53-0.59µm
3 (TM/ETM+), 4 (OLI)	R	0.63-0.69µm	0.63-0.69µm	0.64-0.670µm
4 (TM/ETM+), 5 (OLI)	NIR	0.77-0.90µm	0.77-0.90µm	0.85-0.880µm
5 (TM/ETM+), 6 (OLI)	SWIR1	1.55-1.75µm	1.55-1.75µm	1.57-1.65µm
7 (all sensors)	SWIR2*	2.08-2.35µm	2.09-2.35µm	2.11-2.29µm

*Spectral bands used to produce final forest change probability maps.

Table 5.2: Spectral indices used in this study.

Name	Abbreviation	Equation	Remarks	Reference(s)
Normalized Difference Vegetation Index	NDVI	$\frac{NIR-R}{NIR+R}$	sensitive to photosynethetic activity	(Tucker, 1979)
Normalized Difference Moisture Index	NDMI	$\frac{NIR-SWIR1}{NIR+SWIR1}$	sensitive to canopy moisture content	(Wilson & Sader, 2002; Jin & Sader, 2005)
Normalized Burn Ratio	NBR	$\frac{NIR-SWIR2}{NIR+SWIR2}$	sensitive to disturbances and fire	(Key & Benson, 2006)
Normalized Burn Ratio 2	NBR2	$\frac{SWIR1-SWIR2}{SWIR1+SWIR2}$	sensitive to disturbances and fire	
Tasseled Cap Brightness	TCB	$b_1B + b_2R + b_3G + b_4NIR + b_5SWIR1 + b_6SWIR2$	sensitive to surface brightness	(Crist & Cicone, 1984; Crist, 1985)
Tasseled Cap Greenness	TCG	$g_1B + g_2R + g_3G + g_4NIR + g_5SWIR1 + g_6SWIR2$	sensitive to vegetation greenness	(Crist & Cicone, 1984; Crist, 1985)
Tasseled Cap Wetness	TCW*	$w_1B + w_2R + w_3G + w_4NIR + w_5SWIR1 + w_6SWIR2$	sensitive to vegetation moisture content	(Crist & Cicone, 1984; Crist, 1985; Jin & Sader, 2005)
Tasseled Cap Angle	TCA	$tan^{-1}(\frac{TCB}{TCG})$	sensitive to aboveground biomass	(Gómez et al., 2014; Ahmed et al., 2014)

*Spectral indices used to make final change probability maps.

5.2.5 Deriving Temporal Metrics

Our specific objective in this study was to differentiate between three main forest state classes: deforestation, degradation and no-change. We derived a series of temporal metrics from time series of each of the spectral bands described above and in Tables 5.1 and 5.2, recognizing that these change types can be either gradual or abrupt (i.e. involving a break between adjacent observations). We thus derived temporal metrics which can be divided into two broad categories: (1) full time series and (2) segment-based metrics. We derived these metrics from pixel time series at sites coinciding with local disturbance reports.

For each spectral band, we fit a linear function to the entire time series. We chose the robust linear regression (RLM; (Huber, 1964)) instead of the commonly-used linear regression based on ordinary least squares (OLS). RLM is based on the M-estimator, which seeks to find the best fit to a distribution of data with outliers (Huber, 1964). This choice of fitting method was motivated by the fact that full Landsat time series commonly contain noise due to unmasked clouds or other sources (DeVries et al., 2015; Zhu et al., 2012b; Broich et al., 2011). The output of this method applied to each time series and spectral band thus consisted of (1) the RLM intercept (using the baseline year 1999 as the origin), and (2) the RLM slope.

While an overall RLM trend can help to describe gradual changes or to discriminate between change and no-change classes, abrupt changes or onset of gradual changes late in a time series may not be sufficiently captured using this method. To describe these changes, we tested each pixel time series for each spectral band for the presence or absence of breaks using the "breakpoints" method of Bai and Perron (2003) (Bai & Perron, 2003), which determines the optimal number of breaks in a time series based on the Bayesian Information Criterion (BIC; (Bai & Perron, 2003)). We assumed that in the length of the time series (from 1999 to 2015), a land use or land cover change event would occur only once, and were thus interested in identifying the most important break. We therefore set the maximum number of breaks to one, generating a result representing the presence or absence of a break in the time series (de Jong et al., 2013).

For each segment that resulted from the breakpoint computation above, we fit season-trend models as in Verbesselt et al. (2010) as follows. For a time-dependent response variable y_t, we fit the formula

$$y_t = \alpha_j + \beta_j t + \gamma_j sin(\frac{2\pi t}{f} + \delta_j) \tag{5.1}$$

where α_j is the intercept, β_j is the linear slope, γ_j is the amplitude, f is the frequency of the time series (set to 365 days for LTS data) and δj is the phase for each segment j. Similarly to the overall trend fitting, we used RLM instead of ordinary least squares (OLS) in fitting the season-trend models. The output of the time series segmented applied to

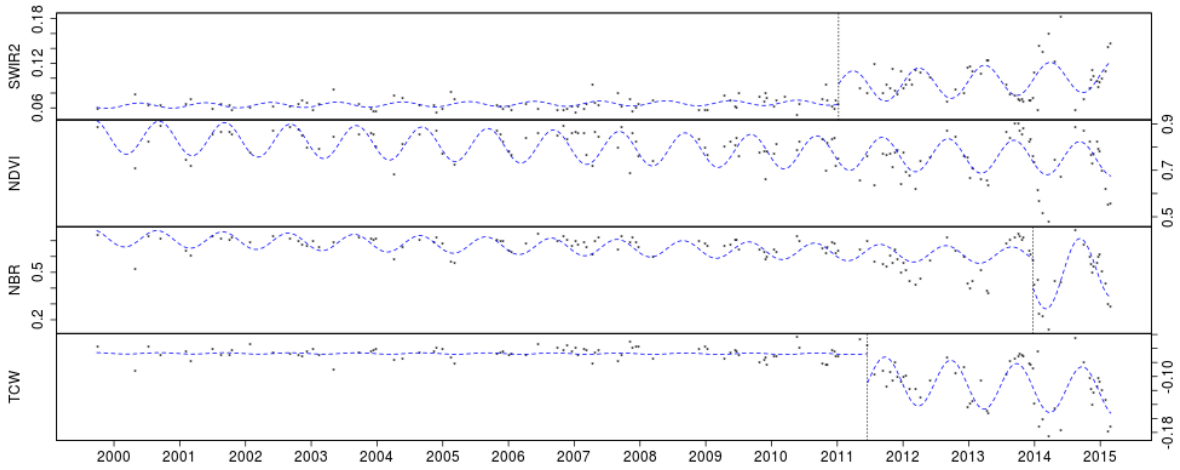

Figure 5.4: Time series over a deforested site for four spectral bands: SWIR2, NDVI, NBR and TCW. The RLM-fitted season-trend model for each segment is shown as a dotted line. VHR imagery and local disturbance photo evidence for this site is shown in Figure 5.3A and B.

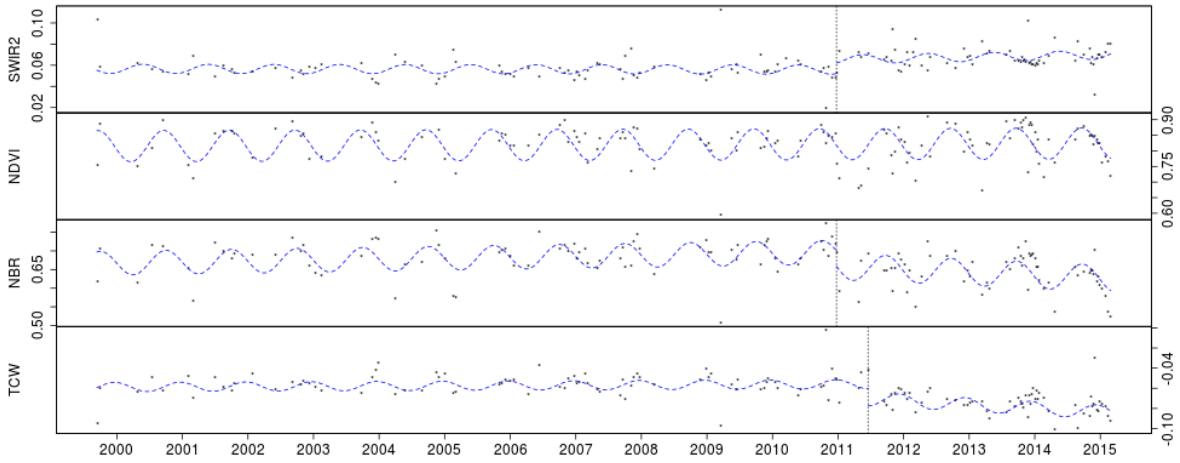

Figure 5.5: Time series over a degraded forest site for four spectral bands: SWIR2, NDVI, NBR and TCW. The RLM-fitted season-trend model for each segment is shown as a dotted line. VHR imagery and local disturbance photo evidence for this site is shown in Figure 5.3C and D.

each time series and spectral band thus consisted of (1) the amplitude of the first segment (γ_1), (2) the amplitude of the second segment (γ_2; equal to the first amplitude if no break was detected), (3) the trend of the first segment (β_1) and (4) the trend of the second segment (β_2; equal to the first trend if no break was detected). These outputs are shown for two sites representing deforestation and degradation in Figures 5.4 and 5.5.

5.2.6 Modelling Forest Change Processes

Random Forest Models.

We used random forests to model change type as a function of LTS spectral-temporal metrics. The random forest classifier is based on a machine learning algorithm which constructs many decision tree classifiers based on bootstrapped samples (Breiman, 2001). Several advantages of the random forest method over other classifiers have been reported in the literature, including the ability to accommodate many predictor variables, as well as the fact that it is a non-parametric classifier (i.e. does not assume any underlying distribution in the training samples) (Breiman, 2001). Random forest classifications generally assign class labels based on the majority vote among all bootstrapped classification trees. In this study, we used the majority votes from 7000 classification trees to analyze the internal out-of-bag (OOB) error estimates per class. We used the class probabilities (also based on the number of votes per class) to study the impact of the updated local data stream and to map change probabilities at several sites (described below).

Iterative Model Updating.

Monitoring activities carried out by local experts were carried out in phases according to project activities in the Kafa BR. Specifically, initial trainings were held with local experts to collaboratively develop ODK-based tools for forest monitoring in 2012, after which several rounds of monitoring were carried out until 2014 (Pratihast et al., 2014). From October 2014, a new Integrated Forest Monitoring System (IFMS) was piloted for the Kafa BR with additional trainings in October, a demonstration phase in November and December 2014, and an operational near real-time monitoring phase from January 2015 onwards (Pratihast et al., 2015).

To demonstrate the use of a continuous data-stream from local experts, we ran the random forest algorithm as described above for two time periods: (1) a training phase and (2) an operational phase roughly according to the project phases described above. We divided the local expert data as outline in Figure 5.6. During an initial "training" phase, we took all local expert data acquired before July 2013 ("period A" in Figure 5.6) and used them with all LTS spectral-temporal covariates to train a random forest model as described above. In addition to the OOB error estimate, we used additional local expert data acquired during the period between July 2013 and October 2014 ("period B" in Figure 5.6) to validate this model. Specifically, we compared the distribution of predicted class probabilities for all disturbance locations reported in period B with the actual change types reported by local experts. During a subsequent "operational" phase, we fused the local expert data from periods A and B, and built a new random forest model using all spectral-temporal covariates. We then used all local expert data acquired after October

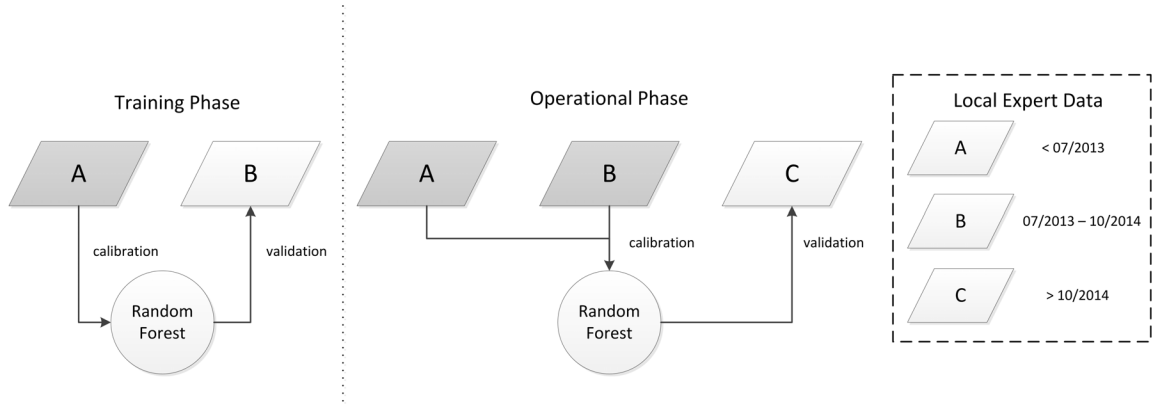

Figure 5.6: Flowchart demonstrating the iterative updating of random forest models. Time of acquisition of local expert data (parallelograms) are shown in the box on the right hand side. In each phase, a subset of the local expert data were used for model calibration (grey), and another subset was used for model validation (white).

2014 ("period C" in Figure 5.6) to compare predicted class probabilities with actual class labels as in the training phase.

Selecting Important Variables.

Mapping forest change classes requires that all covariates used in the change type prediction are computed over all pixels in a scene. The computation of breakpoints for each pixel necessary for deriving temporal metrics was computationally time-consuming and not realistic for producing wall-to-wall change maps. We therefore decided to produce maps using simplified random forest models build with only a subset of the most important spectral-temporal covariates. The importance of individual covariates in random forest models is measured either as the mean decrease in accuracy when each variable is removed from the individual bagged decision trees or as a node impurity coefficient (Breiman, 2001). These measures suffer from two possible drawbacks. First, the model composition is different with every run, resulting in different outcomes for every random forest model. Second, when the covariates included in the model are tightly correlated with each other, interpretation of importance can be problematic (Strobl et al., 2008). For example, if coefficients A and B are both seen to be important predictor variables and are both highly correlated with each other, it is not clear if the importance is due to this correlation or the underlying predictive power of either covariate. To overcome this second drawback, Strobl et al. (2008) proposed a conditional importance measure which involves measuring importance among permuted samples of covariates. With a large number of covariates, however, we found this approach to be computationally unreasonable.

To circumvent this limitation, we derived a scoring algorithm based on iterations of random forests run separately for each spectral band (Tables 5.1 and 5.2), using temporal

metrics derived from each respective band as model covariates. Specifically, we ran the algorithm 1000 times for all temporal metrics derived from only the blue band, the green band, and so forth for all other spectral bands. For each of the 1000 iterations, we ranked the bands based on the overall accuracy as well as the class-specific accuracies. We then derived a score (S) for each band (j) and change class (Δ) by taking the average normalized rank over all iterations as follows:

$$S_{j,\Delta} = \frac{1}{N} \sum_{i}^{N} \frac{x_{i,j} - 1}{n - 1} \tag{5.2}$$

where $x_{i,j}$ is the rank of band j in iteration i, n is the total number of spectral bands and N is the total number of iterations. $x_{i,j}$ was computed such that the bottom ranking band in iteration i was assigned a value of 1, and the top ranking band was assigned a value equal to n. Since it is a normalized rank, S_{Δ} falls within the interval $[0, 1]$, where a maximum score of one indicates a top rank for all N iterations. We selected the most important spectral bands based on this scoring algorithm and produced maps of change class probabilities for several sites. We applied a forest mask produced from a Landsat ETM+ scene acquired on Feburary 2001 to filter out pixels representing stable non-forest from before 2001.

5.3 Results

5.3.1 Model Accuracies and Temporal Variable Importance

The random forest constructed with 7000 trees using all spectral-temporal covariates and training data gave and overall OOB error estimate of 29%. The deforestation class error was 26%, the degradation class error was 31% and the no-change class error was 32%. Although subsequent iterations of the modeling process showed inconsistencies in importance metrics, the overall RLM trends from various spectral bands were consistently ranked as the most important predictors. The amplitude of the second segment (γ_2) was also frequently highly ranked, followed by trends of the first and second segments (β_1 and β_2).

5.3.2 Iterative model updating

The results of the iterative model updating are shown in Figure 5.7. Here, the class probabilities (P) of deforestation (DEF), degradation (DEG) and no-change (NOCH) are shown for reference deforestation and degradation (DEF and DEG on the x-axis, respectively), both for the training phase (top row) and the operational phase (bottom row). In the training phase, the median class probabilities for reference deforestation locations

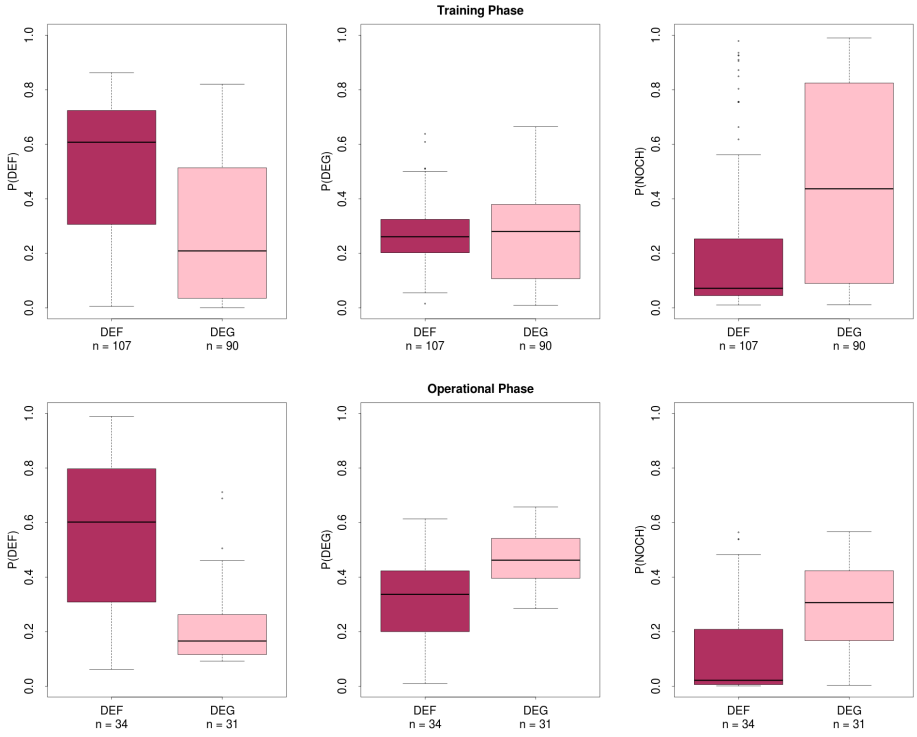

Figure 5.7: Iterative calibration and validation of change classes. Random forest probabilities of deforestation (DEF), degradation (DEG) and no-change (NOCH) are shown for the training phase (top panel) and operational phase (bottom panel) of the monitoring activities. The model updating approach is shown in Figure 5.6.

were 61% for deforestation, 26% for degradation and 7% for no change. These class probabilities remained largely static during the operational phase: 60% for deforestation, 34% for degradation and 2% for no change.

The median class probabilities for reference degradation locations in the training phase were 21% for deforestation, 28% for degradation and 44% for no change. These probabilities changed to 17% for deforestation, 46% for degradation and 31% for no change during the operational period.

5.3.3 Importance of spectral bands in classifying change types

The importance scores for each spectral band are shown in Figure 5.8. SWIR2 and TCW emerged as the most important variables when overall accuracies were considered (i.e. taking all change classes into account). The most important bands for the individual change classes were SWIR2 for deforestation, TCG for degradation and G for no-change. SWIR2 achieved a perfect score of 1 for the deforestation class, implying that it was ranked the highest in terms of deforestation accuracy on every iteration. The NIR band,

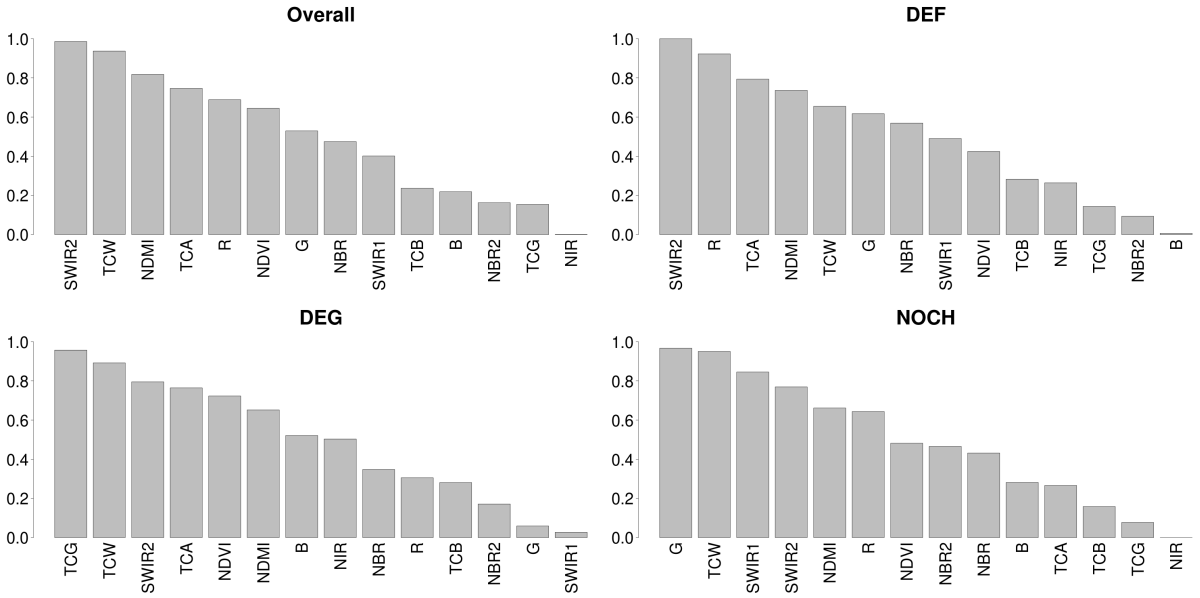

Figure 5.8: Importance scores (S) for each band based on overall accuracies and class accuracies for deforestation (DEF), degradation (DEG) and no-change (NOCH).

on the other hand, received a score of zero for the no-change class, implying that it was consistently the lowest ranked band for that class over all iterations.

5.3.4 Spatial Distribution of Deforestation and Degradation

Based on the results of the importance scoring algorithm, we selected all temporal covariates derived from the SWIR2 and TCW bands for further analysis. We additionally selected the RLM intercept and trend of the green band (G) based on its apparent importance in discriminating stable forest (no-change). Using this subset of the covariates, we derived another random forest model and produced maps of change type probabilities (deforestation, degradation and no-change). The spatial distribution of forest change probabilities (deforestation or degradation) for four sites are shown in Figure 5.9. In general, deforestation between was mapped with high certainty and spatial cohesion. Degradation, on the other hand, was spatially diffuse and probabilities were generally lower. One of the four sites (Figure 5.9B) had noticeably lower deforestation probabilities, despite the fact that an abundance of local expert data confirmed the deforestation events at that site.

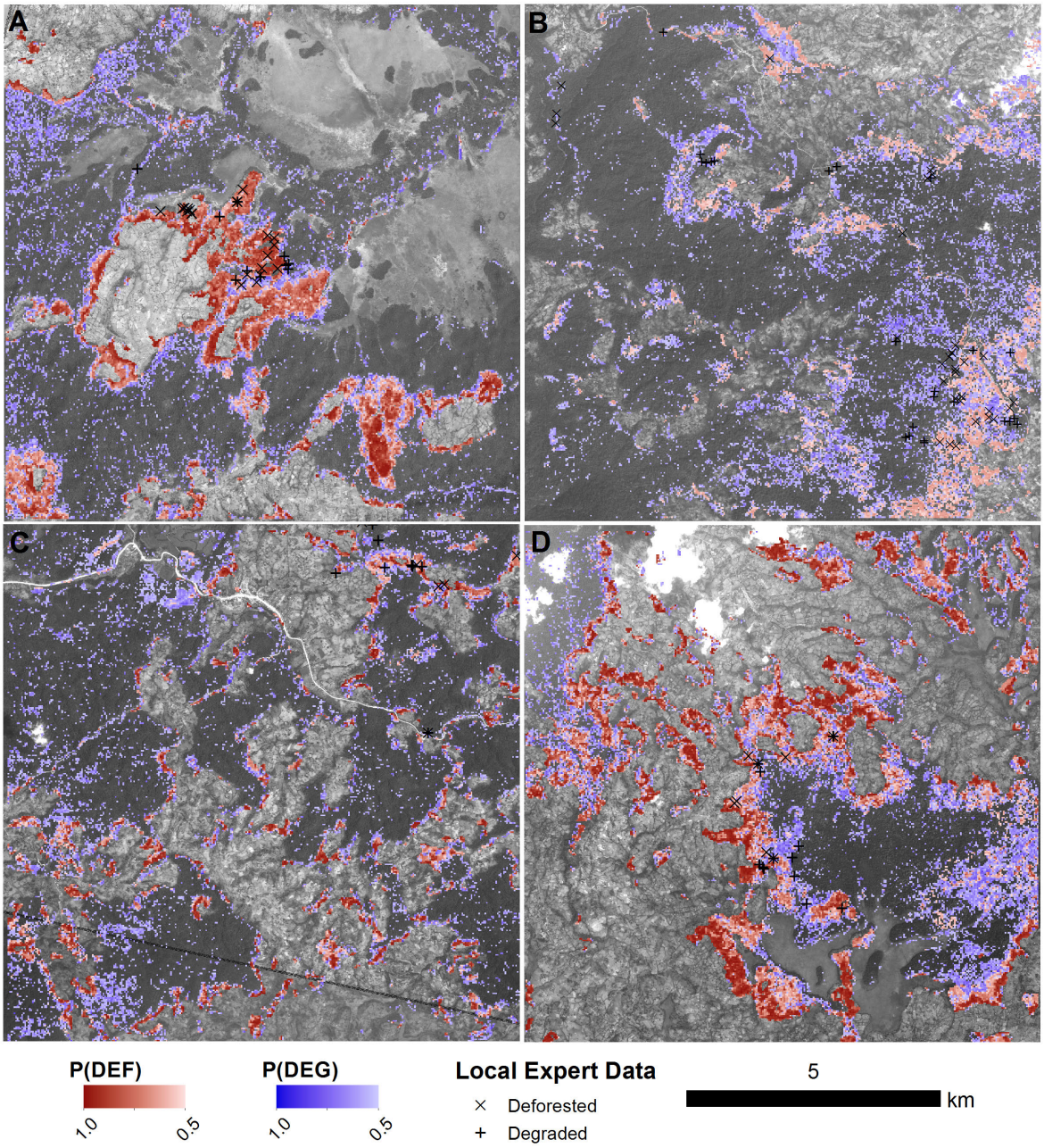

Figure 5.9: Spatial distribution of deforestation and degradation at four sites. The probability of deforestation and degradation are shown as red and blue colour maps, respectively. Local expert reports of deforestation (X) or degradation (+) collected between 2012 and 2015 are overlaid on the maps. The base images are SPOT5 images (band 2; 2.5m spatial resolution) acquired between 2009 and 2011. Dark shaded areas represent forest in the SPOT5 image, and light areas are non-forest land cover types (e.g. cropland or wetland). The locations of each tile (A to D) are shown in Figure 5.1.

5.4 Discussion

5.4.1 Detecting changes using an integrated approach

Our first research question concerned the ability to distinguish deforestation and degradation in our study area using local expert data in combination with LTS. In the current study, we provide evidence that these change types are indeed separable using a random forest approach, with OOB class accuracies for both deforestation and degradation on order of disturbance accuracies reported previously (DeVries et al., 2015). Two main factors contributed to this ability. While a direct comparison between methods and results is difficult, a similar study conducted in the same area achieved similar accuracies in disturbance monitoring using LTS (73% user's and producer's accuracies) (DeVries et al., 2015). Similarly to DeVries et al. (2015), we were able to track small-scale deforestation (Figure 5.9), with the key difference that our models were able to predict degradation above a 50% probability threshold in many cases. Using NDVI time series and an Ordinary Logistic Regression approach, DeVries et al. (2015) were unable to achieve predicted class probabilities above 25% for degradation, precluding the mapping of degraded forest with certainty. In Figure 5.9, on the other hand, we demonstrate how degradation can be mapped alongside deforestation when prediction probabilities are sufficiently high.

Improvements in sensitivity to forest degradation are owed in part to our overall workflow. Most other remote sensing method-related studies validate an existing method using ground-data or visually interpreted data sampled from an existing map or result, and indeed use local expert or community-based monitoring (CBM) data to validate samples selected from existing results (Bellfield et al., 2015). In this study, however, we used *a priori* training data to help to develop the method itself. These existing data underscore the value of the local expert data stream featured in this study. This bottom-up approach was especially important for examining the extent to which we could track forest degradation, since local experts were able to identify cases of below-canopy disturbances independently of any remote sensing based datasets.

5.4.2 A continuous local data stream

The local expert data used in this study were generated as a result of a series of field trainings, local monitoring activities (Pratihast et al., 2014) and the development of an Integrated Forest Monitoring System (IFMS) involving local experts (forest rangers) in the Kafa BR (Pratihast et al., 2015). We divided the dataset into a training and operational phase to represent this process and then compared reference data from each period with predicted class probabilities derived from iteratively trained random forest models. While the median class probabilities between the two phases did not differ substantially,

the spread of probabilities showed a marked change from a wide spread in the training phase (Figure 5.7, top row) to more narrow distributions in the operational phase (Figure 5.7, bottom row). Most importantly, the apparent confusion between degradation and no-change classes in the training phase was reduced as evidenced by the generally lower no-change probabilities among degradation reference samples in the operational phase, an important prerequisite to mapping degradation with a degree of certainty (Figure 5.9).

Two possible factors may influence the improvements in estimated class probabilities seen in Figure 5.6. First, the absolute number of training samples available with subsequent monitoring phases likely have a favourable effect on the random forest models. DeVries et al. (2015) found that degradation samples were associated with and without time series breakpoints and a range of change magnitude values. For this reason, an increase in the number of training samples provides a better range of degradation "states" from which to train the models, particularly considering the fact that local experts are more able to identify degradation from the ground than is possible with optical remote sensing data (Pratihast et al., 2014). Second, it is possible that the quality of the local expert data increase over time as they become more experienced with the monitoring tools and receive subsequent follow-up trainings (Pratihast et al., 2014; Brofeldt et al., 2014). Notably, the last phase corresponds with the kick-off of an IFMS (Pratihast et al., 2015), which is intended to provide a platform for local stakeholders to share local data, experiences and gain access to satellite-based forest change alerts. Such a system is expected to spur increased and enhanced local monitoring data, allowing for further development and testing of forest change models.

5.4.3 Spatial patterns of deforestation and deforestation

The Kafa BR, like many other areas in the tropics, is characterized by forest mosaic landscapes and complex deforestation and degradation patterns (Mertz et al., 2012; DeVries et al., 2015). Characterizing these processes in space is therefore important to understanding forest changes. The spatial distribution of deforestation and degradation shows that deforestation and degradation classes were predicted correctly to a large degree. Previous research in the Kafa BR has shown that deforestation occurs at small scales (DeVries et al., 2015). In general, we found that deforestation probabilities were generally quite high in these change areas, confirming that LTS is a suitable data source for tracking small-scale deforestation (DeVries et al., 2015). Given the fact that the drivers of degradation in the Kafa BR are tightly associated with deforestation (Pratihast et al., 2014), it is not surprising that the areas with relatively high degradation probabilities are spatially correlated with deforested areas in most cases. This mapping approach can thus be used for at least two key purposes. First, deforestation and especially degradation hotspots can be used to alert local stakeholders and monitoring experts of areas with possible dis-

turbances via an interactive monitoring system (Pratihast et al., 2015). Second, these hotspots can be used for activity-based stratification of the area for measuring biomass, biodiversity or other important ecological variables.

Despite the quality of the maps produced, it should be noted that deforestation class probabilities were markedly lower at one of our sites than in the other test sites (Figure5.9B). This particular site is located near the edge of the Landsat scene used in this study, a region where data availability is known to be limiting (DeVries et al., 2015). It is possible that higher uncertainties in the deforestation class are a result of a relative lack of observations in the LTS dataset, which can preclude the fitting of a reliable seasonal model. With a sub-standard season model, the seasonal amplitude of either segment cannot be reliably estimated, causing errors in the deforestation class. Considerations must therefore be made for data availability when choosing temporal variables with which to model forest change.

5.4.4 Limitations to the method

A number of limitations to the approach used in this study are discussed in this section, including definitions of forest degradation, sampling considerations and the timing of forest changes.

Definition of forest degradation.

Making a distinction between deforestation and forest degradation processes is problematic when dealing with the complex forest change processes encountered in this study. While we systematically distinguished between these two processes among local expert disturbance reports, comparison with LTS profiles reveals a more subtle distinction between these processes. Characterizing a disturbance "event" is complicated by the fact that deforestation is preceded by several years of forest degradation when driven by subsistence agriculture (Pratihast et al., 2014; DeVries et al., 2015). Our classification scheme could thus be alternatively viewed as "state variables", in which forest pixels at a given point in time were classified as "deforested" or "degraded" depending on a suite of spectral-temporal variables. Given difficulties with defining degradation (Morales-Barquero et al., 2014), a more practical definition of degradation would be a continuous measurable value (Lambin, 1999). To this end, our approach could be expanded to include other tools, such as hemispherical photography (Gonsamo et al., 2013; Confalonieri et al., 2013) to provide a continuous measure of canopy cover over monitored sites. Additionally, expanding the local monitoring activities to include regular biomass measurement campaigns (Pratihast et al., 2012; Brofeldt et al., 2014) would provide additional continuous forest variables to describe forest change.

Sampling considerations.

The data used in the the iterative validation of the random forest models were not probabilistically sampled, but were rather based on purposive observations by local experts. The internal OOB sample provided by the random forest models provide an alternative robust measure of model accuracy. Additionally, we demonstrated the ability of continuously acquired local expert data to improve and validate the random forest models over time (Figure 5.7). The maps produced by these models (Figure 5.9) can be used to support the continuous training and validation of random forest models by directing local experts to locations with high probability of forest change.

Timing of changes.

The timing of change is an important feature of forest monitoring, for which reference data often consist of visually interpreted imagery (Cohen et al., 2010). Even though local experts also record disturbance timing, we did not attempt to model change timing in this study due especially to uncertainties in the local expert data. These uncertainties arose largely because of the way in which change types and onset times are defined. Pratihast et al. (2014) found that temporal discrepancies between change times recorded by local experts and those observed using very high resolution imagery arose because of two possible differences. First, local rangers are able to detect understorey degradation before this is visible to satellite sensors, causing a temporal lag on the side of the satellite data. Second, local experts tended to define deforestation in terms of land use, implying that preceding degradation acitivites (e.g. for fuelwood and timber harvesting or understorey coffee cultivation) were not interpreted as deforestation, causing a temporal lag on the side of the local experts (Pratihast et al., 2014). To avoid confusion in our change models, we decided therefore to focus on the thematic dimension of forest change.

Overcoming limitations using Integrated Forest Monitoring.

Limitations in sampling and change timing could be addressed by further exploring the idea of an interactive monitoring system between local experts, remote sensing specialists. Pratihast et al. (2015) demonstrate an operational IFMS for the Kafa BR that is designed to support such ongoing monitoring activities. Future research should further investigate how the forest change outputs of our method can be used in an interactive environment to support follow-up monitoring, management and enforcement (Pratihast et al., 2015), including the temporal dimension of change in the context of a near real-time interactive monitoring system, for example (Pratihast et al., 2015).

5.5 Conclusions

In this study, we have provided the first demonstration of local expert forest monitoring data integrated with Landsat Time Series (LTS) using a machine learning (random forest) approach. We found that local expert monitoring data and dense LTS are valuable in training and validation random forest models to predict deforestation and degradation in complex forest matrix landscapes. Notably, we showed that as local expert monitoring data continued to be collected and received, model results improved, demonstrating the potential of an ongoing forest monitoring system featuring both data streams. From the models, we determined that the SWIR2 and TCW spectral bands were the most important for differentiating deforestation and degradation, and used temporal covariates based on these bands to produce spatial predictions of forest change. This study provides a basis on which further research on integrated forest monitoring systems, particularly those seeking to integrate community-based monitoring (CBM) or volunteered geo-information (VGI) data with dense satellite time series (Pratihast et al., 2015). Future research will follow-up on our approach by incorporating other data sources using data fusion methods (Reiche et al., 2015b), such as Sentinel-2, terrestrial or airborne LiDAR or other airborne remote sensing datasets. Furthermore, our approach is flexible to the types of predictions and can include other types of forest change as needed, such as afforestation and reforestation activities.

5.A Appendix

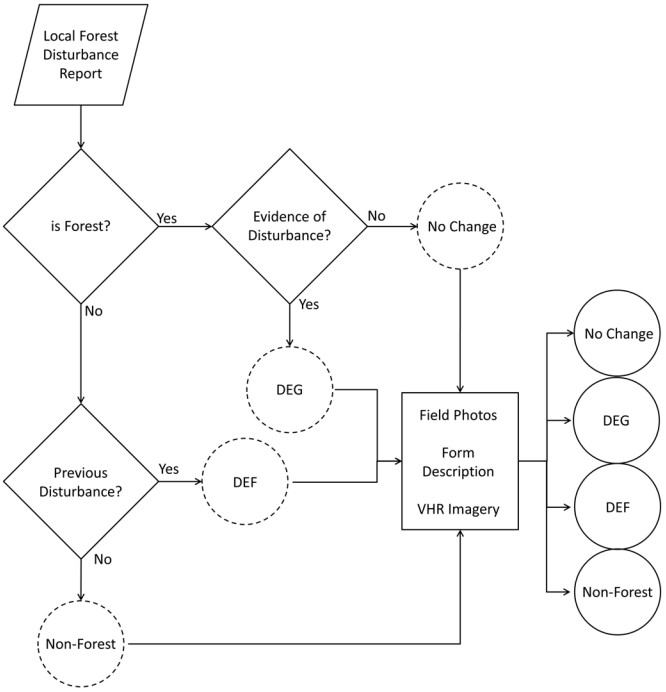

Figure 5.A1: Decision flowchart for classification of local disturbance reports. The primary class labels deforestation (DEF), degradation (DEG), no change (stable forest) or non-forest were assigned based on automatic interpretation of form attributes (circles with hatched outlines). Primary class labels were then verified using plot photos, plot descriptions and very high resolution (VHR) satellite imagery and final class labels (circles with solid outlines) were assigned.

Table 5.A1: Coefficients used to transform reflectance bands from all Landsat sensors into tasseled cap indices.

	B	G	R	NIR	SWIR1	SWIR2
TCB (b)	0.2043	0.4158	0.5524	0.5741	0.3124	0.2303
TCG (g)	-0.1603	0.2819	-0.4934	0.7940	-0.0002	-0.1446
TCW (w)	0.0315	0.2021	0.3102	0.1594	-0.6806	-0.6109

Chapter 6

Synthesis

6.1 Main Results

Remote sensing has come to represent a vital tool for forest monitoring. The opening of satellite archives to the public has resulted in major developments in forest change monitoring methods (Wulder et al., 2012). While forest change detection previously depended on bi-temporal image comparison, recent methods have moved towards describing changes using annual Landsat composite times series (Huang et al., 2010; Kennedy et al., 2010) or even exploiting the entire Landsat archive (Broich et al., 2011; Zhu & Woodcock, 2014; Zhu et al., 2012b). This paradigm shift in forest change monitoring has led to impressive leaps in monitoring capacity evidenced by operational national monitoring systems (INPE, 2014a,b) and global annual forest cover change maps (Hansen et al., 2013). Significant challenges remain, especially with regards to the thematic detail with which forest dynamics can be described using Landsat times series. This thesis seeks to address this research gap by using dense Landsat time series to monitor deforestation, degradation and regrowth in several tropical sites. The main focus was on the application of Landsat time series to monitoring deforestation, forest degradation and post-disturbance forest regrowth. To this end, two potential bridges are described in this thesis. First, the bridge between structural change monitoring as described in the econometrics literature (Bai & Perron, 2003; Zeileis et al., 2005) and LTS is explored in Chapters 2, 3 and 5. Second, the bridge between community-based monitoring (CBM) data and methods and LTS is described in Chapters 4 and 5. Three main research questions were formulated in the Introduction chapter of this thesis and are revisited below.

1. To what extent can we track small-scale forest disturbances in complex forest landscapes using dense LTS? Many of the methods based on dense LTS that have been developed and tested for temperate deciduous or evergreen forests, with few studies utilizing dense LTS over tropical forest areas, where cloud cover and other gaps in the archive present challenges to monitoring forest disturbances (Zhuravleva et al., 2013; Broich et al., 2011). Forest disturbance studies over landscapes in sub-Saharan Africa are particularly lacking. Disturbances in these forest landscapes tend to be driven by small-holder agricultural expansion, which typically involves small incremental changes of only a few hectares at a given time.

A robust approach for monitoring small-scale forest disturbances driven mostly by small-holder agricultural expansion is described in Chapter 2 for a fragmented Afromontane forest landscape in the southwest of Ethiopia. Using a LTS dataset consisting only of ETM+ observations from 1999 to 2013, disturbances are mapped at annual temporal resolution with a user and producer's accuracy of 78%. In Chapter 3, disturbances are shown to be much larger in scale than in Chapter 2 and are mapped with significantly higher accuracies. Both cases demonstrate that LTS data are capable of mapping disturbances

in tropical forest landscapes at high temporal resolution, including in complex forest-agriculture matrix landscapes typically found in sub-Saharan Africa. However, lower accuracies over the Ethiopian site indicate that the nature and scale of forest disturbances has an influence on disturbance accuracies. Similar constraints have been noted in other parts of sub-Saharan Africa, where forest disturbances are largely driven by small-scale agriculture and selective logging, resulting in higher uncertainties in mapped changes (Tyukavina et al., 2013).

An additional limitation faced in the Ethiopian study site is the temporal range with which forest disturbances are mapped. Because of the large gap in observations during the 1990's and a paucity of data from Landsat 5 at the time of conducting the study, only Landsat ETM+ data are used, implying a full time series from 1999 to 2013. Given the need for a defined history period, the analysis is essentially limited to monitoring disturbances from 2005 onwards. In some parts of the study area, disturbances before 2005 could easily have been mapped, since higher data densities (i.e. higher number of total observations) would allow for a shorter history period lengths. However, data densities are markedly low at higher elevations (Figure 2.3), limiting the ability to detect early disturbances.

2. Can structural change monitoring be used with LTS to monitor post-disturbance regrowth in tropical forests? In Chapter 3, a method for detecting post-disturbance regrowth is presented. First, disturbances are mapped using the same method as in Chapter 2. LTS data following a disturbance are then checked for a return to spectral "stability" compared to the modelled stable history (Figure 3.3). This test features the Moving Sums (MOSUM) metric (Equation 3.2), which is a function of the residuals in the monitoring period and the expected noise (variance) in the history period. This method thus provides a data-driven way to monitoring post-disturbance forest regrowth which circumvents the need for annual cloud-free image selection or compositing as in other approaches (Kennedy et al., 2010; Huang & Asner, 2010; Czerwinski et al., 2014). Using all data within the time series also allows for a disturbance-regrowth monitoring method which can ingest data as they come available. In other words, even though regrowth is not a process than can be measured in "near real-time", this flexibility gives the ability to query the regrowth status of a disturbed forest pixel at any time as new observations become available. Finally, the use of all observations in a structural change monitoring context implies that regrowth is determined not based on absolute values or differences between subsequent observations or on pre-defined thresholds, but rather on the temporal *structure* of the post-disturbance time series.

The number of observations in the post-disturbance time series is a strong determinant of regrowth class accuracy. For all disturbances prior to 2002, for example, the producer's accuracy is 88% but decreases to 31% when samples with disturbances before 2009 are also

included (Table 3.6). The user's accuracy, on the other hand, remains relatively constant at between 83% to 89% for similar disturbance times. The sensitivity of the method to omission errors mostly stems from the fact that with later disturbances, less data are available in the time series for follow-up monitoring (Figure 3.9), a problem exacerbated by the decommissioning of Landsat-5 at the end of 2011, effectively reducing the data density at the later stages of the time series. The MOSUM bandwidth (window size) is put forward as a possible parameter that can be adjusted to increase the sensitivity of the method for short or less dense time series. Future research could explore such parameters by identifying conditions under which producer's and user's accuracies are optimized.

3. How can community-based monitoring data and Landsat time series be integrated to enhance forest monitoring? A novel dataset comprised of disturbance reports from local forest experts in the Ethiopian study site, comparable to observations that could be expected from a community-based monitoring (CBM) setting, is presented in Chapter 4. Here, the dataset is compared with professional disturbance observations and very high resolution time series imagery to assess the utility of these data in conjunction with optical remote sensing time series. Several findings of relevance to LTS-based forest monitoring are described in this chapter. First, local experts frequently reported low-level degradation due to fuelwood harvesting, much of which is normally not visible to optical sensors until canopy changes are detected. Second, local experts were able to contextualize forest changes by describing local drivers, such as conversion to small-holder cropland and cultivation of wild or industrialized forest coffee, among other drivers of forest change. Several drawbacks to this dataset are also described, including irregular acquisition of disturbance reports (Figure 4.4), which is related to incentives, local climatic conditions and site accessibility. Discrepancies between optical time series and local expert disturbance data regarding timing of disturbance is also described, arising from both the inability of optical sensors to capture low-level degradation as well as differences in how deforestation "events" are defined by image interpreters and local forest experts (Figure 4.6).

The integration of this local expert dataset with LTS towards characterizing forest changes in greater thematic detail is described in Chapter 5. Here, a subset of the local expert reports described above are classified as "deforestation", "degradation" or "no change" based on attributes, descriptions and photo evidence supplied by local experts. These data are then used to train random forest models, using a wide range of spectral-temporal variables derived by segmenting LTS data over disturbance locations. As local expert data continually become available, the ability of the random forest models to predict deforestation and degradation are shown to improve (Figure 5.6), demonstrating the potential of such a continuous *in situ* data stream to monitor subtle forest change processes over time. Maps showing the spatial distribution of deforestation and degradation class prob-

abilities for a given point in time are also produced using a subset of the most important spectral-temporal variables as predictors (Figure 5.8). While this chapter describes the first operational monitoring system where CBM-type data are integrated with LTS data to describe forest changes, improvements are still needed to further automate the system, especially concerning quality control and consistency of the CBM data.

6.2 Outlook

6.2.1 Forest change definitions revisited

The semantics of land cover classification are critical to the interpretation of change dynamics (Comber et al., 2008; Colson et al., 2009). Three broad forest change classes explored in this thesis are described in Chapter 1 and shown in Figure 1.1. Here, I revisit each of these change definitions and provide a critique on their suitability for forest monitoring.

- **Deforestation:** The definition of deforestation used in this thesis is necessary and sufficient for such monitoring objectives as REDD+ MRV, where carbon stock changes within a reporting period are compared to carbon stock changes within a reference period (DeVries & Herold, 2013). However, defining deforestation based on a tree cover threshold alone does not fully capture the effect of deforestation. For example, follow-up land use or remaining standing biomass in agriculture matrix landscapes (Mertz et al., 2012) are not considered in this definition.
- **Degradation:** While the definition degradation used in this thesis is in line with guidelines put forward by the IPCC (Penman et al., 2003), establishing an operational definition of forest degradation for REDD+ MRV is still elusive (Morales-Barquero et al., 2014; Mertz et al., 2012). Forest degradation could alternatively be described in terms of tree cover loss as a proportion (Kennedy et al., 2012). Other forest parameters, such as vertical structure or above ground biomass (Calders et al., 2015a), may be better descriptors of forest status in response to human intervention.
- **Regrowth:** The definition of regrowth used in this thesis can be interpreted as the presence of a secondary forest canopy following a stand-replacing disturbance. This definition only allows for a binary classification of regrowth, which can indicate whether forest disturbances are transient or permanent land use changes (Broich et al., 2011). However, such a definition neglects important characteristics of forest regrowth, including successional stage classes (Schroeder et al., 2007) or biomass accumulation (related to CO_2 removals; Bongers et al., 2015; Helmer et al., 2009).

A key limitation faced in this thesis, and also partly the motivation behind defining forest changes as described above, is the lack of ground-based reference data by which to fully

characterize forest change processes. The TimeSync method (Cohen et al., 2010) is used in Chapters 2 and 3 to validate disturbances. While this method is sufficient to visually identify and verify discrete stand-replacing disturbances using dense LTS, interpretation of subtle and diffuse degradation with certainty is very difficult. Likewise, secondary regrowth following a disturbance cannot be verified by visual interpretation of Landsat imagery alone, as a non-forest vegetation canopy can be difficult to distinguish from a successional secondary forest canopy. For these reasons, time series of very high resolution (VHR) imagery are used in these chapters to identify degradation (Figure 2.9) and regrowth (Figures 3.7 and 3.8) in sample pixels. Even at such high spatial resolutions (2.5m in the case of SPOT5, for example), the actual extent to which a forest degrades or regrows cannot be fully quantified by visual interpretation of VHR imagery. The validations carried out in Chapters 2, 3 and 4 were thus qualitative. Furthermore, calibration of random forest models in Chapter 5 were likewise qualitative, as forest status was classified based on local expert report attributes and photo evidence.

The conceptualization of forest change described above, while perhaps sufficient for certain monitoring objectives, carries the risk of uncertainties being propagated through the monitoring chain due to differences in forest definitions (Tropek et al., 2013; Ankersen et al., 2015), reference period definition (Pelletier et al., 2011) or other errors. This simplistic view of forest change also risks creating the false illusion that changes between forest states are symmetric or reversible. In reality, forest transitions are probably hysteretic (Hirota et al., 2011; Scheffer & Carpenter, 2003; Scheffer et al., 2001), and past disturbance regimes are important determinants of the fate of regrowing forests (Comita et al., 2010). As forest monitoring priorities shift from being "carbon-centric" to including other co-benefits (Karousakis, 2009; Chhatre et al., 2012), a diversified conceptualization of forest changes is needed to accommodate other objectives, such as the monitoring of Essential Biodiversity Variables (EBV; Pereira et al., 2013).

6.2.2 Towards quantitative forest change monitoring

A more detailed understanding of forest change dynamics is thus necessary to bring LTS-based forest monitoring to a more ecologically relevant level (Kennedy et al., 2014). An alternative to monitoring forest change that can help to achieve the goal described above is to identify and measure variables like canopy cover or biomass at regular intervals, rather than basing change on arbitrary thresholds between forest and non-forest classes (Bontemps et al., 2011). The objective is thus to quantify the biophysical underpinnings of changes on a continual basis. Below, I discuss several specific ways in which quantitative forest monitoring could potentially be supported by LTS in the context of (1) forest degradation and (2) forest regrowth. I then outline how both time series structural change monitoring and integration of *in situ* data streams can support this objective.

Forest degradation

In Chapters 2 and 5, a simple tree cover threshold is used to separate deforestation, degradation and stable forest. Other studies have characterized subtle changes, such as those driven by insect infestations in North American forests, based on LTS trajectories. For example, Meigs et al. (2011) characterized LTS trajectories based on rate and duration of decline and related these observations to tree mortality and surface fuel loadings. Ahmed et al. (2014) combined airborne LiDAR and LTS to estimate canopy cover and height and related these parameters to LTS-derived disturbance parameters. Pflugmacher et al. (2013) similarly combined LTS and airborne LiDAR to describe forest disturbance trajectories and predict current standing above-ground biomass. As shown in Chapter 5, a stream of *a priori* ground-based data can be used to effectively gage the sensitivity of LTS to small-scale forest canopy changes. A multi-scale measuring and monitoring framework is thus envisioned, where LTS, airborne optical data (including LiDAR) and quantitative *in situ* measurements such as canopy gap fraction (Jonckheere et al., 2005), tree mortality (Verbesselt et al., 2009; Meigs et al., 2011) or other plot-based metrics support the characterization of such subtle canopy changes on a continuous basis.

In combination with regrowth patterns observed in Chapter 3, the SWIR bands emerge in Chapters 2 and 5 as important descriptors of forest change processes. In Chapter 2, NDVI time series fail to predict degradation with any certainty, where class probabilities from Ordinal Logistic Regression models do not exceed 25% (Figure 2.8). Inclusion of the SWIR2 band and the tasseled cap wetness band (a weighted difference measure between NIR/visible bands and SWIR bands; Crist, 1985) in Chapter 5, on the other hand, results in degradation class probabilities of greater than 50%, allowing for the mapping of forest areas likely experiencing some form of degradation (Figure 5.9). The SWIR region of the Landsat reflectance spectrum is thus important for capturing subtle forest changes in a time series context. Other studies using LTS to characterize forest disturbances in North American forest sites at high temporal resolution have similarly relied on SWIR1 reflectance (Schroeder et al., 2014), the Noramized Burn Ratio (Zhu et al., 2012b; Kennedy et al., 2010; Huang et al., 2010), tasseled cap wetness (Jin & Sader, 2005) and others. Used in synergy with *in situ* measurements discussed above, SWIR bands and associated indices thus have the potential to enrich the characterization of forest degradation using LTS.

Forest regrowth

The validation of forest regrowth estimates in Chapter 3 faces similar limitations to that of forest degradation in Chapters 2 and 5. While the use of VHR imagery allows for the verification of a secondary forest canopy after disturbance, other characteristics of the successional forest stand cannot be described with such a method without the use

of additional ground-based data, such as forest inventory measurements (Wulder et al., 2009). Estimates of atmospheric CO_2 removals would be especially beneficial to meet some REDD+ MRV objectives (e.g. monitoring of forest carbon enhancements). These estimates are often based on stand age after a disturbance fed into a carbon budget model (Houghton et al., 2012). The MOSUM-based regrowth algorithm presented in Chapter 3 is a novel data-driven method for flagging regrowth among disturbed forest stands. Stand age of regrowing forests could not be validated due to a paucity of VHR reference imagery. Linking the regrowth detection algorithm with *in situ* data on stand age and growth rates would allow for a more quantitative estimate of regrowth rates following disturbances. Helmer et al. (2009) describe an approach for achieving these estimates by linking disturbance data with space-borne LiDAR data. Combining the MOSUM-based regrowth method presented in Chapter 3 with such a stand age estimating approach could be a step towards data-driven models for forest succession and CO_2 removals.

The contribution of LTS and structural change monitoring

This thesis shows that the application of structural change monitoring (Zeileis et al., 2005; Verbesselt et al., 2010, 2012) to LTS can help to track small-scale changes or complex change processes such as degradation or regrowth. The findings described in this thesis have implications on the ability to realize the objectives described above. These implications can be summarized into several advantages. First, the use of dense LTS provides evidence of forest change at a spatial grain relevant to ecological processes (Kennedy et al., 2014). Time series derived from coarse-resolution sensors like MODIS and AVHRR have enormous value to large area environmental analyses due to their long term gap-free coverage (de Jong et al., 2013; Fensholt & Proud, 2012; Fensholt et al., 2015). However, the use of all available LTS data in this thesis, similarly to other recent studies (Zhu et al., 2015; Zhu & Woodcock, 2014; Zhu et al., 2012b), combined with the prospect of fusion with future datasets such as the Sentinel-2 mission (Drusch et al., 2012) could be a step towards approaching temporal resolutions currently possible with coarse-resolution datasets, but at much higher spatial resolution.

Second, structural change monitoring is shown in this thesis to provide a data-driven way to describe different change processes in a time series. Three general implementations of structural change monitoring are taken to describe time series: (1) breakpoint detection based on stable history models (disturbance monitoring in Chapters 2 and 3); (2) time series similarity (post-disturbance regrowth monitoring in Chapter 3); and (3) segmentation based on statistically significant breakpoints (derivation of spectral-temporal variables in Chapter 5). The underlying feature of all three implementations is the fact that breakpoints are determined based on statistical hypothesis testing (Bai & Perron, 2003; Zeileis et al., 2003, 2005), minimizing the need for user-driven thresholds. Future research could further explore the relationship between disturbance-regrowth parameters

derived in Chapters 2 and 3, or segment-derived variables derived in Chapter 5 (e.g. segment amplitude and trend) and the dynamics of quantitative forest variables.

Finally, robustness against time series noise is a key advantage of the structural change monitoring methods employed in this thesis. Inclusion of a noise term in the MOSUM parameter (Verbesselt et al., 2012) when monitoring LTS (disturbance and regrowth monitoring in Chapters 2 and 3) confers robustness (e.g. demonstrated in Figure 2.6) and circumvents the need for time series smoothing or compositing. In effect, a high incidence of noise in the "stable" portion of the time series will lower MOSUM values and reduce the chances of flagging false breakpoints due to noisy data. This approach thus represents an alternative to temporal compositing that can ingest new data as they become available towards a continuous change monitoring framework (Verbesselt et al., 2012).

The contribution of CBM data

Integration of *in situ* data streams, such as professional, CBM or VGI data, provide "eyes on the ground" and allow for characterization and quantification of subtle change drivers and processes not easily detected from space (Chapters 4 and 5). Furthermore, this data stream is key to gaging the extent to which space-borne data streams such as LTS can monitor small-scale diffuse change processes (Chapter 5). Several studies have demonstrated how CBM or VGI data can provide measurements that can be used to monitor forest-related variables over time. Pratihast et al. (2012) showed that above-ground biomass measurements using CBM are comparable to professional forest inventory measurements. Similarly to findings in Chapter 5 of this thesis, Brofeldt et al. (2014) found that CBM-based biomass measurements improve over time, lending support to the operational integration of CBM data in national forest monitoring systems. Ferster & Coops (2015) used VGI and RapidEye data to estimate forest fuel load, facilitated by a novel smart-phone application, demonstrating how citizen science can be operationally linked to satellite-based forest monitoring. Finally, Coops et al. (2012) linked digital photography and MODIS time series to map phenological parameters for the purpose of habitat mapping. Among other examples, these studies demonstrate the potential of CBM or similar *in situ* data streams to enhance satellite-based time series ecosystem monitoring in an operational setting. These studies all measure quantitative forest variables rather than classifying change types, demonstrating the clear potential of such a data stream.

6.2.3 Sensor Integration

An increasing number of satellite sensors, coupled with the opening image archives to the public (Wulder et al., 2012), is resulting in moves towards more integrated monitoring strategies (Wulder & Coops, 2014). As such, sensor integration is specifically poised to

address the objective of quantitative forest monitoring set out above. One obvious advantage to fusing other datasets is related to the continuity of the Landsat legacy, as future Landsat missions are discussed (NASA, 2015) and the European Landsat "analogue", Sentinel-2 (Drusch et al., 2012), has recently been launched.

Fusion of LTS data with other sensors need not be limited to optical sensors with comparable features, however. Use of other sensor types in LTS-based monitoring will in fact broaden the types of variables that can be measured at high temporal resolution. Several studies have prototyped across-sensor fusion methods, a number of examples of which are discussed below.

- **Coarse-resolution optical:** Fusion of LTS with MODIS, AVHRR or other coarse resolution time series result in essentially the same types of forest variables being measured, namely canopy reflectance. Demonstrated benefits of fusing with coarse-resolution time series include increased temporal resolution (Hilker et al., 2009; Masek et al., 2006a) and inclusion of climate proxies as external regressors in time series models (Lhermitte et al., 2011; Dutrieux et al., 2015).
- **Synthetic Aperture Radar (SAR):** Active SAR sensors are sensitive to canopy structure and volume, adding additional dimensionality to measured forest variables. Integration of SAR with LTS has been shown to increased temporal resolution (Reiche et al., 2015a,b). SAR also has the potential of measuring carbon stocks (Englhart et al., 2011).
- **space-borne or airborne LiDAR:** Active optical LiDAR data describe vertical forest structure and phenology (Calders et al., 2015a,b). Airborne or space-borne LiDAR can thus provide wall-to-wall coverage of these variables, which have been shown to be useful in measuring carbon stocks (Asner, 2009). Fusion with LTS has been demonstrated to be useful in describing forest disturbances based on forest structural parameters (Ahmed et al., 2014).

6.2.4 Targeted Stratification and Sampling

The approaches for quantifying the physical underpinnings of forest change discussed up to this point all focus on "bottom-up" approaches to calibrating LTS reflectance data as a proxy for certain forest state variables. Additionally, a "top-down" approach can be taken to broaden forest change definitions used in forest monitoring. In short, knowledge on the spatial and temporal distribution of changes as determined by LTS-based methods can be used to prioritize highly dynamic areas in sampling exercises. While this approach can be used for various monitoring objectives, such as biodiversity monitoring within REDD+ (Dickson & Kapos, 2012), the example of above-ground biomass measurements, is described below.

A key challenge in estimating above-ground biomass (AGB) in forests is the scaling up from plot level to landscape level. To achieve landscape-scale estimates of AGB, stratified random sampling designs are often employed (Herold & Johns, 2007; Fagan & Defries, 2009; McRoberts et al., 2013). When random samples in a particular forest stratum are scarce (due to large stratum size, for example), uncertainties in AGB estimates may be high for those strata, propagating through the MRV chain and hampering efforts to demonstrate performance under REDD+ (Pelletier et al., 2011; Grassi et al., 2008). It would therefore be useful to understand forest dynamics in space and time prior to sampling to be able to prioritize areas undergoing change. To this end, a targeted "activity-based" sampling design is proposed, whereby forest strata are defined based on previous high temporal resolution change estimates. Such targeted strata could thus be defined based on distance to disturbances from the previous year (Chapters 2 and 3), presence or absence of regrowing forests (Chapter 3) or the likelihood of small-scale degradation (Chapter 5). Concentrating samples in such strata would theoretically increase confidence of AGB change estimates (and hence CO_2 emissions and removals estimates) in area where AGB is probably most dynamic.

6.2.5 Towards an integrated forest monitoring framework

The need for local-scale monitoring

The release of large archives of satellite imagery has resulted in development of regional to global map products such as pan-tropical maps of above-ground biomass (Saatchi et al., 2011; Baccini et al., 2012), which are being increasingly used in operational settings. One such product with an unprecedented spatial and temporal resolution and extent is the global forest cover loss map developed by Hansen et al. (2013). The potential impact of such products has inevitably resulted in controversies surrounding their utility for objectives such as REDD+ MRV. Tropek et al. (2013) critiqued the global forest cover loss map of Hansen et al. (2013) based on classification errors or forest definition issues, resulting in a mis-representation of forest gain and loss. While this limitation can be overcome through the local optimization and calibration of these datasets according to national or sub-national monitoring objectives (Hansen et al., 2014), the extent to which this forest change product can capture all change types is still an open question.

For the purposes of operational monitoring systems, a question thus arises: With the emergence of these large area datasets, is there still a need for developing monitoring approaches at local scales? To illustrate this question, I present comparisons of change maps generated in this thesis and those of Hansen et al. (2013) over small subsets of the Peru and Ethiopia study sites in Figures 6.1 and 6.2, respectively. These comparisons show that different forest change dynamics result in different performance of the global dataset over local sites, as described in more detail below.

In the case of the Peruvian study site, estimates of disturbed area from Chapter 3 (Figure 6.1A) are comparable to annual forest loss estimates from Hansen et al. (Figure 6.1B). Despite the low producer's accuracies (and thus high omission errors) for the regrowth class reported in Chapter 3, forest gain estimates over the same period are markedly more conservative in the Hansen et al. map. Two conclusions can be drawn from this example. First, large discrete forest disturbances, such as those driven by livestock agriculture and gold mining in Peru, are generally easy to detect with dense LTS and are largely consistent between the two maps. Second, the MOSUM-based regrowth method, while conservative in itself, is indeed more sensitive to post-disturbance forest regrowth in this study area than the "forest gain" class in the Hansen et al. dataset.

A comparison between forest disturbance products for the Ethiopian study site is shown in Figure 6.2. The map from Hansen et al. reports disturbances from 1999 to 2013, while those from Chapter 2 only extend back to 2005, owing to limitations in the LTS and the need for a stable history period. On the other hand, the disturbance estimates produced in Chapter 2 (shown as disturbance years in Figure 6.2A) seem to be much more comprehensive than those of Hansen et al.. In fact, forest area included in the "forest loss" class of the Hansen et al. map (Figure 6.2B) represent only one third of the forest area classified as disturbed in Chapter 2, when considering overlapping disturbance years only. Additionally, integration of CBM data as described in Chapter 5 allows for the classification of remaining forest areas based on probability of degradation at a given time (blue pixels in Figure 6.2A), providing additional thematic depth to the map product.

An integrated monitoring framework

The two demonstrations described above lend credence to the fact that, despite the vast potential global maps have for inclusion in operational monitoring systems, locally calibrated monitoring approaches are needed to understand the drivers and impacts of changes to forests over time. To this end, I propose a local monitoring framework which features the continuous integration of space-borne and *in situ* data streams, such as LTS and CBM as described in this thesis. This framework incorporates findings and concepts described above in this chapter and is below and in Figure 6.3.

1. *Continuous, independent space-borne and* in situ *data streams.* Both data originating from space-borne (e.g. LTS) and *in situ* (e.g. CBM) data streams are continually ingested and pre-processed for use in the integrated monitoring system. Except in the case of regularly acquired data, such as MODIS 16-day composites, these data streams are essentially processed "on demand". Data acquired *in situ* can be opportunistically sampled as in Chapter 4 as well as with other types of CBM or VGI data streams, or can be sampled based on existing maps (described under point number 3).

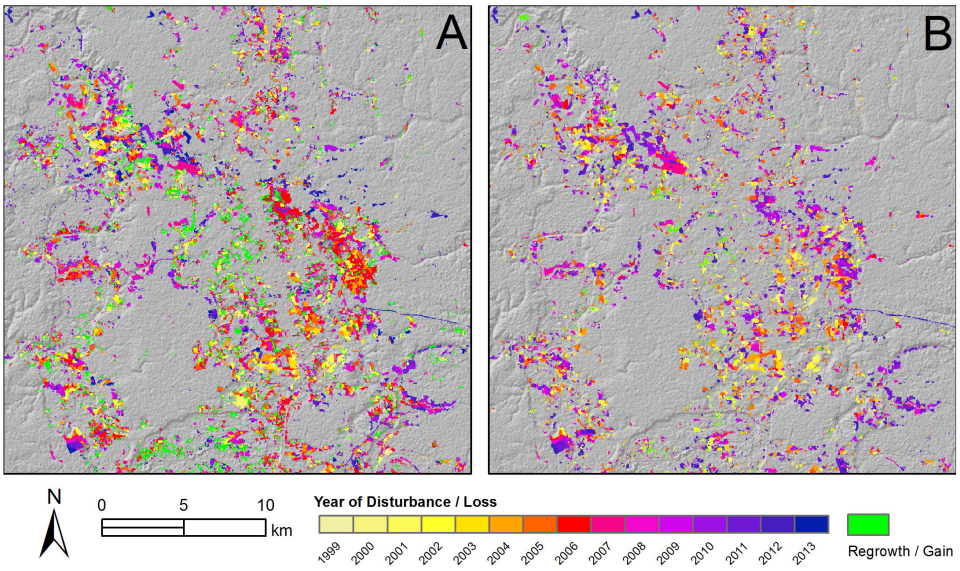

Figure 6.1: Mapped forest dynamics in Madre de Dios, Peru. Disturbance and regrowth described in Chapter 3 are shown in the left panel. Forest gain and loss from Hansen et al. (2013) are shown in the right panel. All results are from between 1999 and 2013.

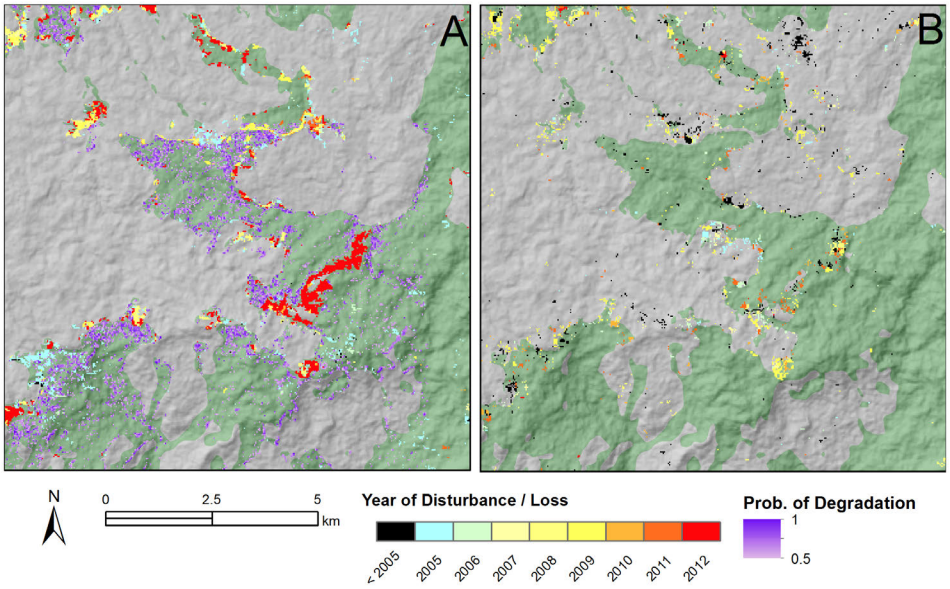

Figure 6.2: Mapped forest dynamics in Kafa, Ethiopia. Disturbance dates (described in Chapter 2) and degradation probabilities for March 2015 described in Chapter 5 are shown in the left panel. Forest gain and loss from Hansen et al. (2013) are shown in the right panel. Disturbance results in the left panel are only available from 2005 to 2012, while disturbance results in the right panel are available from 1999 to 2012.

2. *Calibration and validation of methods and map products.* Methods for quantifying forest dynamics or classifying forest or other land cover types are calibrated and validated using existing *in situ* data. As described in Chapter 5, *a priori* identification and measurement of subtle forest changes are used to enhance time series algorithms. Key outputs include maps of forest disturbance, forest regrowth and other potential forest state variables.

3. *Targeted stratification and sampling.* Continuous ground-based monitoring efforts are aided by knowledge of the spatial distribution of mapped forest change attributes. Field samples are chosen from a stratified random sample, where strata are defined based on previous disturbances (Chapters 2 and 3) or other forest-related state variables such as regrowth (Chapter 3) or degradation (Chapter 5). To monitor forest carbon changes, for example, biomass measurements can be carried out at randomly selected plots from strata defined based on different degrees of canopy cover change (chrono-sequencing). Other quantitative forest variables can be integrated into the system at this point.

4. *Near real-time disturbance alerts.* Near real-time disturbance alerts are fed back to local stakeholders who then have the opportunity to provide verification of the alerts (Pratihast et al., 2015). Such action may lead to subsequent re-calibration or validation of near real-time change detection algorithms (e.g. to reduce false positives) as described in point number 2 above.

5. *Multi-scale reporting.* Regular accounting and *ad hoc* reports are produced from the integrated monitoring system to support a number of objectives and users of the system. Regular accounting is carried out according to REDD+ MRV guidelines, for example, including area change and carbon stock estimates (DeVries & Herold, 2013). Additional local-level reporting is carried out on an *ad hoc* basis in response to near real-time disturbance alerts, triggering follow-up actions such as law enforcement or verification of alerts, as necessary (Souza et al., 2009; Pratihast et al., 2015).

6.3 Concluding Remarks

Satellite remote sensing is entering a new era, in which a multitude of space-borne sensors continually acquire data over the earth's surface. At the same time, advances in *in situ* monitoring imply that ground-based data are also becoming increasingly available for environmental monitoring applications. Not only are new methods and approaches needed to exploit synergies in remote sensing data sources (De Sy et al., 2012), but also methods which can consistently and effectively integrate *in situ* and space-borne time series data streams. This thesis demonstrates how data-driven methods, such as those encompassed within structural change monitoring, can be applied to LTS towards forest monitoring objectives. Some of the first evidence of CBM data being used to improve forest change estimates in tropical landscapes are also shown in this thesis. Future research

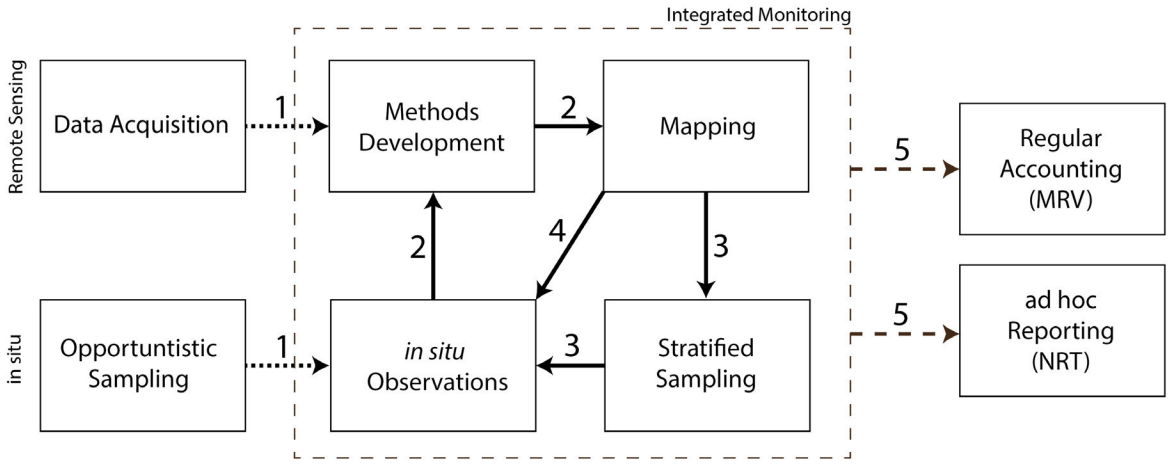

Figure 6.3: Schematic describing an integrated monitoring framework featuring remote sensing (top row) and *in situ*(bottom row) data streams.

can capitalize on these findings by exploring how these two data streams can be further utilized to the benefit of forest monitoring programmes. Effective integration of these data streams will provide greater depth in spatial, temporal and thematic domains.

References

Achard, F., Mollicone, D., Stibig, H.-J., Aksenov, D., Laestadius, L., Li, Z., Popatov, P., & Yaroshenko, A. (2006). Areas of rapid forest-cover change in boreal eurasia. *Forest Ecology and Management*, *237*, 322–334.

Achard, F., Stibig, H., Eva, H., Lindquist, E. J., Bouvet, A., Arino, O., & Mayaux, P. (2010). Estimating tropical deforestation from Earth observation data. *Carbon Management*, *1*, 271–287.

Aerts, R., Berecha, G., & Honnay, O. (2015). Protecting coffee from intensification. *Science*, *347*, 139.

Aerts, R., Hundera, K., Berecha, G., Gijbels, P., Baeten, M., Van Mechelen, M., Hermy, M., Muys, B., & Honnay, O. (2011). Semi-forest coffee cultivation and the conservation of Ethiopian Afromontane rainforest fragments. *Forest Ecology and Management*, *261*, 1034–1041.

Ahmed, O. S., Franklin, S. E., & Wulder, M. a. (2014). Interpretation of forest disturbance using a time series of Landsat imagery and canopy structure from airborne lidar. *Canadian Journal of Remote Sensing*, *39*, 521–542.

Akaike, H. (1973). Information theory and an extension of the maximum likelihood principle. In *Proceeding of the Second International Symposium on Information Theory* (pp. 267–281). Budapest.

Alexandridis, T. K., Cherif, I., Kalogeropoulos, C., Monachou, S., Eskridge, K., & Silleos, N. (2013). Rapid error assessment for quantitative estimations from Landsat 7 gap-filled images. *Remote Sensing Letters*, *4*, 920–928.

Alvarez-Berríos, N. L., & Mitchell Aide, T. (2015). Global demand for gold is another threat for tropical forests. *Environmental Research Letters*, *10*, 014006.

Amazon Conservation Association (2015). Monitoring of the Andean Amazon Project (MAAP). URL: `http://www.maaproject.org/`. Accessed on: 01/07/2015.

Angelsen, A. (2009). *Realising REDD+: National strategy and policy options*. Bogor, Indonesia: Center for International Forestry Research (CIFOR).

Ankersen, J., Grogan, K., Mertz, O., Fensholt, R., Castella, J.-C., Lestrelin, G., Nguyen,

D. T., Danielsen, F., Brofeldt, S. r., & Rasmussen, K. (2015). Vietnam's Forest Transition in Retrospect: Demonstrating Weaknesses in Business-as-Usual Scenarios for REDD+. *Environmental Management*, *55*, 1080–1092.

Anokwa, Y., Hartung, C., & Brunette, W. (2009). Open Source Data Collection in the Developing World. *Computer*, *42*, 97–99.

Arima, E. Y., Walker, R. T., Sales, M., Jr, C. S., & Perz, S. G. (2008). The Fragmentation of Space in the Amazon Basin: Emergent Road Networks. *Photogrammetric Engineering & Remote Sensing*, *74*, 699–709.

Asner, G. P. (2001). Cloud cover in Landsat observations of the Brazilian Amazon. *International Journal of Remote Sensing*, *22*, 37–41.

Asner, G. P. (2009). Tropical forest carbon assessment: integrating satellite and airborne mapping approaches. *Environmental Research Letters*, *4*, 034009.

Asner, G. P., Llactayo, W., Tupayachi, R., & Luna, E. R. (2013). Elevated rates of gold mining in the Amazon revealed through high-resolution monitoring. *Proceedings of the National Academy of Sciences of the United States of America*, *110*, 18454–9.

Assefa, E., & Bork, H.-R. (2014). Deforestation and forest management in southern Ethiopia: investigations in the Chencha and Arbaminch areas. *Environmental management*, *53*, 284–99.

Baccini, a., Goetz, S. J., Walker, W. S., Laporte, N. T., Sun, M., Hackler, J., Beck, P. S. a., Dubayah, R., Friedl, M. a., Samanta, S., Houghton, R. a., Sulla-Menashe, D. et al. (2012). Estimated carbon dioxide emissions from tropical deforestation improved by carbon-density maps. *Nature Climate Change*, *2*, 182–185.

Bach, W. (1976). Global air pollution and climatic change. *Reviews of Geophysics*, *14*, 429–474.

Bai, J. (1997). Estimation of a change point in multiple regression models. *Review of Economics and Statistics*, *74*, 551–563.

Bai, J., & Perron, P. (2003). Computation and analysis of multiple structural change models. *Journal of Applied Econometrics*, *18*, 1–22.

Banskota, A., Kayastha, N., Falkowski, M. J., Wulder, M. A., Froese, R. E., White, J. C., Banskota, A., Kayastha, N., & Falkowski, M. J. (2014). Forest monitoring using Landsat time-series data- A review. *Canadian Journal of Remote Sensing*, *40*, 1–37.

Bédard, F., Reichert, G., Dobbins, R., & Trépanier, I. (2008). Evaluation of segment-based gap-filled Landsat ETM+ SLC-off satellite data for land cover classification in southern Saskatchewan, Canada. *International Journal of Remote Sensing*, *29*, 2041–2054.

Bellfield, H., Sabogal, D., Goodman, L., & Leggett, M. (2015). Case Study Report: Community-Based Monitoring Systems for REDD+ in Guyana. *Forests*, *6*, 133–156.

Belt, T. (1874). *The Naturalist in Nicaragua* volume 9. London: Everyman's Library.

Bernstein, I. S., Balcaen, P., Dresdale, L., Gouzoules, H., Kavanagh, M., Patterson, T., & Neyman-Warner, P. (1976). An appeal for the preservation of habitats in the interests of primate conservation. *Primates*, *17*, 413–415.

Bigagli, L., Santoro, M., Mazzetti, P., & Nativi, S. (2015). Architecture of a Process Broker for Interoperable Geospatial Modeling on the Web. *ISPRS International Journal of Geo-Information*, *4*, 647–660.

Boissière, M., Beaudoin, G., Hofstee, C., & Rafanoharana, S. (2014). Participating in REDD+ Measurement, Reporting, and Verification (PMRV): Opportunities for local people? *Forests*, *5*, 1855–1878.

Bonan, G. B. (2008). Forests and climate change: forcings, feedbacks, and the climate benefits of forests. *Science*, *320*, 1444–1449.

Bongers, F., Chazdon, R., Poorter, L., & Peña Claros, M. (2015). The potential of secondary forests. *Science*, *348*, 642–643.

Bontemps, S., Herold, M., Kooistra, L., van Groenestijn, a., Hartley, a., Arino, O., Moreau, I., & Defourny, P. (2011). Revisiting land cover observations to address the needs of the climate modelling community. *Biogeosciences Discussions*, *8*, 7713–7740.

Bowler, D. E., Buyung-Ali, L. M., Healey, J. R., Jones, J. P., Knight, T. M., & Pullin, A. S. (2012). Does community forest management provide global environmental benefits and improve local welfare? *Frontiers in Ecology and the Environment*, *10*, 29–36.

Breiman, L. (2001). Random forests. *Machine Learning*, *45*, 5–32.

Brofeldt, S., Theilade, I., Burgess, N. D., Danielsen, F., Poulsen, M. K., Adrian, T., Bang, T. N., Budiman, A., Jensen, J., Jensen, A. E., Kurniawan, Y., Læ gaard, S. B. L. et al. (2014). Community monitoring of carbon stocks for REDD+: Does accuracy and cost change over time? *Forests*, *5*, 1834–1854.

Broich, M., Hansen, M. C., Potapov, P., Adusei, B., Lindquist, E., & Stehman, S. V. (2011). Time-series analysis of multi-resolution optical imagery for quantifying forest cover loss in Sumatra and Kalimantan, Indonesia. *International Journal of Applied Earth Observation and Geoinformation*, *13*, 277–291.

Brooks, E. B., Wynne, R. H., Thomas, V. A., Blinn, C. E., Coulston, J. W., & Background, A. (2014). On-the-Fly Massively Multitemporal Change Detection Using Statistical Quality Control Charts and Landsat Data. *IEEE Transactions on Geoscience and Remote Sensing*, *52*, 3316–3332.

Brown, S., & Zarin, D. (2013). What Does Zero Deforestation Mean? *Science*, *342*, 805–807.

Bucki, M., Cuypers, D., Mayaux, P., Achard, F., Estreguil, C., & Grassi, G. (2012). Assessing REDD+ performance of countries with low monitoring capacities: the matrix

approach. *Environmental Research Letters*, *7*.

Calders, K., Newnham, G., Burt, A., Murphy, S., Raumonen, P., Herold, M., Culvenor, D., Avitabile, V., Disney, M., Armston, J., & Kaasalainen, M. (2015a). Nondestructive estimates of above-ground biomass using terrestrial laser scanning. *Methods in Ecology and Evolution*, *6*, 198–208.

Calders, K., Schenkels, T., Bartholomeus, H., Armston, J., Verbesselt, J., & Herold, M. (2015b). Monitoring spring phenology with high temporal resolution terrestrial LiDAR measurements. *Agricultural and Forest Meteorology*, *203*, 158–168.

Carlson, T. N., & Ripley, D. A. (1997). On the relation between NDVI, fractional vegetation cover, and leaf area index. *Remote sensing of Environment*, *62*, 241–252.

Carreiras, J. a. M. B., Jones, J., Lucas, R. M., & Gabriel, C. (2014). Land Use and Land Cover Change Dynamics across the Brazilian Amazon: Insights from Extensive Time-Series Analysis of Remote Sensing Data. *PloS ONE*, *9*, e104144.

Castro, P., Alonso, J., Guerra, C., Gonçalves, J., Pôças, I., Marcos, B., & Honrado, J. (2013). Novel tools to improve the management of spatial data quality in the context of ecosystem and biodiversity monitoring. In *Proceedings of the GI Forum*.

Caviglia-Harris, J. L., Toomey, M., Harris, D. W., Mullan, K., Bell, A. R., Sills, E. O., & Roberts, D. a. (2014). Detecting and interpreting secondary forest on an old Amazonian frontier. *Journal of Land Use Science*, (pp. 1–24).

Chavez, A. B. (2013). Landscape dynamics of Amazonian deforestation between 1986 and 2007 in southeastern Peru: policy drivers and road implications. *Journal of Land Use Science*, (pp. 1–24).

Chen, J., Zhu, X., Vogelmann, J. E., Gao, F., & Jin, S. (2011). A simple and effective method for filling gaps in Landsat ETM+ SLC-off images. *Remote Sensing of Environment*, *115*, 1053–1064.

Chhatre, A., Lakhanpal, S., Larson, A., Nelson, F., Ojha, H., & Rao, J. (2012). Social safeguards and co-benefits in redd+: A review of the adjacent possible. *Current Opinion in Environmental Sustainability*, *4*, 654–660.

Chu, C.-S., Hornik, K., & Kuan, C.-M. (1992). Mosum Tests for Parameter Constancy. *Biometrika*, *82*, 603–617.

Cihlar, J., Latifovic, R., Chen, J., Trishchenko, a., Du, Y., Fedosejevs, G., & Guindon, B. (2004). Systematic corrections of AVHRR image composites for temporal studies. *Remote Sensing of Environment*, *89*, 217–233.

Cihlar, J., Ly, H., Li, Z., & Chen, J. (1997). Multitemporal, multichannel AVHRR data sets for land biosphere studies - artifacts and corrections. *Remote Sensing of Environment*, *60*, 35–57.

Cohen, W. B., Yang, Z., & Kennedy, R. (2010). Detecting trends in forest disturbance

and recovery using yearly Landsat time series: 2. TimeSync - Tools for calibration and validation. *Remote Sensing of Environment*, *114*, 2911–2924.

Colson, F., Bogaert, J., Filho, A. C., Nelson, B., Pinagé, E. R., & Ceulemans, R. (2009). The influence of forest definition on landscape fragmentation assessment in Rondônia, Brazil. *Ecological Indicators*, *9*, 1163–1168.

Comber, A., See, L., Fritz, S., Van der Velde, M., Perger, C., & Foody, G. (2013). Using control data to determine the reliability of volunteered geographic information about land cover. *International Journal of Applied Earth Observation and Geoinformation*, *23*, 37–48.

Comber, A., Wadsworth, R., & Fisher, P. (2008). Using semantics to clarify the conceptual confusion between land cover and land use: the example of 'forest'. *Journal of Land Use Science*, *3*, 37–41.

Comita, L. S., Thompson, J., Uriarte, M., Jonckheere, I., Canham, C. D., & Zimmerman, J. K. (2010). Interactive effects of land use history and natural disturbance on seedling dynamics in a subtropical forest. *Ecological applications : a publication of the Ecological Society of America*, *20*, 1270–1284.

Confalonieri, R., Foi, M., Casa, R., Aquaro, S., Tona, E., Peterle, M., Boldini, a., De Carli, G., Ferrari, a., Finotto, G., Guarneri, T., Manzoni, V. et al. (2013). Development of an app for estimating leaf area index using a smartphone. Trueness and precision determination and comparison with other indirect methods. *Computers and Electronics in Agriculture*, *96*, 67–74.

Conrad, C., & Hilchey, K. (2011). A review of citizen science and community-based environmental monitoring: Issues and opportunities. *Environmental Monitoring and Assessment*, *176*, 273–291.

Coops, N. C., Hilker, T., Bater, C. W., Wulder, M. a., Nielsen, S. E., McDermid, G., & Stenhouse, G. (2012). Linking ground-based to satellite-derived phenological metrics in support of habitat assessment. *Remote Sensing Letters*, *3*, 191–200.

Coppin, P., Jonckheere, I., Nackaerts, K., Muys, B., & Lambin, E. (2004). Digital change detection methods in ecosystem monitoring: a review. *International Journal of Remote Sensing*, *25*, 1565–1596.

Corbera, E., Estrada, M., & Brown, K. (2010). Reducing greenhouse gas emissions from deforestation and forest degradation in developing countries: revisiting the assumptions. *Climatic Change*, *100*, 355–388.

Crist, E. (1985). A TM Tasseled Cap Equivalent Transformation for Reflectance Factor Data. *Remote Sensing of Environment*, *306*, 301–306.

Crist, E., & Kauth, R. (1986). The tasseled cap de-mystified. *Photogrammetric Engineering & Remote Sensing*, *52*, 81–86.

Crist, E. P., & Cicone, R. C. (1984). A Physically-Based Transformation of Thematic Mapper Data—The TM Tasseled Cap. *IEEE Transactions on Geoscience and Remote Sensing*, *GE-22*, 256–263.

Czerwinski, C. J., King, D. J., & Mitchell, S. W. (2014). Mapping forest growth and decline in a temperate mixed forest using temporal trend analysis of Landsat imagery, 1987–2010. *Remote Sensing of Environment*, *141*, 188–200.

Danielsen, F., Adrian, T., Brofeldt, S., van Noordwijk, M., Poulsen, M., Rahayu, S., Rutishauser, E., Theilade, I., Widayati, A., An, N., Bang, T., Budiman, A. et al. (2013). Community monitoring for REDD+: International promises and field realities. *Ecology and Society*, *18*.

Danielsen, F., Burgess, N., & Balmford, A. (2005). Monitoring matters: Examining the potential of locally-based approaches. *Biodiversity and Conservation*, *14*, 2507–2542.

Danielsen, F., Burgess, N., Balmford, A., Donald, P., Funder, M., Jones, J., Alviola, P., Balete, D., Blomley, T., Brashares, J., Child, B., Enghoff, M. et al. (2009). Local participation in natural resource monitoring: A characterization of approaches. *Conservation Biology*, *23*, 31–42.

Danielsen, F., Burgess, N., Jensen, P., & Pirhofer-Walzl, K. (2010). Environmental monitoring: The scale and speed of implementation varies according to the degree of peoples involvement. *Journal of Applied Ecology*, *47*, 1166–1168.

Danielsen, F., Jensen, P., Burgess, N., Altamirano, R., Alviola, P., Andrianandrasana, H., Brashares, J., Burton, A., Coronado, I., Corpuz, N., Enghoff, M., Fjeldså, J. et al. (2014). A multicountry assessment of tropical resource monitoring by local communities. *BioScience*, *64*, 236–251.

Danielsen, F., Skutsch, M., Burgess, N., Jensen, P., Andrianandrasana, H., Karky, B., Lewis, R., Lovett, J., Massao, J., Ngaga, Y., Phartiyal, P., Poulsen, M. et al. (2011). At the heart of REDD+: A role for local people in monitoring forests? *Conservation Letters*, *4*, 158–167.

De Sy, V., Herold, M., Achard, F., Asner, G. P., Held, A., Kellndorfer, J., & Verbesselt, J. (2012). Synergies of multiple remote sensing data sources for REDD+ monitoring. *Current Opinion in Environmental Sustainability*, *4*, 1–11.

Defries, R., Achard, F., Brown, S., Herold, M., Murdiyarso, D., Schlamadinger, B., & Desouzajr, C. (2007). Earth observations for estimating greenhouse gas emissions from deforestation in developing countries. *Environmental Science & Policy*, *10*, 385–394.

DeFries, R., Hansen, A., Newton, A. C., & Hansen, M. C. (2005). Increasing Isolation of Protected Areas in Tropical Forests Over the Past Twenty Years. *Ecological Applications*, *15*, 19–26.

Delbart, N., Beaubien, E., Kergoat, L., & Le Toan, T. (2015). Comparing land surface

phenology with leafing and flowering observations from the PlantWatch citizen network. *Remote Sensing of Environment*, *160*, 273–280.

Devillers, R., Bédard, Y., Jeansoulin, R., & Moulin, B. (2007). Towards spatial data quality information analysis tools for experts assessing the fitness for use of spatial data. *International Journal of Geographical Information Science*, *21*, 261–282.

DeVries, B., & Herold, M. (2013). The Science of Measuring, Reporting and Verification (MRV). In R. Lyster, C. MacKenzie, & C. McDermott (Eds.), *Law, Tropical Forests and Carbon: The Case of REDD+* chapter 8. (pp. 151–183). Cambridge: Cambridge Univ Press.

DeVries, B., Verbesselt, J., Kooistra, L., & Herold, M. (2015). Robust monitoring of small-scale forest disturbances in a tropical montane forest using Landsat time series. *Remote Sensing of Environment*, *161*, 107–121.

Dickson, B., & Kapos, V. (2012). Biodiversity monitoring for REDD+. *Current Opinion in Environmental Sustainability*, *4*, 717–725.

Dourojeanni, M. J. (2006). *Estudio de caso sobre la carretera Interoceánica en la amazonía sur del Perú*. Bank Information Centre (BIC). Lima. URL: `http://www.bicusa.org/en/Document.100135.pdf`.

Dresen, E., DeVries, B., Herold, M., Verchot, L., & Müller, R. (2014). Fuelwood Savings and Carbon Emission Reductions by the Use of Improved Cooking Stoves in an Afromontane Forest, Ethiopia. *Land*, *3*, 1137–1157.

Drusch, M., Del Bello, U., Carlier, S., Colin, O., Fernandez, V., Gascon, F., Hoersch, B., Isola, C., Laberinti, P., Martimort, P., Meygret, A., Spoto, F. et al. (2012). Sentinel-2: Esa's optical high-resolution mission for gmes operational services. *Remote Sensing of Environment*, *120*, 25–36.

Dutrieux, L. P., Verbesselt, J., Kooistra, L., & Herold, M. (2015). Monitoring forest cover loss using multiple data streams, a case study of a tropical dry forest in Bolivia. *ISPRS Journal of Photogrammetry and Remote Sensing*, . In press.

Duveiller, G., Defourny, P., Desclée, B., & Mayaux, P. (2008). Deforestation in Central Africa: Estimates at regional, national and landscape levels by advanced processing of systematically-distributed Landsat extracts. *Remote Sensing of Environment*, *112*, 1969–1981.

Englhart, S., Keuck, V., & Siegert, F. (2011). Aboveground biomass retrieval in tropical forests — The potential of combined X- and L-band SAR data use. *Remote Sensing of Environment*, *115*, 1260–1271.

Ernst, C., Mayaux, P., Verhegghen, A., Bodart, C., Christophe, M., & Defourny, P. (2013). National forest cover change in Congo Basin: deforestation, reforestation, degradation and regeneration for the years 1990, 2000 and 2005. *Global change biology*, *19*, 1173–87.

Evangelidis, K., Ntouros, K., Makridis, S., & Papatheodorou, C. (2014). Geospatial services in the Cloud. *Computers and Geosciences*, *63*, 116–122.

Fagan, M., & Defries, R. (2009). *Measurement and Monitoring of the World's Forests*. Resources for the Future.

FAO (2014). *State of the World's Forests*. Food and Agriculture Organization of the United Nations. Rome.

Feldpausch, T. R., Prates-Clark, C. D. C., Fernandes, E. C., & Riha, S. J. (2007). Secondary forest growth deviation from chronosequence predictions in central Amazonia. *Global Change Biology*, *13*, 967–979.

Fensholt, R., Horion, S., Tagesson, T., Ehammer, A., Ivits, E., & Rasmussen, K. (2015). Global-scale mapping of changes in ecosystem functioning from earth observation-based trends in total and recurrent vegetation. *Global Ecology and Biogeography*, . In press.

Fensholt, R., & Proud, S. R. (2012). Evaluation of Earth Observation based global long term vegetation trends — Comparing GIMMS and MODIS global NDVI time series. *Remote Sensing of Environment*, *119*, 131–147.

Fernandes, R., & G. Leblanc, S. (2005). Parametric (modified least squares) and non-parametric (Theil–Sen) linear regressions for predicting biophysical parameters in the presence of measurement errors. *Remote Sensing of Environment*, *95*, 303–316.

Ferster, C. J., & Coops, N. C. (2015). Integrating volunteered smartphone data with multispectral remote sensing to estimate forest fuels. *International Journal of Digital Earth*, (pp. 1–26).

Finegan, B. (1996). Pattern and process in neotropical secondary rain forests: The first 100 years of succession. *Trends in Ecology and Evolution*, *11*, 119–124.

Fiorella, M., & Ripple, W. (1993). Analysis of conifer forest regeneration using Landsat Thematic Mapper data. *Photogrammetric Engineering & Remote Sensing*, *59*, 1383–1388.

Fisher, B. (2010). African exception to drivers of deforestation. *Nature Geoscience*, *3*, 375–376.

Foody, G. M., & Boyd, D. S. (2002). Sharpened Mapping of Tropical Forest Biophysical Properties from Coarse Spatial Resolution Satellite Sensor Data. *Neural Computing & Applications*, *11*, 62–70.

Foody, G. M., & Boyd, D. S. (2013). Using volunteered data in land cover map validation: Mapping west African forests. *IEEE Journal of Selected Topics in Applied Earth Observations and Remote Sensing*, *6*, 1305–1312.

Frazier, R. J., Coops, N. C., Wulder, M. a., & Kennedy, R. (2014). Characterization of aboveground biomass in an unmanaged boreal forest using Landsat temporal segmentation metrics. *ISPRS Journal of Photogrammetry and Remote Sensing*, *92*, 137–146.

Freitas, S. R., Mello, M. C. S., & Cruz, C. B. M. (2005). Relationships between forest structure and vegetation indices in Atlantic Rainforest. *Forest Ecology and Management*, *218*, 353–362.

Gamon, J. a., Field, C. B., Goulden, M. L., Griffin, K. L., Applications, S. E., & Feb, N. (1995). Relationships Between NDVI, Canopy Structure, and Photosynthesis in Three Californian Vegetation Types. *Ecological Applications*, *5*, 28–41.

Gao, B. (1996). NDWI - a normalized difference water index for remote sensing of vegetation liquid water from space. *Remote sensing of environment*, *266*, 257–266.

Garedew, E., Sandewall, M., Söderberg, U., & Campbell, B. M. (2009). Land-use and land-cover dynamics in the central rift valley of Ethiopia. *Environmental management*, *44*, 683–94.

Gebrehiwot, S. G., Bewket, W., Gärdenäs, A. I., & Bishop, K. (2013). Forest cover change over four decades in the Blue Nile Basin, Ethiopia: comparison of three watersheds. *Regional Environmental Change*, *14*, 253–266.

Getahun, K., Van Rompaey, a., Van Turnhout, P., & Poesen, J. (2013). Factors controlling patterns of deforestation in moist evergreen Afromontane forests of Southwest Ethiopia. *Forest Ecology and Management*, *304*, 171–181.

Gibbs, H., & Herold, M. (2007). Tropical deforestation and greenhouse gas emissions. *Environmental Research Letters*, *2*.

Goetz, S., & Dubayah, R. (2011). Advances in remote sensing technology and implications for measuring and monitoring forest carbon stocks and change. *Carbon Management*, *2*, 231–244.

GOFC-GOLD (2010). *A sourcebook of methods and procedures for monitoring and reporting anthropogenic greenhouse gas emissions and removals caused by deforestation, gains and losses of carbon stocks in forests remaining forests, and forestation*. GOFC-GOLD Land Cover Office.

Gómez, C., White, J. C., Wulder, M. a., & Alejandro, P. (2014). Historical forest biomass dynamics modelled with Landsat spectral trajectories. *ISPRS Journal of Photogrammetry and Remote Sensing*, *93*, 14–28.

Gonsamo, A., D'odorico, P., & Pellikka, P. (2013). Measuring fractional forest canopy element cover and openness - definitions and methodologies revisited. *Oikos*, *122*, 1283–1291.

Goodchild, M. (2007). Citizens as sensors: The world of volunteered geography. *GeoJournal*, *69*, 211–221.

Grassi, G., Monni, S., Federici, S., Achard, F., & Mollicone, D. (2008). Applying the conservativeness principle to REDD to deal with the uncertainties of the estimates. *Environmental Research Letters*, *3*, 035005.

Griffiths, P., Kuemmerle, T., Baumann, M., Radeloff, V. C., Abrudan, I. V., Lieskovsky, J., Munteanu, C., Ostapowicz, K., & Hostert, P. (2013). Forest disturbances, forest recovery, and changes in forest types across the Carpathian ecoregion from 1985 to 2010 based on Landsat image composites. *Remote Sensing of Environment*, *151*, 72–88.

Gullison, R., Frumhoff, P., Canadell, J., Field, C., Nepstad, D., Hayhoe, K., Avissar, R., Curran, L., Friedlingstein, P., Jones, C., & Nobre, C. (2007). Tropical forests and climate policy. *Science*, *316*, 985–986.

Hajek, F., Ventresca, M. J., Scriven, J., & Castro, A. (2011). Regime-building for REDD+: Evidence from a cluster of local initiatives in south-eastern Peru. *Environmental Science & Policy*, *14*, 201–215.

Haklay, M. (2010). How good is volunteered geographical information? a comparative study of openstreetmap and ordnance survey datasets. *Environment and Planning B: Planning and Design*, *37*, 682–703.

Hansen, M., & Loveland, T. (2012). A review of large area monitoring of land cover change using landsat data. *Remote Sensing of Environment*, *122*, 66–74.

Hansen, M., Potapov, P., Margono, B., Stehman, S., Turubanova, S., & Tyukavina, a. (2014). Response to comment on "High-resolution global maps of 21st-century forest cover change". *Science*, *344*, 981.

Hansen, M. C., DeFries, R. S., Townshend, J. R. G., Carroll, M., Dimiceli, C., & Sohlberg, R. a. (2003). Global Percent Tree Cover at a Spatial Resolution of 500 Meters: First Results of the MODIS Vegetation Continuous Fields Algorithm. *Earth Interactions*, *7*, 1–15.

Hansen, M. C., Potapov, P. V., Moore, R., Hancher, M., Turubanova, S. a., Tyukavina, a., Thau, D., Stehman, S. V., Goetz, S. J., Loveland, T. R., Kommareddy, a., Egorov, a. et al. (2013). High-resolution global maps of 21st-century forest cover change. *Science*, *342*, 850–3.

Hardisky, M. A., Klemas, V., & Smart, R. M. (1983). The influence of soil salinity, growth form, and leaf moisture on the spectral radiance of Spartina alterniflora canopies. *Photogrammetric Engineering and Remote Sensing*, *49*, 77–83.

Healey, S., Cohen, W., Zhiqiang, Y., & Krankina, O. (2005). Comparison of Tasseled Cap-based Landsat data structures for use in forest disturbance detection. *Remote Sensing of Environment*, *97*, 301–310.

Hein, L., & Gatzweiler, F. (2006). The economic value of coffee (Coffea arabica) genetic resources. *Ecological Economics*, *60*, 176–185.

Helmer, E. H., Lefsky, M. a., & Roberts, D. a. (2009). Biomass accumulation rates of Amazonian secondary forest and biomass of old-growth forests from Landsat time series and the Geoscience Laser Altimeter System. *Journal of Applied Remote Sensing*, *3*,

033505.

Herold, M., & Johns, T. (2007). Linking requirements with capabilities for deforestation monitoring in the context of the UNFCCC-REDD process. *Environmental Research Letters*, *2*, 045025.

Herold, M., Roman-Cuesta, R. M. R., Mollicone, D., Hirata, Y., Van Laake, P., Asner, G. G. P., Souza, C., Skutsch, M., Avitabile, V., & MacDicken, K. (2011). Options for monitoring and estimating historical carbon emissions from forest degradation in the context of REDD+. *Carbon Balance and Management*, *6*, 13.

Herold, M., & Skutsch, M. (2011). Monitoring, reporting and verification for national REDD+ programmes: Two proposals. *Environmental Research Letters*, *6*.

Hilker, T., Wulder, M. a., Coops, N. C., Linke, J., McDermid, G., Masek, J. G., Gao, F., & White, J. C. (2009). A new data fusion model for high spatial- and temporal-resolution mapping of forest disturbance based on Landsat and MODIS. *Remote Sensing of Environment*, *113*, 1613–1627.

Hirota, M., Holmgren, M., Van Nes, E. H., & Scheffer, M. (2011). Global Resilience of Tropical Forest and Savanna to Critical Transitions. *Science*, *334*, 232–235.

Hirschmugl, M., Steinegger, M., Gallaun, H., & Schardt, M. (2014). Mapping Forest Degradation due to Selective Logging by Means of Time Series Analysis: Case Studies in Central Africa. *Remote Sensing*, *6*, 756–775.

Holling, C. S. (1973). Resilience and Stability of Ecological Systems. *Annual Review of Ecology and Systematics*, *4*, 1–23.

Holmgren, P., & Marklund, L.-G. (2007). National Forest Monitoring Systems - purposes, options and status. In P. Freer-Smith, M. Broadmeadow, & J. Lynch (Eds.), *Forestry & Climate Change* (pp. 163–173). CAB International.

Hosonuma, N., Herold, M., De Sy, V., De Fries, R. S., Brockhaus, M., Verchot, L., Angelsen, A., & Romijn, E. (2012). An assessment of deforestation and forest degradation drivers in developing countries. *Environmental Research Letters*, *7*, 044009.

Houghton, R. a., House, J. I., Pongratz, J., van der Werf, G. R., DeFries, R. S., Hansen, M. C., Le Quéré, C., & Ramankutty, N. (2012). Carbon emissions from land use and land-cover change. *Biogeosciences*, *9*, 5125–5142.

Howorth, R. T., & Pendry, C. a. (2006). Post-cultivation secondary succession in a Venezuelan lower montane rain forest. *Biodiversity and Conservation*, *15*, 693–715.

Huang, C., Goward, S. N., Masek, J. G., Thomas, N., Zhu, Z., & Vogelmann, J. E. (2010). An automated approach for reconstructing recent forest disturbance history using dense Landsat time series stacks. *Remote Sensing of Environment*, *114*, 183–198.

Huang, M., & Asner, G. P. (2010). Long-term carbon loss and recovery following selective logging in Amazon forests. *Global Biogeochemical Cycles*, *24*, 1–15.

Huber, P. J. (1964). Robust Estimation of a Location Parameter. *The Annals of Mathematical Statistics*, *35*, 73–101.

Huete, a., Didan, K., Miura, T., Rodriguez, E. P., Gao, X., & Ferreira, L. G. (2002). Overview of the radiometric and biophysical performance of the MODIS vegetation indices. *Remote Sensing of Environment*, *83*, 195–213.

Hunt Jr, E. R., & Rock, B. N. (1989). Detection of changes in leaf water content using Near- and Middle-Infrared reflectances. *Remote Sensing of Environment*, *30*, 43–54.

INPE (2014a). Detecção de Desmatamento em Tempo Real. URL: `http://obt.inpe.br/deter/`.

INPE (2014b). Projeto PRODES: Monitoramento da Floresta Amazônica Brasileira por Satélite. URL: `http://obt.inpe.br/prodes/index.php`.

Irons, J. R., Dwyer, J. L., & Barsi, J. a. (2012). The next Landsat satellite: The Landsat Data Continuity Mission. *Remote Sensing of Environment*, *122*, 11–21.

ISO/TC211 (2002). *Geographic information - Quality principles*. International Organization for Standardization.

Jamali, S., Jönsson, P., Eklundh, L., Ardö, J., & Seaquist, J. (2015). Remote Sensing of Environment Detecting changes in vegetation trends using time series segmentation. *Remote Sensing of Environment*, *156*, 182–195.

Jin, S., & Sader, S. a. (2005). Comparison of time series tasseled cap wetness and the normalized difference moisture index in detecting forest disturbances. *Remote Sensing of Environment*, *94*, 364–372.

Johnson, N., Kotz, S., & Kemp, A. (1992). *Univariate Discrete Distributions*. Wiley-Interscience.

Jonckheere, I., Nackaerts, K., Muys, B., & Coppin, P. (2005). Assessment of automatic gap fraction estimation of forests from digital hemispherical photography. *Agricultural and Forest Meteorology*, *132*, 96–114.

de Jong, R., Verbesselt, J., Zeileis, A., & Schaepman, M. (2013). Shifts in Global Vegetation Activity Trends. *Remote Sensing*, *5*, 1117–1133.

Joseph, S., Herold, M., Sunderlin, W. D., & Verchot, L. V. (2013). REDD+ readiness: early insights on monitoring, reporting and verification systems of project developers. *Environmental Research Letters*, *8*, 034038.

Joshi, N., Mitchard, E. T. A., Woo, N., Torres, J., Moll-rocek, J., & Ehammer, A. (2015). Mapping dynamics of deforestation and forest degradation in tropical forests using radar satellite data. *Environmental Research Letters*, *10*, 34014.

Ju, J., & Roy, D. P. (2008). The availability of cloud-free Landsat ETM+ data over the conterminous United States and globally. *Remote Sensing of Environment*, *112*,

1196–1211.

Karousakis, K. (2009). *Promoting Biodiversity Co-Benefits in REDD*. 11 OECD Environment Working Papers.

Kennedy, R., Cohen, W., & Schroeder, T. (2007). Trajectory-based change detection for automated characterization of forest disturbance dynamics. *Remote Sensing of Environment*, *110*, 370–386.

Kennedy, R. E., Andréfouët, S., Cohen, W. B., Gómez, C., Griffiths, P., Hais, M., Healey, S. P., Helmer, E. H., Hostert, P., Lyons, M. B., Meigs, G. W., Pflugmacher, D. et al. (2014). Bringing an ecological view of change to Landsat-based remote sensing. *Frontiers in Ecology and the Environment*, *12*, 339–346.

Kennedy, R. E., Yang, Z., & Cohen, W. B. (2010). Detecting trends in forest disturbance and recovery using yearly Landsat time series: 1. LandTrendr - Temporal segmentation algorithms. *Remote Sensing of Environment*, *114*, 2897–2910.

Kennedy, R. E., Yang, Z., Cohen, W. B., Pfaff, E., Braaten, J., & Nelson, P. (2012). Spatial and temporal patterns of forest disturbance and regrowth within the area of the Northwest Forest Plan. *Remote Sensing of Environment*, *122*, 117–133.

Key, C. H., & Benson, N. C. (2006). *Landscape assessment: Ground measure of severity, the composite burn index; and remote sensing of severity, the Normalized Burn Ratio. FIREMON: Fire effects monitoring and inventory system, USDA Forest Service General Technical Report RMRS-GTR-164-CD*. USDA Forest Service Rocky Mountain Research Station. Fort Collins, CO.

Kim, D.-H., Sexton, J. O., Noojipady, P., Huang, C., Anand, A., Channan, S., Feng, M., & Townshend, J. R. (2014). Global, Landsat-based forest-cover change from 1990 to 2000. *Remote Sensing of Environment*, *155*, 178—193.

Kissinger, G., Herold, M., & Sy, V. D. (2012). *Drivers of Deforestation and Forest Degradation*. Lexeme Consulting. Vancouver.

Lambin, E. F. (1999). Monitoring forest degradation in tropical regions by remote sensing: some methodological issues. *Global Ecology and Biogeography*, *8*, 191–198.

Laurance, W. F., Useche, D. C., Rendeiro, J., Kalka, M., Bradshaw, C. J. a., Sloan, S. P., Laurance, S. G., Campbell, M., Abernethy, K., Alvarez, P., Arroyo-Rodriguez, V., Ashton, P. et al. (2012). Averting biodiversity collapse in tropical forest protected areas. *Nature*, *489*, 290–4.

Lawlor, K., Madeira, E., Blockhus, J., & Ganz, D. (2013). Community participation and benefits in redd+: A review of initial outcomes and lessons. *Forests*, *4*, 296–318.

Lee, K., & Kang, S. (2013). Mobile cloud service of geo-based image processing functions: a test iPad implementation. *Remote Sensing Letters*, *4*, 37–41.

van de Leemput, I. a., van Nes, E. H., & Scheffer, M. (2015). Resilience of Alternative

States in Spatially Extended Ecosystems. *PLoS ONE*, *10*, e0116859.

Leisch, F., Hornik, K., & Kuan, C. (2000). Monitoring structural changes with the generalized fluctuation test. *Econometric Theory*, *16*, 835–854.

Lewis, S. L., Phillips, O. L., Baker, T. R., Lloyd, J., Malhi, Y., Almeida, S., Higuchi, N., Laurance, W. F., Neill, D. a., Silva, J. N. M., Terborgh, J., Lezama, a. T. et al. (2004). Concerted changes in tropical forest structure and dynamics: evidence from 50 South American long-term plots. *Philosophical transactions of the Royal Society of London. Series B, Biological sciences*, *359*, 421–436.

Lhermitte, S., Verbesselt, J., Verstraeten, W., & Coppin, P. (2011). A comparison of time series similarity measures for classification and change detection of ecosystem dynamics. *Remote Sensing of Environment*, *115*, 3129—3152.

Li, X., Wang, S., Ge, Y., Jin, R., Liu, S., Ma, M., Shi, W., Li, R., & Liu, Q. (2013). Development and experimental verification of key techniques to validate remote sensing products. In *International Archives of the Photogrammetry, Remote Sensing and Spatial Information Sciences: 8th International Symposium on Spatial Data Quality* (pp. 25–30). volume 40.

Loveland, T. R., & Dwyer, J. L. (2012). Landsat: Building a strong future. *Remote Sensing of Environment*, *122*, 22–29.

Main-Knorn, M., Cohen, W. B., Kennedy, R. E., Grodzki, W., Pflugmacher, D., Griffiths, P., & Hostert, P. (2013). Monitoring coniferous forest biomass change using a Landsat trajectory-based approach. *Remote Sensing of Environment*, *139*, 277–290.

Malhi, Y., Roberts, J., Betts, R., & Killeen, T. (2008). Climate change, deforestation, and the fate of the Amazon. *Science*, *319*, 169–173.

Masek, J., Schwaller, M., & Hall, F. (2006a). On the blending of the Landsat and MODIS surface reflectance: predicting daily Landsat surface reflectance. *IEEE Transactions on Geoscience and Remote Sensing*, *44*, 2207–2218.

Masek, J. G., Vermote, E. F., Saleous, N. E., Wolfe, R., Hall, F. G., Huemmrich, K. F., Gao, F., Kutler, J., & Lim, T.-K. (2006b). A Landsat surface reflectance dataset for North America, 1990-2000. *IEEE Geoscience and Remote Sensing Letters*, *3*, 68–72.

Maxwell, S. K., Schmidt, G. L., & Storey, J. C. (2007). A multi-scale segmentation approach to filling gaps in Landsat ETM+ SLC-off images. *International Journal of Remote Sensing*, *28*, 5339–5356.

a.J. McDonald, Gemmell, F., & Lewis, P. (1998). Investigation of the Utility of Spectral Vegetation Indices for Determining Information on Coniferous Forests. *Remote Sensing of Environment*, *66*, 250–272.

McRoberts, R. E., Tomppo, E. O., Vibrans, A. C., & Freitas, J. V. D. (2013). Design considerations for tropical forest inventories. *Pesquisa Florestal Brasileira*, *33*, 189–202.

Meigs, G. W., Kennedy, R. E., & Cohen, W. B. (2011). A Landsat time series approach to characterize bark beetle and defoliator impacts on tree mortality and surface fuels in conifer forests. *Remote Sensing of Environment*, *115*, 3707–3718.

Mertz, O., Müller, D., Sikor, T., Hett, C., Heinimann, A., Castella, C., Lestrelin, G., Ryan, C. M., Reay, D. S., Danielsen, F., Theilade, I., Noordwijk, M. V. et al. (2012). The forgotten D: challenges of addressing forest degradation in complex mosaic landscapes under REDD. *Geografisk Tidsskrift-Danish Journal of Geography*, *112*, 37–41.

Mitchard, E. T. a., Saatchi, S. S., White, L. J. T., Abernethy, K. a., Jeffery, K. J., Lewis, S. L., Collins, M., Lefsky, M. a., Leal, M. E., Woodhouse, I. H., & Meir, P. (2011). Mapping tropical forest biomass with radar and spaceborne LiDAR: overcoming problems of high biomass and persistent cloud. *Biogeosciences Discussions*, *8*, 8781–8815.

Morales-Barquero, L., Skutsch, M., Jardel-Peláez, E., Ghilardi, A., Kleinn, C., & Healey, J. (2014). Operationalizing the Definition of Forest Degradation for REDD+, with Application to Mexico. *Forests*, *5*, 1653–1681.

Myers, N. (1979). U.S. State Department/A.I.D. Conference on Deforestation in the Tropics, held in Washington, D.C., 12?14 June 1978. *Environmental Conservation*, *6*, 71–71.

Myers, N., Mittermeier, R. a., Mittermeier, C. G., da Fonseca, G. a., & Kent, J. (2000). Biodiversity hotspots for conservation priorities. *Nature*, *403*, 853–8.

NASA (2015). NASA, USGS Begin Work on Landsat 9 to Continue Land Imaging Legacy. URL: `http://www.nasa.gov/`.

Neeti, N., & Eastman, J. R. (2011). A Contextual Mann-Kendall Approach for the Assessment of Trend Significance in Image Time Series. *Transactions in GIS*, *15*, 599–611.

Neeti, N., Rogan, J., Christman, Z., Eastman, J. R., Millones, M., Schneider, L., Nickl, E., Schmook, B., Turner, B. L., & Ghimire, B. (2012). Mapping seasonal trends in vegetation using AVHRR-NDVI time series in the Yucatán Peninsula, Mexico. *Remote Sensing Letters*, *3*, 433–442.

Neigh, C., Bolton, D., Diabate, M., Williams, J., & Carvalhais, N. (2014). An Automated Approach to Map the History of Forest Disturbance from Insect Mortality and Harvest with Landsat Time-Series Data. *Remote Sensing*, *6*, 2782–2808.

Nepstad, D., & Carvalho, G. (2001). Road paving, fire regime feedbacks, and the future of Amazon forests. *Forest Ecology and Management*, *154*, 395–407.

Nielsen, A., Conradsen, K., & Simpson, J. (1998). Multivariate Alteration Detection (MAD) and MAF Postprocessing in Multispectral, Bitemporal Image Data: New Approaches to Change Detection Studies. *Remote Sensing of Environment*, *64*, 1–19.

Olander, L. P., Gibbs, H. K., Steininger, M., Swenson, J. J., & Murray, B. C. (2008). Reference scenarios for deforestation and forest degradation in support of REDD: a review of data and methods. *Environmental Research Letters*, *3*, 025011.

Olofsson, P., Foody, G. M., Stehman, S. V., & Woodcock, C. E. (2013). Making better use of accuracy data in land change studies: Estimating accuracy and area and quantifying uncertainty using stratified estimation. *Remote Sensing of Environment*, *129*, 122–131.

Palmer Fry, B. (2011). Community forest monitoring in REDD+: the 'M' in MRV? *Environmental Science & Policy*, *14*, 181–187.

Pan, Y., Birdsey, R. a., Fang, J., Houghton, R., Kauppi, P. E., Kurz, W. a., Phillips, O. L., Shvidenko, a., Lewis, S. L., Canadell, J. G., Ciais, P., Jackson, R. B. et al. (2011). A Large and Persistent Carbon Sink in the World's Forests. *Science*, *988*, 1–28.

Pelletier, J., Ramankutty, N., & Potvin, C. (2011). Diagnosing the uncertainty and detectability of emission reductions for REDD + under current capabilities: an example for Panama. *Environmental Research Letters*, *6*, 024005.

Penman, J., Gytarsky, M., Hiraishi, T., Krug, T., Kruger, D., Pipatti, R., Buendia, L., Miwa, K., & Ngara, T. (2003). *Good Practice Guidance for Land Use, Land-Use Change and Forestry*. Intergovernmental Panel on Climate Change (IPCC).

Pereira, H. M., Ferrier, S., Walters, M., Geller, G. N., Jongman, R. H. G., Scholes, R. J., Bruford, M. W., Brummitt, N., Butchart, S. H. M., Cardoso, A. C., Coops, N. C., Dulloo, E. et al. (2013). Essential biodiversity variables. *Science*, *339*, 277–278.

Peru: Ministerio del Ambiente (2011). *Forest Carbon Partnership Fund (FCPF): Readiness Preparation Proposal (R-PP)*. Ministerio del Ambiente.

Petitjean, F., Inglada, J., & Gançarski, P. (2012). Satellite image time series analysis under time warping. *IEEE Transactions on Geoscience and Remote Sensing*, *50*, 3081–3095.

Pfaff, A. (1999). What drives deforestation in the Brazilian Amazon?: evidence from satellite and socioeconomic data. *Journal of Environmental Economics and Management*, *37*, 26–43.

Pflugmacher, D., Cohen, W. B., & E. Kennedy, R. (2012). Using Landsat-derived disturbance history (1972–2010) to predict current forest structure. *Remote Sensing of Environment*, *122*, 146–165.

Pflugmacher, D., Cohen, W. B., Kennedy, R. E., & Yang, Z. (2013). Using Landsat-derived disturbance and recovery history and lidar to map forest biomass dynamics. *Remote Sensing of Environment*, *151*, 124–137.

Phillips, O. L., Malhi, Y., Higuchi, N., Laurance, W. F., Núñez, P. V., Vásquez, R. M., Laurance, S. G., Ferreira, L. V., Stern, M., Brown, S., & Grace, J. (1998). Changes in

the carbon balance of tropical forests: Evidence from long-term plots. *Science*, *282*, 439–442.

Pinzon, J., & Tucker, C. (2014). A Non-Stationary 1981-2012 AVHRR NDVI3g Time Series. *Remote Sensing*, *6*, 6929–6960.

Pohl, C., & Van Genderen, J. (1998). Multisensor image fusion in remote sensing: Concepts, methods and applications. *International Journal of Remote Sensing*, *19*, 823–854.

Potapov, P. V., Dempewolf, J., Talero, Y., Hansen, M. C., Stehman, S. V., Vargas, C., Rojas, E. J., Castillo, D., Mendoza, E., Calderón, a., Giudice, R., Malaga, N. et al. (2014). National satellite-based humid tropical forest change assessment in Peru in support of REDD+ implementation. *Environmental Research Letters*, *9*, 124012.

Potapov, P. V., Turubanova, S. a., Hansen, M. C., Adusei, B., Broich, M., Altstatt, A., Mane, L., & Justice, C. O. (2012). Quantifying forest cover loss in Democratic Republic of the Congo, 2000–2010, with Landsat ETM+ data. *Remote Sensing of Environment*, *122*, 106–116.

Powell, S. L., Cohen, W. B., Kennedy, R. E., Healey, S. P., & Huang, C. (2013). Observation of Trends in Biomass Loss as a Result of Disturbance in the Conterminous U.S.: 1986–2004. *Ecosystems*, *17*, 142–157.

Pratihast, A., DeVries, B., Avitabile, V., de Bruin, S., Kooistra, L., Tekle, M., & Herold, M. (2014). Combining Satellite Data and Community-Based Observations for Forest Monitoring. *Forests*, *5*, 2464–2489.

Pratihast, A., Herold, M., Avitabile, V., de Bruin, S., Bartholomeus, H., Souza, J., C.M., & Ribbe, L. (2012). Mobile devices for community-based REDD+ monitoring: a case study for Central Vietnam. *Sensors*, *13*, 21–38.

Pratihast, A., Herold, M., De Sy, V., Murdiyarso, D., & Skutsch, M. (2013). Linking community-based and national REDD+ monitoring: A review of the potential. *Carbon Management*, *4*, 91–104.

Pratihast, A. K., DeVries, B., Avitabile, V., de Bruin, S., Herold, M., & Bergsma, A. (2015). Design and implementation of an interactive web-based near real-time forest monitoring system. *PLoS ONE*, . Submitted.

R Core Team (2014). *R: A Language and Environment for Statistical Computing*. R Foundation for Statistical Computing Vienna, Austria.

Ratner, B., & Terry, P. (2012). *Building coalitions across sectors and scales in Cambodia*.

Reiche, J., de Bruin, S., Hoekman, D., Verbesselt, J., & Herold, M. (2015a). A Bayesian Approach to Combine Landsat and ALOS PALSAR Time Series for Near Real-Time Deforestation Detection. *Remote Sensing*, *7*, 4973–4996.

Reiche, J., Souzax, C. M., Hoekman, D. H., Verbesselt, J., Persaud, H., & Herold, M.

(2013). Feature level fusion of multi-temporal ALOS PALSAR and Landsat data for mapping and monitoring of tropical deforestation and forest degradation. *IEEE Journal of Selected Topics in Applied Earth Observations and Remote Sensing*, *6*, 2159–2173.

Reiche, J., Verbesselt, J., Hoekman, D., & Herold, M. (2015b). Fusing Landsat and SAR time series to detect deforestation in the tropics. *Remote Sensing of Environment*, *156*, 276–293.

Reynolds, M. R., & Cho, G.-Y. (2011). Multivariate Control Charts for Monitoring the Mean Vector and Covariance Matrix with Variable Sampling Intervals. *Sequential Analysis*, *30*, 1–40.

Roerink, G., Menenti, M., Soepboer, W., & Su, Z. (2003). Assessment of climate impact on vegetation dynamics by using remote sensing. *Physics and Chemistry of the Earth, Parts A/B/C*, *28*, 103–109.

Roerink, G. J., Menenti, M., & Verhoef, W. (2000). Reconstructing cloudfree NDVI composites using Fourier analysis of time series. *International Journal of Remote Sensing*, *21*, 1911–1917.

Romijn, E., Herold, M., Kooistra, L., Murdiyarso, D., & Verchot, L. (2012). Assessing capacities of non-Annex I countries for national forest monitoring in the context of REDD+. *Environmental Science & Policy*, *19-20*, 33–48.

Roy, D., Wulder, M., Loveland, T., C.E., W., Allen, R., Anderson, M., Helder, D., Irons, J., Johnson, D., Kennedy, R., Scambos, T., Schaaf, C. et al. (2014). Landsat-8: Science and product vision for terrestrial global change research. *Remote Sensing of Environment*, *145*, 154–172.

Saatchi, S. S., Harris, N. L., Brown, S., Lefsky, M., Mitchard, E. T. a., Salas, W., Zutta, B. R., Buermann, W., Lewis, S. L., Hagen, S., Petrova, S., White, L. et al. (2011). Benchmark map of forest carbon stocks in tropical regions across three continents. *Proceedings of the National Academy of Sciences*, *2005*.

Salk, C. F., Chazdon, R. L., & Andersson, K. P. (2013). Detecting landscape-level changes in tree biomass and biodiversity: methodological constraints and challenges of plot-based approaches. *Canadian Journal of Forest Research*, *43*, 799–808.

Sanz-Sanchez, M., Herold, M., & Penman, J. (2013). Conference Report: REDD+ related forest monitoring remains a key issue: A report following the recent un climate conference in Doha. *Carbon Management*, *4*, 125–127.

Scheffer, M., Carpenter, S., Foley, J. a., Folke, C., & Walker, B. (2001). Catastrophic shifts in ecosystems. *Nature*, *413*, 591–596.

Scheffer, M., & Carpenter, S. R. (2003). Catastrophic regime shifts in ecosystems: Linking theory to observation. *Trends in Ecology and Evolution*, *18*, 648–656.

Schmidt, L., & Scholz, I. (2008). *Reducing Emissions from Deforestation and Forest*

Degradation in Developing Countries: Meeting the main challenges ahead. Briefing Paper 6.. Deutsches Institut für Entwicklungspolitik.

Schmidt, M., Lucas, R., Bunting, P., Verbesselt, J., & Armston, J. (2015). Multi-resolution time series imagery for forest disturbance and regrowth monitoring in Queensland, Australia. *Remote Sensing of Environment*, *158*, 156–168.

Schmitt, C. B., Denich, M., Demissew, S., Friis, I., & Boehmer, H. J. (2010a). Floristic diversity in fragmented Afromontane rainforests: Altitudinal variation and conservation importance. *Applied Vegetation Science*, (pp. 291–304).

Schmitt, C. B., Senbeta, F., Denich, M., Preisinger, H., & Boehmer, H. J. (2010b). Wild coffee management and plant diversity in the montane rainforest of southwestern Ethiopia. *African Journal of Ecology*, *48*, 78–86.

Schroeder, T., Wulder, M., Healey, S., & Moisen, G. (2011). Mapping wildfire and clearcut harvest disturbances in boreal forests with landsat time series data. *Remote Sensing of Environment*, *115*, 1421–1433.

Schroeder, T. a., Cohen, W. B., & Yang, Z. (2007). Patterns of forest regrowth following clearcutting in western Oregon as determined from a Landsat time-series. *Forest Ecology and Management*, *243*, 259–273.

Schroeder, T. a., Healey, S. P., Moisen, G. G., Frescino, T. S., Cohen, W. B., Huang, C., Kennedy, R. E., & Yang, Z. (2014). Improving estimates of forest disturbance by combining observations from Landsat time series with U.S. Forest Service Forest Inventory and Analysis data. *Remote Sensing of Environment*, *154*, 61–73.

Scullion, J. J., Vogt, K. a., Sienkiewicz, A., Gmur, S. J., & Trujillo, C. (2014). Assessing the influence of land-cover change and conflicting land-use authorizations on ecosystem conversion on the forest frontier of Madre de Dios, Peru. *Biological Conservation*, *171*, 247–258.

Sen, P. (1968). Estimates of the regression coefficient based on Kendall's tau. *Journal of the American Statistical Association*, *63*, 1379–1389.

Shepard, G. H., Rummenhoeller, K., Ohl-Schacherer, J., & Yu, D. W. (2010). Trouble in Paradise: Indigenous Populations, Anthropological Policies, and Biodiversity Conservation in Manu National Park, Peru. *Journal of Sustainable Forestry*, *29*, 252–301.

Shrestha, R. (2010). Participatory carbon monitoring: An experience from the koshi hills, nepal. *Proceedings of the National Conference on Forest-People Interaction*, (pp. 1–14).

Sigrist, P., Coppin, P., & Hermy, M. (1999). Impact of forest canopy on quality and accuracy of gps measurements. *International Journal of Remote Sensing*, *20*, 3595–3610.

Skarlatidou, A., Haklay, M., & Cheng, T. (2011). Trust in Web GIS: The role of the trustee attributes in the design of trustworthy Web GIS applications. *International*

Journal of Geographical Information Science, *25*, 1913–1930.

Skutsch, M., McCall, M., & Larrazabal, A. (2014a). Balancing views on community monitoring: The case of REDD+: A response to "towards a more balanced view on the potentials of locally-based monitoring". *Biodiversity and Conservation*, *23*, 233–236.

Skutsch, M., Torres, A., Mwampamba, T., Ghilardi, A., & Herold, M. (2011). Dealing with locally-driven degradation: A quick start option under REDD+. *Carbon Balance and Management*, *6*.

Skutsch, M., Turnhout, E., Vijge, M. J., Herold, M., Wits, T., Den Besten, J. W., & Torres, A. B. (2014b). Options for a national framework for benefit distribution and their relation to community-based and national REDD+ monitoring. *Forests*, *5*, 1596–1617.

Souza, C. M., Pereira, K., Lins, V., Haiashy, S., & Souza, D. (2009). Web-oriented GIS system for monitoring, conservation and law enforcement of the Brazilian Amazon. *Earth Science Informatics*, *2*, 205–215.

Souza, C. M., Roberts, D. A., & Cochrane, M. A. (2005). Combining spectral and spatial information to map canopy damage from selective logging and forest fires. *Remote Sensing of Environment*, *98*, 329–343.

Stehman, S. V., Wickham, J. D., Smith, J. H., & Yang, L. (2004). Thematic accuracy of the 1992 National Land-Cover Data for the western United States. *Remote Sensing of Environment*, *91*, 452–468.

Stickler, C., Nepstad, D., Coe, M., McGrath, D., Rodrigues, H., Walker, W., Soares-Filho, B., & Davidson, E. (2009). The potential ecological costs and cobenefits of redd: A critical review and case study from the amazon region. *Global Change Biology*, *15*, 2803–2824.

Strahler, A., Boschetti, L., Foody, G., Friedl, M., Hansen, M., Herold, M., Mayaux, P., Morisette, J., Stehman, S., & Woodcock, C. (2006). *Global land cover validation: Recommendations for evaluation and accuracy assessment of global land cover maps*. EUR 22156 EN GOFC-GOLD.

Strobl, C., Boulesteix, A.-L., Kneib, T., Augustin, T., & Zeileis, A. (2008). Conditional variable importance for random forests. *BMC bioinformatics*, *9*, 307.

Tadesse, G., Zavaleta, E., & Shennan, C. (2014a). Coffee landscapes as refugia for native woody biodiversity as forest loss continues in southwest Ethiopia. *Biological Conservation*, *169*, 384–391.

Tadesse, G., Zavaleta, E., Shennan, C., & FitzSimmons, M. (2014b). Policy and demographic factors shape deforestation patterns and socio-ecological processes in southwest Ethiopian coffee agroecosystems. *Applied Geography*, *54*, 149–159.

Teketay, D. (1997). The impact of clearing and conversion of dry Afromontane forests

into arable land on the composition and density of soil seed banks. *Acta Oecologica*, *18*, 557–573.

Thiel, C., Drezet, P., Weise, C., Quegan, S., & Schmullius, C. (2006). Radar remote sensing for the delineation of forest cover maps and the detection of deforestation. *Forestry*, *79*, 589–597.

Thompson, I. D., Guariguata, M. R., Okabe, K., Bahamondez, C., Nasi, R., Heymell, V., & Sabogal, C. (2013). An operational framework for defining and monitoring forest degradation. *Ecology and Society*, *18*.

Tomppo, E., Gschwantner, T., Lawrence, M., & McRoberts, R. (2010). *National Forest Inventories: Pathways for Common Reporting*. Springer.

Topp-Jørgensen, E., Poulsen, M., Lund, J., & Massao, J. (2005). Community-based monitoring of natural resource use and forest quality in montane forests and miombo woodlands of Tanzania. *Biodiversity and Conservation*, *14*, 2653–2677.

Torres, A., & Skutsch, M. (2012). Splitting the difference: A proposal for benefit sharing in reduced emissions from deforestation and forest degradation (REDD+). *Forests*, *3*, 137–154.

Tropek, R., Beck, J., Keil, P., Musilová, Z., Irena, v., & Storch, D. (2013). Comment on "High-resolution global maps of 21st-century forest cover change". *Science*, *344*.

Tucker, C., Pinzon, J., Brown, M., Slayback, D., Pak, E., Mahoney, R., Vermote, E., & El Saleous, N. (2005). An extended AVHRR 8-km NDVI dataset compatible with MODIS and SPOT vegetation NDVI data. *International Journal of Remote Sensing*, *26*, 4485–4498.

Tucker, C. J. (1979). Red and photographic infrared linear combinations for monitoring vegetation. *Remote Sensing of Environment*, *8*, 127–150.

Tyukavina, a., Stehman, S. V., Potapov, P. V., Turubanova, S. a., Baccini, a., Goetz, S. J., Laporte, N. T., Houghton, R. a., & Hansen, M. C. (2013). National-scale estimation of gross forest aboveground carbon loss: a case study of the Democratic Republic of the Congo. *Environmental Research Letters*, *8*, 044039.

UNFCCC (2001). *Report of the Conference of the Parties on its Seventh Session, Held in Marrakech from Oct.–Nov. 2001. Addendum Part Two: Action Taken by the Conference of the Parties (FCCC/CP/2001/13/Add. 1 vol I)*. United Nations Framework Convention on Climate Change Secretariat. Bonn.

UNFCCC (2009a). *Cost of implementing methodologies and monitoring systems relating to estimates of emissions from deforestation and forest degradation , the assessment of carbon stocks and greenhouse gas emissions from changes in forest cover , and the enhancement of for*.

UNFCCC (2009b). *Outcome of the work of the Ad Hoc Working Group*

on Long-term Cooperative Action under the Convention Draft decision FCCC/AWGLCA/2009/L.7/Add.6. Copenhagen.

UNFCCC (2010). *Outcome of the Work of the ad Hoc Working Group on Long-Term Cooperative Action under the Convention Policy Approaches and Positive Incentives on Issues Relating to Reducing Emissions from Deforestation and Forest Degradation in Developing Countries and the Role of Conservation*. United Nations Framework Convention on Climate Change Secretariat. Bonn.

UNFCCC (2013). *Guidelines and Procedures for the Technical Assessment of Submissions from Parties on Proposed Forest Reference Emission Levels and/or Forest Reference Levels*. United Nations Framework Convention on Climate Change Secretariat. Bonn.

Vargas, R., Paz, F., & De Jong, B. (2013). Quantification of forest degradation and belowground carbon dynamics: Ongoing challenges for monitoring, reporting and verification activities for redd+. *Carbon Management*, *4*, 579–582.

Veblen, T. T. (1976). The urgent need for forest conservation in highland Guatemala. *Biological Conservation*, *9*, 141–154.

Verbesselt, J., Hyndman, R., Zeileis, A., & Culvenor, D. (2010). Phenological change detection while accounting for abrupt and gradual trends in satellite image time series. *Remote Sensing of Environment*, *114*, 2970–2980.

Verbesselt, J., Robinson, A., Stone, C., & Culvenor, D. (2009). Forecasting tree mortality using change metrics derived from MODIS satellite data. *Forest Ecology and Management*, *258*, 1166–1173.

Verbesselt, J., Zeileis, A., & Herold, M. (2012). Near real-time disturbance detection using satellite image time series. *Remote Sensing of Environment*, *123*, 98–108.

Verburg, P., Neumann, K., & Nol, L. (2011). Challenges in using land use and land cover data for global change studies. *Global Change Biology*, *17*, 974–989.

Vermote, E. F., Deuzé, J. L., Herman, M., & Morcrette, J. J. (1997). Second simulation of the satellite signal in the solar spectrum, 6S: An overview. *IEEE Transactions on Geoscience and Remote Sensing*, *35*, 675–686.

Visseren-Hamakers, I., Gupta, A., Herold, M., Peña-Claros, M., & Vijge, M. (2012). Will REDD+ work? The need for interdisciplinary research to address key challenges. *Current Opinion in Environmental Sustainability*, *4*, 590–596.

Walker, R., Browder, J., Arima, E., Simmons, C., Pereira, R., Caldas, M., Shirota, R., & Zen, S. D. (2009). Ranching and the new global range: Amazônia in the 21st century. *Geoforum*, *40*, 732–745.

Walker, S., & Duncan, D. (1967). Estimation of the probability of an event as a function of several independent variables. *Biometrika*, *54*, 167–179.

van der Werf, G. R., Morton, D. C., DeFries, R. S., Olivier, J. G. J., Kasibhatla, P. S.,

Jackson, R. B., Collatz, G. J., & Randerson, J. T. (2009). CO2 emissions from forest loss. *Nature Geoscience*, *2*, 737–738.

Williams, D. L., Goward, S., & Arvidson, T. (2006). Landsat: Yesterday, Today, and Tomorrow. *Photogrammetric Engineering and Remote Sensing*, *72*, 1171–1178.

Wilson, E. H., & Sader, S. a. (2002). Detection of forest harvest type using multiple dates of Landsat TM imagery. *Remote Sensing of Environment*, *80*, 385–396.

World Resources Institute (2014). Global Forest Watch. URL: `http://www.globalforestwatch.org/`.

Wulder, M. A., & Coops, N. C. (2014). Satellites: Make Earth observations open access. *Nature*, *513*, 30–1.

Wulder, M. a., Masek, J. G., Cohen, W. B., Loveland, T. R., & Woodcock, C. E. (2012). Opening the archive: How free data has enabled the science and monitoring promise of Landsat. *Remote Sensing of Environment*, *122*, 2–10.

Wulder, M. a., White, J. C., Andrew, M. E., Seitz, N. E., & Coops, N. C. (2009). Forest fragmentation, structure, and age characteristics as a legacy of forest management. *Forest Ecology and Management*, *258*, 1938–1949.

Zeileis, A., Kleiber, C., Walter, K., & Hornik, K. (2003). Testing and dating of structural changes in practice. *Computational Statistics and Data Analysis*, *44*, 109–123.

Zeileis, A., Leisch, F., Hornik, K., & Kleiber, C. (2002). strucchange: An R Package for Testing for Structural Change in Linear Regression Models. *Journal of Statistical Software*, *7*, 1–38.

Zeileis, A., Leisch, F., Kleiber, C., & Hornik, K. (2005). Monitoring structural change in dynamic econometric models. *Journal of Applied Econometrics*, *20*, 99–121.

Zhang, C., Li, W., & Travis, D. (2007). Gaps-fill of SLC-off Landsat ETM+ satellite image using a geostatistical approach. *International Journal of Remote Sensing*, *28*, 5103–5122.

Zhu, X., Liu, D., & Chen, J. (2012a). A new geostatistical approach for filling gaps in Landsat ETM+ SLC-off images. *Remote Sensing of Environment*, *124*, 49–60.

Zhu, Z., & Woodcock, C. E. (2012). Object-based cloud and cloud shadow detection in Landsat imagery. *Remote Sensing of Environment*, *118*, 83–94.

Zhu, Z., & Woodcock, C. E. (2014). Continuous change detection and classification of land cover using all available Landsat data. *Remote Sensing of Environment*, *144*, 152–171.

Zhu, Z., Woodcock, C. E., Holden, C., & Yang, Z. (2015). Generating synthetic Landsat images based on all available Landsat data: Predicting Landsat surface reflectance at any given time. *Remote Sensing of Environment*, *162*, 67–83.

Zhu, Z., Woodcock, C. E., & Olofsson, P. (2012b). Continuous monitoring of forest disturbance using all available Landsat imagery. *Remote Sensing of Environment*, *122*, 75–91.

Zhuravleva, I., Turubanova, S., Potapov, P., Hansen, M., Tyukavina, a., Minnemeyer, S., Laporte, N., Goetz, S., Verbelen, F., & Thies, C. (2013). Satellite-based primary forest degradation assessment in the Democratic Republic of the Congo, 2000–2010. *Environmental Research Letters*, *8*, 024034.

List of publications

Peer-reviewed journal publications

DeVries, B., Pratihast, A.K., Verbesselt, J., Kooistra, L. and Herold, M. 2015. Characterizing forest change using community-based monitoring data and Landsat time series. *PLoS ONE Forests*, under review.

Pratihast, A.K., **DeVries, B.**, Avitabile, V., de Bruin, S., Herold, M. and Bergsma, A. 2015. Design and implementation of an interactive web-based near real-time forest monitoring system. *PLoS ONE Forests*, under review.

Avitabile V., Herold M., Heuvelink G.B.M., Lewis S.L., Phillips O.L., Asner G.P., Asthon P., Banin L.F., Bayol N., Berry N., Boeckx P., de Jong B., **DeVries B.**, Girardin C., Kearsley E., Lindsell J.A., Lopez-Gonzalez G., Lucas R., Malhi Y., Morel A., Mitchard E., Nagy L., Qie L., Quinones M., Ryan C.M., Slik F., Sunderland, T., Vaglio Laurin G., Valentini R., Verbeeck H., Wijaya A. and Willcock S. 2015. An integrated pan-tropical biomass maps using multiple reference datasets. *Global Change Biology*, under review

DeVries, B., Decuyper, M., Verbesselt, J., Zeileis, A., Herold, M. and Joseph, S. 2015. Tracking disturbance-regrowth dynamics in the tropics using structural change monitoring and Landsat time series. *Remote Sensing of Environment* 169:320-334.

DeVries, B., Verbesselt, J., Kooistra L. and Herold, M. 2015. Robust monitoring of small-scale forest disturbances in a tropical montane forest using Landsat time series. *Remote Sensing of Environment*, 161:107-121.

Pratihast, A.K., **DeVries, B.**, Avitabile, V., de Bruin, S., Kooistra, L. and Herold, M. 2014. Combining satellite data and community-based observations for forest monitoring. *Forests*, 5:2464-2489.

Dresen, E., **DeVries, B.**, Herold, M., Verchot, L. and Müller, R. 2014. Fuelwood savings and carbon emission reductions by the use of improved cooking stoves in an Afromontane forest, Ethiopia. *Land*, 3(3):1137-1157.

Buerger, C., **DeVries, B.** and Stambolic, V. 2006. Localization of Rheb to the endomembrane is critical for its signaling function. *Biochemical and Biophysical Research Communications*, 344(3):869-880.

Peer-reviewed book chapter

DeVries, B. and Herold, M. 2013. The Science of Measuring, Reporting and Verification (MRV). In R. Lyster, C. MacKenzie, & C. McDermott (Eds.), Law, Tropical Forests and Carbon: The Case of REDD+, pp. 151-183. Cambridge: Cambridge Univ Press.

Other scientific publications

DeVries, B., Verbesselt, J., Kooistra, L. and Herold, M. 2014. Detecting tropical deforestation and degradation using Landsat time series. In *International Geoscience and Remote Sensing Symposium*, 13-18 July 2014, Québec, QC, Canada.

Hamunyela, E., Verbesselt, J., Schultz, M., Penndorf, A., Frotscher, K., Herold, M., Reiche, J., **DeVries, B.**, Dutrieux, L.P. and Calders, K. 2014. Tracking forest cover change using Landsat & Rapid Eye towards S2. In *Sentinel-2 for Science Workshop*, 20-22 May 2014, ESA-ESRIN, Frascati, Italy.

Avitabile, V., Herold, M., Calders, K., **DeVries, B.** and Ribeiro Sales, M.H. 2014. Multiple data sources for analyzing, integrating and validating biomass maps. In *Proceedings of the First Joint Workshop of the EARSeL Special Interest Group on Land Use & Land Cover and the NASA LCLUC Program on "Frontiers in Earth Observation for Land System Science"*, 17-18 March 2014, Berlin, Germany.

Avitabile, V., Herold, M., Lewis, S.L., Phillips, O.L., Aguilar-Amuchastegui, N., Asner, G.P., Brienen, R.J.W., **DeVries, B.**, Gazolla Gatti, R., Feldpausch, T.R., Girardin, C., Jong, B. de; Kearsley, E., Klop, E., Lin, X., Lindsell, J., Lopez-Gonzalez, G., Lucas, R., Malhi, Y., Morel, A., Mitchard, E., Pandey, D., Piao, S., Ryan, C., Sales, M., Santoro, M., Vaglio Laurin, G., Valentini, R., Verbeeck, H., Wijaya, A. and Willcock, S. Comparative analysis and fusion for improved global biomass mapping. 2014. In *International Conference Global Vegetation Monitoring and Modeling (GV2M)*, 3-7 February 2014, Avignon, France.

DeVries, B., Verbesselt, J., Kooistra, L. and Herold, M. 2013. Detecting tropical deforestation and forest degradation at high temporal resolution in support of REDD+ MRV. In *Proceedings ESA Living Planet Symposium*, 9-13 September 2013, Edinburgh, Scotland.

Pratihast, A.K., **DeVries, B.**, Kooistra, L., de Bruin, S. and Herold, M. 2013. Interactive Forest Monitoring System: A case study of Kafa, Ethiopia. In *Proceedings ESA Living Planet Symposium*, 9-13 September 2013, Edinburgh, Scotland.

DeVries, B., Pratihast, A.K., Verbesselt, J., Kooistra, L., de Bruin, S. and Herold, M. 2013. Near real-time tropical forest disturbance monitoring using Landsat time series and local expert monitoring data. In *MultiTemp 2013: 7th International Workshop on the Analysis of Multi-temporal Remote Sensing Images*, 25-27 June 2013, Banff, AB, Canada.

Dutrieux, L.P., Verbesselt, J., Kooistra, L., **DeVries, B.** and Herold, M. 2013. Combining medium and high-resolution data in multi-scale approach to detect breaks in satellite image time-series. In *MultiTemp 2013: 7th International Workshop on the Analysis of Multi-temporal Remote Sensing Images*, 25-27 June 2013, Banff, AB, Canada.

DeVries, B., Avitabile, V., Kooistra, L. and Herold, M. - 2012. Monitoring the impact of REDD+ implementation in the Unesco Kafa biosphere reserve, Ethiopia. In *International Geoscience and Remote Sensing Symposium*, 22-27 July 2012, Munich, Germany.

DeVries, B. 2010. Monitoring the effects of restoration efforts in degraded tropical peatlands, Central Kalimantan, Indonesia. *MSc thesis, Wageningen University, The Netherlands.* 59 p.

DeVries, B. 2010. Developing a tool for carbon accounting through hydrological modeling in the Sebangau peatlands, Central Kalimantan, Indonesia. *MSc thesis, Wageningen University, The Netherlands.* 54 p.

Short biography

Ben DeVries was born in St.Thomas, Ontario, Canada on August 1, 1981, where he grew up and attended primary school. He completed his secondary school diploma at Parkside Collegiate Institute in St.Thomas.

Ben completed his Honours Bachelor of Science in Biochemistry at the University of Toronto, Canada in 2005. He then completed an internship in Sri Lanka through the Canadian International Youth Internship Programme (IYIP) and went on to work in Eastern and Southern Africa as a Disaster Response Coordinator for the Christian Reformed World Relief Committee while stationed in Kampala, Uganda.

Ben began his MSc studies at Wageningen University in 2008 through the International Land and Water Management MSc programme. He completed a major and minor MSc theses with the Land Degradation and Development Group at Wageningen University. Both theses were related to field-based and model-based methods for monitoring tropical peatland hydrology and associated carbon emissions and were undertaken through Alterra in partnership with WWF Germany and Indonesia.

Upon completion of his MSc degree in 2010, Ben took on a PhD position at the Laboratory of Geo-Information Science and Remote Sensing at Wageningen University. Here, he developed novel methods based on dense remote sensing time series for the monitoring of forest change dynamics in tropical systems. Much of this research was undertaken in the UNESCO Kafa Biosphere Reserve in southern Ethiopia, with support from the Nature and Biodiversity Conservation Union (NABU), Germany and Ethiopia. Ben was actively involved in educational and capacity building activities during his PhD studies, assisting in the teaching of MSc level courses and holding various trainings and capacity workshops at the local and national scales.

Ben's current research interests are concerned with the monitoring and characterization of forest and other land cover dynamics at high temporal resolution using remote sensing time series and ground-based data streams. Following his PhD, he will be continuing his research career as a post-doctoral researcher at the Department of Geographical Sciences, University of Maryland.

PE&RC Training and Education Statement

With the training and education activities listed below the PhD candidate has complied with the requirements set by the C.T. de Wit Graduate School for Production Ecology and Resource Conservation (PE&RC) which comprises of a minimum total of 32 ECTS (= 22 weeks of activities)

Review of literature (6 ECTS)

- The science of MRV; published in *Law, Tropical Forests and Carbon: The Case of REDD+*, Cambridge University Press (2013)

Writing of project proposal (4.5 ECTS)

- Local REDD monitoring and implementation in the UNESCO Biosphere Reserve, Kafa Region, Ethiopia

Post-graduate courses (4.5 ECTS)

- Geostatistics; PE&RC (2011)
- Sampling in space and time; PE&RC (2013)
- Multivariate analysis; SENSE (2013)

Invited review of (unpublished) journal manuscript (2 ECTS)

- Science of the Total Environment: forest change and climate interactions (2014)
- Remote Sensing of Environment: tropical deforestation monitoring using remote sensing (2015)

Competence strengthening / skills courses (1.5 ECTS)

- Career orientation; WUR (2014)

PE&RC Annual meetings, seminars and the PE&RC weekend (1.2 ECTS)

- PE&RC PhD Weekend (2012)
- PE&RC Day (2014)

Discussion groups / local seminars / other scientific meetings (6.4 ECTS)

- REDD+ Discussion group; WUR (2011-2014)
- Sensing a changing world symposium; oral presentation; WUR (2012)
- Ethiopia REDD+ MRV road map workshop; member of facilitation team; Addis Ababa, Ethiopia (2012)
- Ecology discussion group; WUR (2014-2015)

International symposia, workshops and conferences (11.9 ECTS)

- IGARSS; poster presentation; Munich, Germany (2011)
- MultiTemp; oral presentation; Banff, Canada (2013)
- ESA Living planet symposium; oral presentation; Edinburgh, UK (2014)
- IGARSS; oral presentation; Québec, Canada (2014)
- ISRSE; oral presentation; Berlin, Germany (2015)

Lecturing / supervision of practicals / tutorials (4.8 ECTS)

- Geo-scripting (2014)
- Advanced earth observation (2015)

Supervision of 3 MSc students

- F. Tessema: remote sensing time series analysis for tracking forest change in support of local REDD+ implementation (2011)
- K. Mulatu: integrating biodiversity monitoring in REDD+ MRV (2012)
- D. Beyene: assessing the impact of the UNESCO biosphere reserves on forest cover change (2013)